THESIS

DESIGN AND ANALYSIS OF ACTUAL AND ALTERNATIVE EXHAUST GAS RECIRCULATION SYSTEMS ON SOLAR TURBINES CENTAUR 40 3.5MWE GAS TURBINE ENGINE FOR THE PURPOSE OF CARBON CAPTURE OPTIMIZATION

Submitted by

Bianca R Jeremiah

Department of Mechanical Engineering

In partial fulfillment of the requirements

For the Degree of Master of Science

Colorado State University

Fort Collins, Colorado

Fall 2025

Master's Committee:

Advisor: Bret Windom

Todd Bandhauer

Daniel Herber

ABSTRACT

DESIGN AND ANALYSIS OF ACTUAL AND ALTERNATIVE EXHAUST GAS RECIRCULATION SYSTEMS ON SOLAR TURBINES CENTAUR 40 3.5MWE GAS TURBINE ENGINE FOR THE PURPOSE OF CARBON CAPTURE OPTIMIZATION

Power generation plants on land as well as in marine applications are massively contributing to carbon dioxide emissions, causing accelerated climate change throughout the globe. Decarbonization of the energy production industry is imperative, especially as energy demand continues to grow. As the power grid decarbonizes through new energy solutions and alternative technologies, retrofitting the current power generation system is an essential step in bridging the existing infrastructure with the emerging one. One way to bridge the gap is by retrofitting existing engines with exhaust gas recirculation systems for improved carbon capture capability. This work discusses the design and deployment implications of an EGR system on a 3.5 MWe Solar Turbines Centaur 40 gas turbine at Colorado State University (CSU), utilizing Flownex simulation software to model various system configurations. System requirements and design considerations of a gas turbine EGR system are presented, along with detailed analysis of a bottled gas manifold that will serve as a surrogate of an EGR system. Detailed analysis of the cooling load, footprint, and steam production associated with multiple cooling systems are explored as it pertains to actual EGR systems, as well as the combustion composition of the recirculated exhaust gases. For the surrogate EGR system, careful consideration of the required gas mass flow rates to reproduce the expected EGR composition is taken with respect to available bulk delivery capacities and delivery technology. Both natural gas and diesel fuel compositions are considered in system models to develop the EGR system as an applicable technology on both

land and marine based gas turbine power production plants. The optimal system design for applying EGR to CSU's Solar Turbines Centaur 40 gas turbine engine was determined to be the surrogate gas system, as it avoids high cooling loads and space requirements that would be restrictive if attempted in the available research facility. An exhaust gas system was constructed to enable future experimental testing of the surrogate EGR system, which includes both internal and external building modifications.

ACKNOWLEDGEMENTS

This work was funded by the Decarbonization Research Consortium under the Office of Naval Research; awarded as part of N00014-23-S-B001. The study was supported with technical guidance by Solar Turbines. The CSU Energy Institute at the Powerhouse Energy Campus provided lab space, equipment, and facilities which made this work possible.

Dr. Bret Windom, thank you for your guidance throughout my degree, and for your shining clarity in every situation. Andrew Zdanowicz, your mentorship and attitude shaped my experience at CSU. Thank you for your endless patience and counsel in every aspect of this project. Dr. Toluwalase Fosudo, your investment in my success was felt and appreciated from the very start.

Andrew Harrod, I couldn't have asked for a better research colleague and friend. Infinite thanks to all the friends I made - thank you for your love and support throughout the journey.

TABLE OF CONTENTS

LIST OF TABLES

LIST OF FIGURES

CHAPTER 1- INTRODUCTION

1.1 Motivation

The global call to decrease carbon emissions, balanced with the increasing demand for reliable and energy-dense power production, has driven the Navy and other maritime industries to consider retrofit carbon capture (CC) technologies on their existing gas turbine powered vessels. These systems can offer short-term carbon emission solutions while meeting expectations for mission readiness and vessel performance. Gas turbines power the majority of the Navy's fleet and have characteristically high air-fuel ratios due to their working principle and material limitation that make conventional carbon capture and storage (CCS) technologies prohibitively large and energy consuming for onboard vessels. Exhaust gas recirculation (EGR) is a process that portions a segment of exhaust gas to mix with intake air and reenter the engine inlet. EGR systems have been proposed to increase carbon dioxide (CO_2) concentrations in gas turbine exhaust and thereby substantially reduce the burden of point-source CCS systems.

Literature on large scale applications of EGR is limited, and designs of alternative EGR systems intended to support turbine performance testing are virtually nonexistent. This study evaluates design considerations of both real and alternative EGR systems. The alternative system, also referred to as the surrogate system, includes utilizing bottled supply gases to match the GT intake composition expected with EGR. These systems are considered for their specific implementation on CSU's Centaur 40 research engine through the lens of both marine and land-based applications.

1.2 Carbon Dioxide Emissions

Greenhouse gases (GHG) are a major contributor to the acceleration of climate change, a phenomenon majorly disruptive to weather, the environment, and various sectors of socio-environmental sustainability. Carbon dioxide (CO_2), as well as methane (CH_4) and nitrous oxide (N_2O) are known long-lived GHG, meaning they persist in the atmosphere for decades or centuries once produced. Anthropogenically sourced GHG emissions accounted for a 49% rise in direct warming influence between 1990 and 2022 [1]. The most significant contributor to GHG emissions is CO_2, as it accounts for about 80% of the increased heat since 1990 and is produced at roughly 36 billion metric tons each year from electrical generation, transportation, and other processes [1].

Electric power generation is a primary contributor to CO_2 in the atmosphere, accounting for as much as 1,427 million metric tons emissions in 2024 [2]. Stationary power plants are integral to the United States power grid and are largely reliant on gas turbine engines, as they accounted for a majority of all power generation in the US in 2024, and their utilization is projected to increase as the demand for energy grows. While combustion gas turbine engines are lean burning by design, there are still considerable emissions. The most prominent emissions from gas turbine engines are CO_2 and NOx, due to the combustion characteristics of the hydrocarbon fuels. The National Energy Technology Laboratory compiled a map showing the carbon dioxide emissions of all operating gas turbines installed in the United States between 2010 and 2023, shown as Figure 1 [3]. The map shows CO_2 emissions of each GT installation ranging from zero to one million tonnes per year.

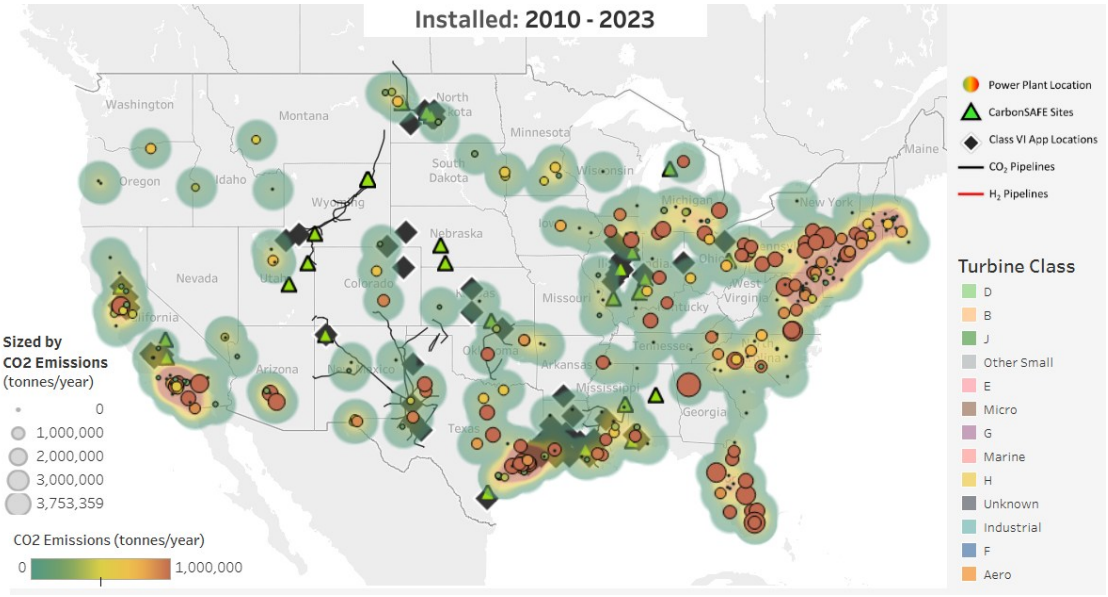

Figure 1: Map of CO_2 emissions from all gas turbines installed in the United States between 2010 and 2023 shown on a scale from 0-1,000,000 tonnes CO_2 per year [3].

Gas turbine engines can run on various fuels and have characteristic emissions profiles associated with each fuel type. While many gas turbines are also capable of running on hydrogen blends and other alternative fuels, they will not be discussed in this work. Rather, we will focus on the main fuel sources currently used for energy consumption in the United States. Natural gas and petroleum fuel sources account for nearly identical shares of the national energy consumption across all energy consumption sectors, at 38% and 35% respectively [4]. This breakdown includes electric power generation, transportation, industrial, residential, and commercial. In electric power generation alone, natural gas accounted for 39% and petroleum less than 1% in 2022 [5]. The navy reported emissions of 16.7 million metric tons of CO_2 in 2021, which composed of 70% operational and 30% installation sourced emissions [6]. The operational emissions sources are petroleum-derived fuels: 50% jet fuel (JP-5) and 50% ship fuel (F-76) [6].

Given the major share of the energy production network and the marine sector that is reliant on gas turbine energy production, it is valuable to determine the specific CO_2 and NOx emissions associated with GT combustion. Burns et al. found that the CO_2 mole fraction in exhaust gas of a typical gas turbine burning natural gas to be around 3% without EGR [7]. This is similar to offsite emissions testing results of CSU's Solar Turbines Centaur 40 engine shown in Figure 2, which shows that running at full load without EGR, the CO_2 mass fraction in the exhaust ranges from 2.5% - 3.25% depending on natural gas or liquid diesel fuel.

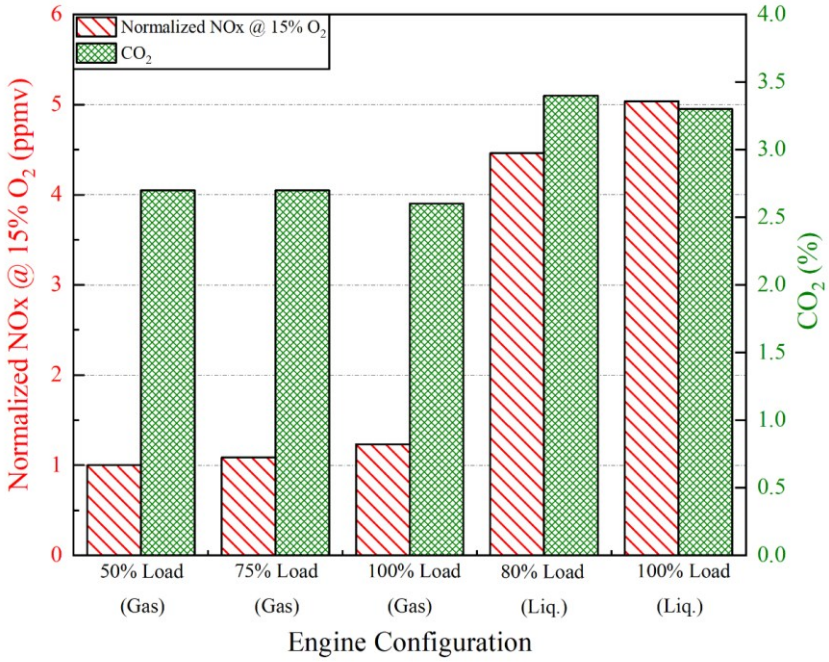

Figure 2: Results of offsite testing of the CSU dual-fuel gas turbine C40 engine showing normalized NOx and CO_2 emissions from 50%-100% load. G indicates pipeline natural gas and is measured for loads 50%-100%. L indicates liquid fuel Diesel tested on load range 80%-100%.

1.3 Decarbonization Motivation, Policy, and Technology

There are three recognized methods of decarbonizing power generation: pre combustion, post combustion, and oxy-combustion [8]. While pre-combustion decarbonization methods present promising alternatives for the energy transition, the current state of the energy generation network

has deep roots in fossil fuel consumption and demands we decarbonize through post combustion methods. Despite combustion gas turbine emissions production associated with fossil fuels, they are a necessary component of the U.S. energy economy and cannot immediately be replaced with alternative methods or fuels. Therefore, the emissions produced from the existing gas turbine infrastructure must be managed in a retrofit manner. Fortunately, stationary power plant emissions present a unique and effective method of global decarbonization: point source carbon capture (PSCC). PSCC captures emissions directly from their source, typically from separating the desired emission from exhaust flues at power plants or industrial factories by means of carbon capture systems, most notably amine absorption.

Processing exhaust gases for CO_2 sequestration and utilization provides both environmental benefits through emissions reduction as well as financial motivation through downstream carbon usage. Captured CO_2 can be used either directly or indirectly in a multitude of ways such as enhanced oil and natural gas recovery, fertilizer products, CO_2 based synthetic fuel production, etc. Carbon capture is proven to be a feasible and profitable method of emissions mitigation. Between 2016 and 2023, 147 million metric tons of CO_2 were captured from industrial sources in the US with the majority finding end use in enhanced oil and gas recovery, and 63.1 million metric tons were stored through geological sequestration [9].

Policy action provides additional motivation to carbon capture, such as the United States 2022 Inflation Reduction Act which includes the 45Q tax credit for CCUS as well as the Clean Fuels & Products Shot. These policies provide credits for capturing and sequestering carbon, at a value of \$60 per tonne of CO_2 [10] and promote decarbonization of the fuel and chemical industry by instating the 2050 net-zero emissions goal [11].

Typical percentages of CO_2 in GT exhaust flue are relatively low when considering the high total mass flow of the exhaust, such as the 68,365 kg/hr exhaust flow of the Centaur 40 [12]. This is especially relevant when considering feasibility of post combustion carbon capture systems (PCCCS). PCCCS size is determined by the volume of flue gas it must process, the scrubbing percentage, and the amount of carbon in the flue stream. Burnes et al. found the relationship between amine process carbon separation system size and concentration of CO_2 in the process gas, shown in Figure 3. They noted that the absorber is the largest part of the amine system, which is driven by the capture requirement and residence time required to complete capture [7]. Considering a commercially available CO_2 absorber, the capture capacity was found to be linear once CO_2 levels of 10% are reached, but CO_2 concentrations less than 10% are much more influential to absorber diameter [7] . Doubling the CO_2 concentration from 3-6% could have more significant gains on the PCCCS size and cost.

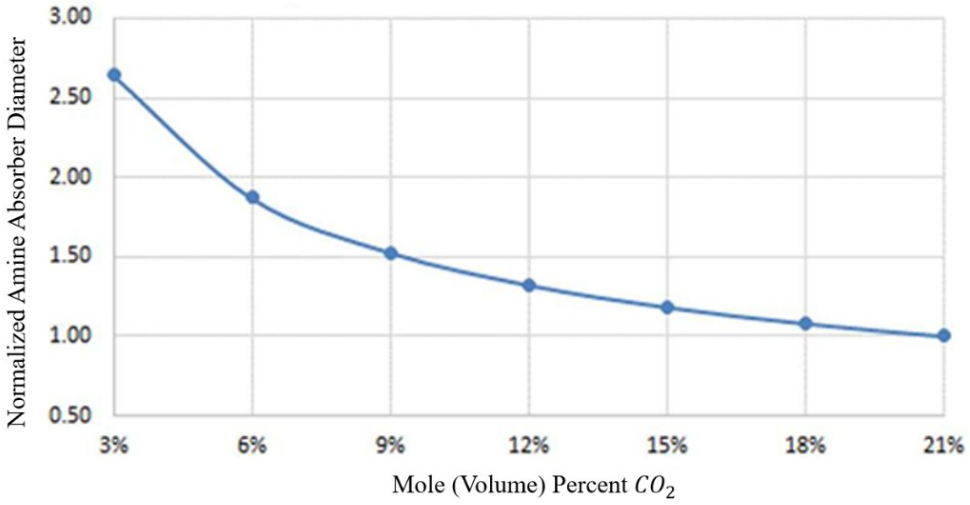

Figure 3: Normalized CO2 capture amine absorber system diameter vs CO2 inlet purity [7]. The plot shows that increasing the CO2 volume percent at the inlet directly relates to a reduction in amine absorber system diameter.

From Figure 3, which shows mole percent CO_2 versus normalized absorber diameter, it is obvious that with a higher percentage of CO_2 in the exhaust flue, a smaller absorber is required for

processing. Furthermore, Sammak et al. found the carbon capture absorber diameter to be determined by flue gas flow and velocity, and packing height determined by the required level of CO_2 capture efficiency [13]. Therefore, a higher concentration of CO_2 in the exhaust gas coupled with a lower flue gas mass flow will result in a smaller footprint, and subsequently cost, of the PCCCS.

1.4 EGR Technology and Use in Post Combustion Carbon Capture

Exhaust gas recirculation (EGR) presents a solution to high capital expenses post combustion carbon capture systems by increasing the concentration of CO_2 at the inlet, thus reducing the mass flow of flue gas, reducing footprint and, subsequently, cost. Figure 4 is a representative EGR cycle, developed by Burnes et al. [7]. It shows air and oxygen mixing and entering the gas turbine engine, with exhaust gas being processed through a water separation unit and being split into two paths: recirculation loop and exhaust and carbon capture processing system.

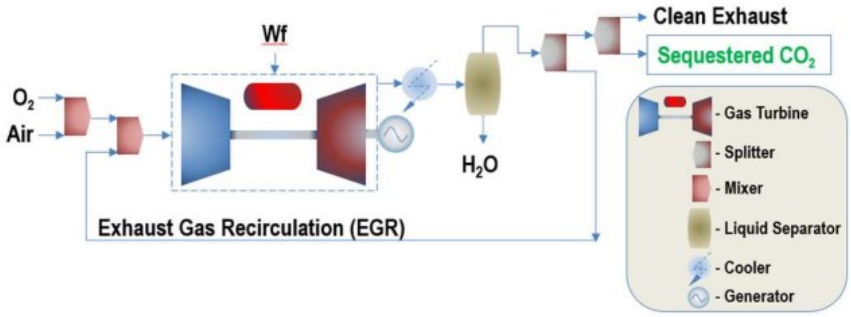

Figure 4: Simplified schematic of EGR/gas turbine system model showing ambient air intake mixing with recirculated exhaust before entering a gas turbine compressor. The Gas turbine exhaust flow exists the turbine and enters a water separator unit, then a mass splitter where some fraction of the exhaust is sent through the recirculation loop and some is sent to another splitter. The final splitter directs gas to a CO_2 sequestration unit or into ambient air [7].

EGR is a common application on reciprocating diesel engines and is used for the purpose of NOx emissions reduction [14], as NOx formation is dependent on peak in-cylinder temperature, and EGR can contribute to temperature reduction. EGR systems typically function by reintroducing a

controlled amount of cooled, dry exhaust gas back into the engine intake, displacing a portion of the incoming air. In industrial applications, EGR systems are commonly comprised of the engine, an EGR cooler, a diverter valve to control the amount of recirculation, and a reentry point.

In gas turbine engines, EGR has potential to greatly increase carbon concentration and reduce NOx in the exhaust. However, as temperature is controlled in GT applications, oxygen depletion with EGR plays a more prevalent role in NOx formation. Burnes et al. conducted a study using a chemical reactor network in Chemkin Pro, a combustion simulation software, to simulate a 16.5 MWe Titan 130 industrial gas turbine operating at full load with 37 ℃ ambient temperature condition, and found that a range of inlet O_2 from 14% to 16% optimal for minimizing NOx levels, shown in Figure 5. Similarly, ElKady et al. found that EGR can reduce NOx production but related it to EGR given a constant relative flame temperature, depicted in Figure 6 [15].

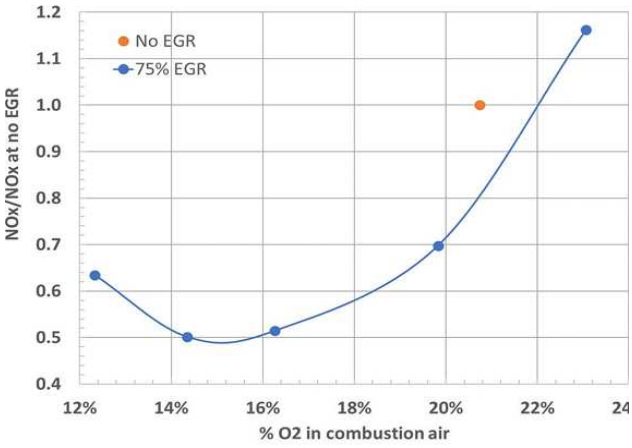

Figure 5: Ratio of corrected (15% O2, dry) actual NOx to NOx at no EGR. NOx dips between 14-16% O2 in the combustion chamber, and then increases at more than 18% [7].

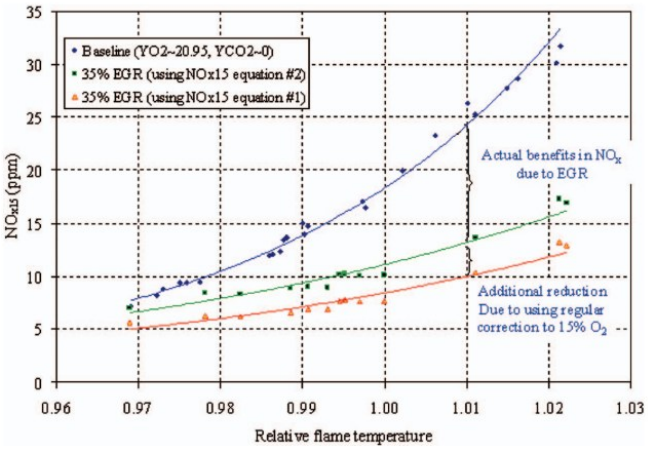

Figure 6: Effect of EGR on NOx as a function of flame temperature, showing 35% EGR reduces NOx ppm in exhaust demonstrated by two calculation methods [15].

From these results we can conclude that EGR has an impact in reducing NOx production, most likely through regulation of available oxygen entering the combustor, as well as localized lower

flame temperatures in the primary reaction zone of the gas turbine combustor as a result of increased dilution. Inverse trends to NOx are seen for CO_2, as EGR is proven to increase CO_2 concentration in the exhaust. ElKady et al. found that 35% EGR resulted in a 50% increase in exhaust CO_2, shown in Figure 7 [15]. Similarly, Burnes et al. found that 50% EGR resulted in a 100% increase in exhaust CO_2, doubling the non-EGR concentration, shown in Figure 8 [7].

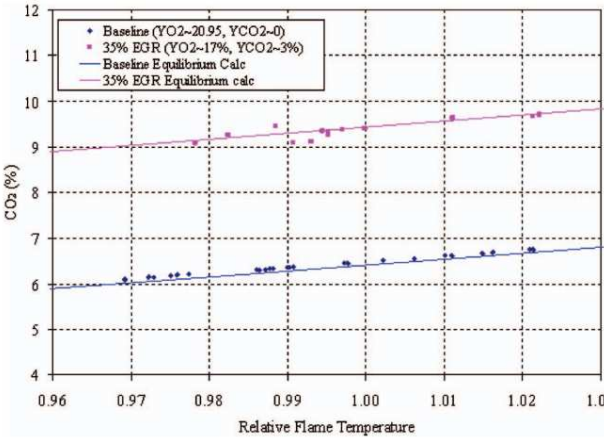

Figure 7: Exhaust CO2 as a function of flame temperature, showing a 150% increase in CO2 in the exhaust at 35% EGR [15].

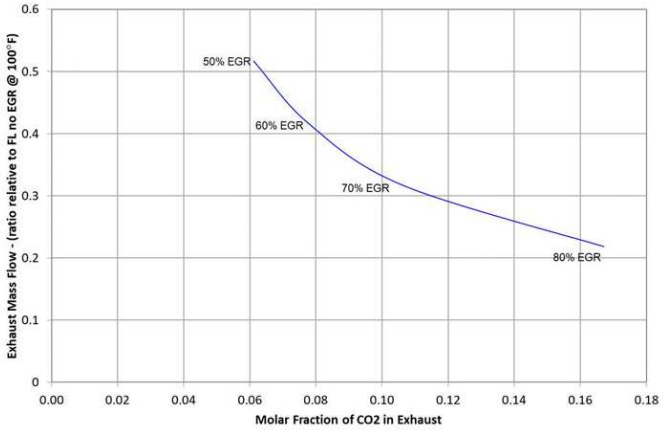

Figure 8: EGR parametric study with 100°F inlet comparing Exhaust mass flow vs Exhaust CO_2 mass fraction for a Cold End Drive Gas Turbine. With increasing EGR%, CO_2 mass fraction increases notably from 0.03 to 0.06 with 50% EGR [7].

As size and cost relate to exhaust composition, Sammak et al. found that EGR reduces the size and cost of the flue gas cleaning system, estimating a 7% reduction in overall CCP cost at just 30% EGR [13]. The main factors in the reduction in size and cost are the increased CO_2 concentration in flue gas and reduced volume of gas to be processed through the carbon capture system because of EGR.

While EGR is proven to increase CO_2 in the exhaust stream, it also reduces O_2 levels both in the exhaust and at the inlet by displacing ambient air with combustion products, of which oxygen is consumed at stoichiometric conditions. Lowered oxygen levels can impact proper combustion,

even leading to blow out. It is advantageous to find the maximum recirculation capacity to maximize CO_2 concentration without depleting O_2 levels below acceptable inlet requirements. There exists some literature that defines minimum O_2 levels for robust combustion maintenance with EGR [15].

Elkady et al. conducted their experimental studies with an oxidizer composition of 3% CO_2, 17% O_2 and 80% N_2 to simulate 35% - 40% EGR on a single dry low NOx (DLN) nozzle combustor with the conditions of General Electric's F-class heavy duty gas turbines [15]. They found lower oxygen levels correspond to higher fuel to oxidizer ratios and less consumption of CO, resulting in high CO emissions due to flame starvation [15], and therefore set O_2 levels at the stated percentage. Burnes et al. found that an EGR limit of 50% is required to maintain robust combustion. The red band in Figure 9 denotes the approximate range of O_2 level where robust combustion can be sustained and should not be exceeded without the addition of supplemental O_2.

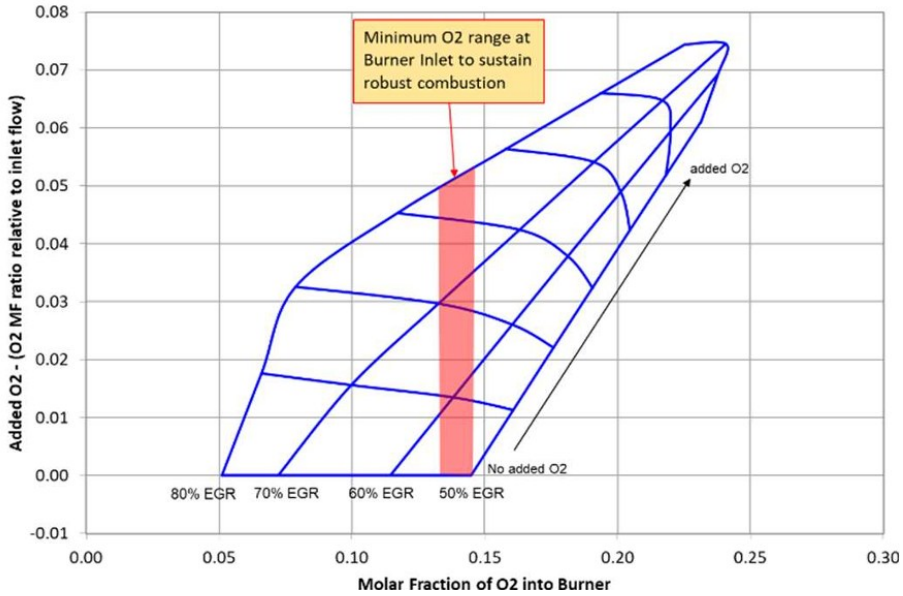

Figure 9: EGR parametric study with 100°F inlet modeling supplemental O_2 vs O_2 mass fraction (MF) into the burner for cold end drive gas turbine system [7].

Introducing the carbon capture system as a retrofit application to an existing GT power plant or industrial facility is a competitive method of point source decarbonization, however the additional load required to run the carbon capture systems - amine-based absorption in this particular study - can reduce overall efficiency. Fortunately, opportunities exist to offset the power loss in carbon capture system operation, including bottoming cycles and boiler systems, as it is already necessary to cool the exhaust for integration with carbon capture systems [13]. Gülen and Hall [16] studied the system efficiency and cost of gas turbine combined cycle (GTCC) systems designed to optimize post combustion carbon capture. They found that by combining two bottoming cycle modifications with high supplementary firing in the heat recovery steam generator (HRSG) and recirculating HRSG exhaust gas, it is possible to achieve a nearly 65% reduction in CO_2 capture penalty and 35% reduction in capital cost when compared to an existing gas-fired GTCC power plant with post combustion capture [16]. When considering a retrofit of a single cycle gas turbine to increase carbon capture feasibility, HRSG bottoming cycles present a feasible opportunity to reduce operational and capital cost. This work will consider HRSG opportunity in the EGR system, utilizing the heat recovery cycle in dual purpose at the heat recovery point. The heat from the exhaust flue will be transferred to the HRSG system for steam turbine power, leaving the processed flue cooled for recirculation into the inlet of the gas turbine. An alternative use of the exhaust flue waste heat might be in a boiler system, which could provide an opportunity for hot water generation or other applications that can directly integrate onboard navy vessels.

The literature circulating on EGR and its application in optimizing PCCC is mostly limited to theoretical studies and analyses. In 2009 General Electric published a study describing experimental work evaluating the performance and risks of using DLN technology in EGR. They developed a research combustor to explore the performance of nozzles operating in low O_2

environments, and used N_2 and CO_2 to simulate EGR conditions. They found that up to 35% EGR, GT combustors can operate with high efficiencies and can determine CO_2 levels of more than 10% by volume, but that EGR levels are limited by CO emissions regulation [15]. In 2014 GE published a patent on power generation system utilizing EGR and a HRSG bottoming cycle [17]. Another GE publication presented in 2025 showed the analysis of EGR in its ability to improve and enable a post-combustion carbon capture plant with the natural gas combined cycle [13] using Promax and Aspen Process Economic Analyzer. They referenced an earlier (2024) Front End Engineering Design study [18] analyzing the design to retrofit an existing electric generating plant in Bucks, Alabama with carbon capture and combined cycle technology. Thielens et al. conducted experimental studies on a MTT EnerTwin micro gas turbine with power generation on the 1-3.2 kWe scale, adding an external EGR loop to the micro GT and finding exhaust CO_2 concentration to reach up to 7.9% at 84% EGR with a notable reduction in NOx emissions, and limitations being combustion instability and CO production [19].

1.5 Objectives and Overview

Carbon emissions have been presented as a major contributor to global emissions, and require immediate, urgent action to greatly reduce or eliminate them. Carbon capture presents an opportune technology for reducing point source emissions from power plants and naval vessels, but complications are presented in the low carbon percent in the exhaust relative to total mass flow specifically for gas turbine carbon capture applications. It has been proven in the literature that exhaust gas recirculation can increase carbon concentration in the exhaust, which directly reduces the size and cost of carbon capture systems. Detrimental impacts of EGR on plant efficiency can be managed through use of combined bottoming cycles or offset with carbon credits and reuse.

The preceding review of the existing literature on EGR and gas turbines shows that many studies conducted are limited to modeling and design analysis of combined cycle systems, while experimental research is limited to micro turbine generators on the scale of 30-200kWe [20] with low pressure and temperature ranges [19] that make extrapolating data to represent full scale GT, which is of interest in this study, unreasonable.

It is crucial to understand EGR implications on single cycle gas turbine engines and their overall plant footprint and operational limitations. The objective of this thesis is to address the implication of EGR on single cycle gas turbine engines for the purpose of improved post-combustion carbon capture and investigate alternative EGR strategies and methods that can facilitate testing of EGR when research establishments are resource or size limited. With this context in mind, the research objectives are as follows:

- Explore the design and analysis of retrofit EGR systems to be applied to existing gas turbines for the purpose of improved carbon capture.
- Design a surrogate EGR system for large scale testing and validation of EGR in affecting exhaust CO_2 concentration on a GT engine.
- Construction of a test facility to investigate EGR on overall engine performance to aid subsequent versions of EGR system modeling.
- Analyze various model types for both actual and surrogate EGR while considering limiting operational obstacles in real-world applications.

The contents of this document are as follows: Chapter 2 describes the experimental methods, including the system configuration, the combusted gas composition used for modeling, and an overview and definition of each flow model simulation. Chapter 3 presents the results of the recirculated EGR model including heat exchange options and requirements and flow

redirection methods. Chapter 4 presents results of the surrogate EGR simulation study, namely the gas flow and pressure requirements for each surrogate gas, and the associated piping system configured to the research facility. Chapter 5 presents the design process and completed manufacturing work contributed toward final commissioning of the exhaust system for the Centaur 40. Finally, Chapters 6 and 7 will summarize simulation conclusions as well as offer recommendations for future work.

CHAPTER 2 – METHODS

2.1 Experimental Methods

The flow schematic of the gas turbine engine assembly with a fully cooled EGR system is pictured in Figure 10. The schematic incorporates fuel supply and skid, the gas turbine, and CCS system, as well as the EGR system including a heat exchanger, variable exhaust gas diverter, recirculation loop, and mixer. This network represents the EGR and CCS unit as it would be applied in the real world.

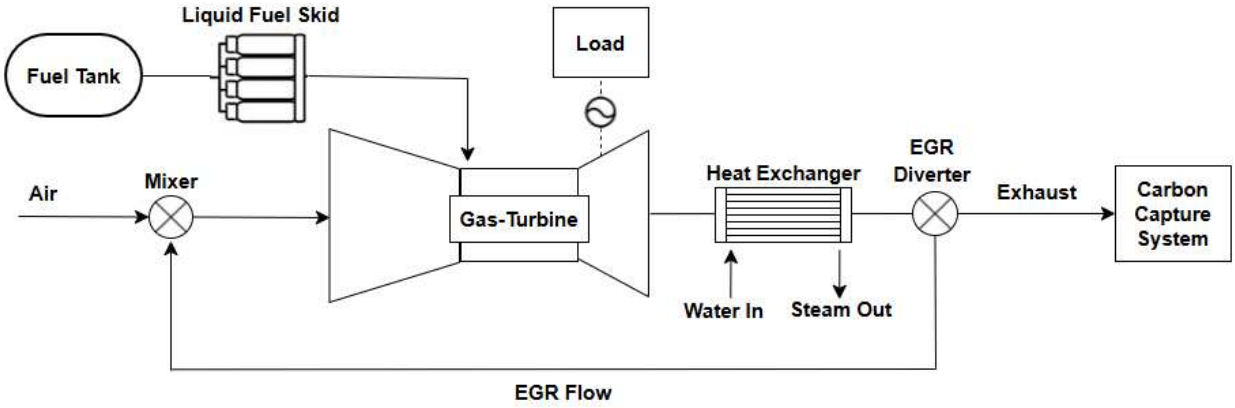

Figure 10: Flow chart of actual EGR schematic modeled in this study, showing inlet air mixing with recirculated exhaust, entering the gas turbine and exhausting into a heat exchanger, before splitting between the EGR recirculation loop or carbon capture system.

Determining the location of the system components is dependent on the goals of the system. Various configurations are possible when utilizing EGR, but for integration with a CCS system, full variability of EGR percentage, and to optimize heat recovery processes, the prime orientation is demonstrated in Figure 10 and examined in this paper.

In Figure 10, the entirety of the exhaust gas is cooled before the diverter valve. The recirculating exhaust gases should be cooled as low as possible, ideally to ambient temperatures, to avoid excessive reduction in gas turbine performance [12] and to integrate with the CCS unit,

which requires inlet temperatures in the range of 45°C-55°C [13], or depending on carbon capture technology. Additionally, maximum heat recovery opportunity exists through cooling the full exhaust flow prior to parting off for recirculation. Cooling the exhaust gas to target temperatures will result in water drop-out thus avoiding excessive moisture damage when exhaust gases enter the engine [21] and excessive heat damage from exhaust gases entering the CCS equipment. Condensed water can be collected after the heat exchanger in real world applications, as is simulated in this study. After cooling, a diverter valve splits the exhaust stream into flow that is recirculated and flow that is directed to a generalized CCS system. In some cases, the diverter may need to be assisted by an auxiliary fan to achieve the desired recirculation rates.

Note that it is not within the scope of this work to analyze CCS system type or performance or gas turbine combustion, merely the upstream gas handling practices. Previous studies have discussed the impact of EGR on combustion characteristics and CCS system behavior with flue gas composition. For more information on the mixing component of the system, reference Jeremiah, Harrod, et al. [22].

A surrogate EGR system offers an alternative to the demands of recirculating, cooling and treating hot exhaust gases required for actual EGR. In marine applications, the cooling requirements are more reasonable, given the abundance of seawater. However, in the lab setting, and other applications where the presence of a large thermal sink is impossible, the cooling capacity may be difficult and expensive to achieve. A more feasible study may be to simulate the EGR using surrogate gases – specifically, the direct introduction of bottled CO_2 and additional N_2 into the engine intake. The volume of surrogate gases required to simulate EGR in this way is substantial, but combustion characteristics and engine performance can be assessed without the previously stated demands of true EGR loop.

The envisioned surrogate EGR system is depicted in Figure 11. Here, the heat exchanger and recirculation loop depicted in Figure 10 are replaced with a surrogate gas supply and blending skid.

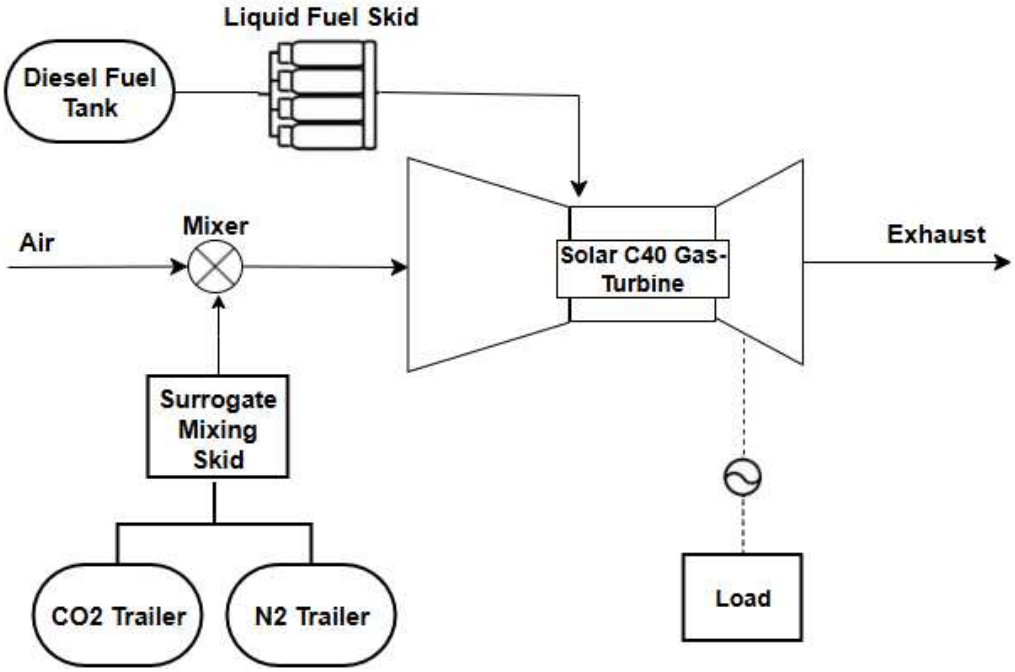

Figure 11: Flow chart of surrogate gas EGR schematic as is modeled in this study, showing ambient air inlet mixing with surrogate gases mixed and vaporized, entering the gas turbine and exiting through the exhaust.

The surrogate gas system consists of a reservoir for each gas, labeled as CO_2 trailer and N_2 trailer in Figure 11, as well as the surrogate gas mixing skid, which includes gas processing/handling components such as electrically heated vaporizers and an EGR/air mixer. Vaporizers are required to change both surrogate gases from liquid to gaseous phase to allow proper mixing with ambient intake air. Both CO_2 and N_2 will be delivered in liquid form due to the high-volume requirement for the surrogate system, which requires the gases delivered in their most dense form (liquid) to allow for maximum time capacity during an experimental test.

2.2 Experimental Equipment

Figure 12: Solar Centaur 40 3.5 MWe gas turbine engine in research facility located at CSU powerhouse energy campus.

Figure 12 depicts a Solar Turbines Centaur 40 gas turbine in the process of commissioning. This engine is rated at 3.5 MWe and is equipped with dual-fuel SoLoNOx injectors permitting operation on natural gas, diesel, and a variety of alternative fuels. The Centaur 40 engine contains an 11 stage axial compressor with a 10:1 pressure ratio, an inlet airflow of 18.7 kg/s, a 3 stage clockwise reaction turbine, a 445°C exhaust temperature, and a 12910 kJ/kWe-hr heat rate [12]. The engine is coupled to a 13.8 kV 60 Hz generator and the power produced will be dissipated by resistive load banks. Since it is entirely independent from the electrical grid and the university does not rely on the unit for its own power demand, it will be dedicated solely for research purposes, allowing for singular test flexibility. The simulation results presented herein will inform the design and implementation of EGR delivery systems on this Centaur 40 unit for future experimental studies.

2.3 Modeling Software Selection

Flownex is a simulation environment that enables the study of flow and heat transfer systems and how they will behave in application. Flownex is used in this study to evaluate the feasibility of EGR in the lab environment and design the EGR delivery system. Existing case studies use Flownex simulation environment to solve heat transfer and flow related issues including a study on a Gas Turbine combustor design [23], a Combined Cycle Power Plant [24], as well as journal publications such as K. Zolińska et al. on the study of waste heat recovery using the Flownex plate heat exchanger element [25], and Muksin et al. in their simulation coupling Flownex and LabVIEW to study an experimental power reactor [26].

2.4 Ambient Conditions and Combustion Composition

The following assumptions are made to simplify simulations in this study:

- Inlet and outlet pressure conditions will be considered as atmospheric for CSU's research facility at 84 kPa.
- Ambient air humidity is neglected.
- Ambient Temperature is 20 °C.
- Combustion composition for the fluid in simulations is determined by a combustion model depicted in Figure 13.
- The GT inlet mass flow is 18.7 kg/s.
- The GT pressure ratio is 10:1.

Two fuels will be modeled in Flownex, one being a standard composition of natural gas according to the North American Energy Standards Board, and one a representative of diesel fuel. As mentioned in Chapter 1, natural gas is a primary fuel used in gas turbine power production. As

such, its chemical composition is utilized to perform realistic simulations in this study. It is well known that natural gas composition varies throughout the vast U.S. pipeline network. The composition utilized in the following studies will be a direct replication of the composition dictated in Table 1.

Table 1: Chemical composition of Natural Gas, outlining the union gas system and typical ranges for these values, which accounts for variance from different sources [27].

Component	Typical Analysis (mole %)	Range (mole %)
Methane	94.9	87.0 - 96.0
Ethane	2.5	1.8 - 5.1
Propane	0.2	0.1 - 1.5
iso - Butane	0.03	0.01 - 0.3
normal - Butane	0.03	0.01 - 0.3
iso - Pentane	0.01	trace - 0.14
normal - Pentane	0.01	trace - 0.04
Hexanes plus	0.01	trace - 0.06
Nitrogen	1.6	1.3 - 5.6
Carbon Dioxide	0.7	0.1 - 1.0
Oxygen	0.02	0.01 - 0.1
Hydrogen	trace	trace - 0.02
Specific Gravity	0.585	0.57 - 0.62
Gross Heating Value (MJ/m^3), dry basis *	37.8	36.0 - 40.2

Natural gas is the main fuel used for land-based power generation, but its composition varies depending on supplier and location. For simulation purposes, a fuel was created in Flownex with the chemical composition cataloged in Table 1.

The mole percent listed in Table 1 was converted to mass fraction using molecular weights of the species and mixture and their relationship as expressed in [28], solved in EES.

Equation 1 $$Y_i = x_i MW_i MW_{mix}$$

Diesel fuel is modeled as its combustion products, solved by a simple combustion balance combusting the chemical formula diesel $C_{12}H_{23}$ with air, assuming stoichiometric conditions.

Table 2: Diesel combustion products for simulated exhaust composition with no EGR as mass fraction.

Species	Pre-Cooled Exhaust Gas
H_2O	0.0210
Ar	0.0127
CO_2	0.0520
N_2	0.7440
O_2	0.1690

Each fuel will be processed through a recirculation model in Flownex with a combustion component to determine recirculation composition utilized, shown in Figure 13. To validate the combustion component in determining exhaust composition with EGR, CO_2, O_2, and NOx values will be compared to values accepted in literature, namely the studies mentioned in Chapter 1.

Label	Description
1	Ambient Air Intake
2	Mixer
3	Compressor
4	Fuel Injection
5	Combustion Chamber
6	Turbine
7	Turbine Outlet
8	Splitter
9	Exhaust/CCS
10	Fluid Conversion
11	Heat Exchanger
12	Water Separator
13	Fluid Conversion

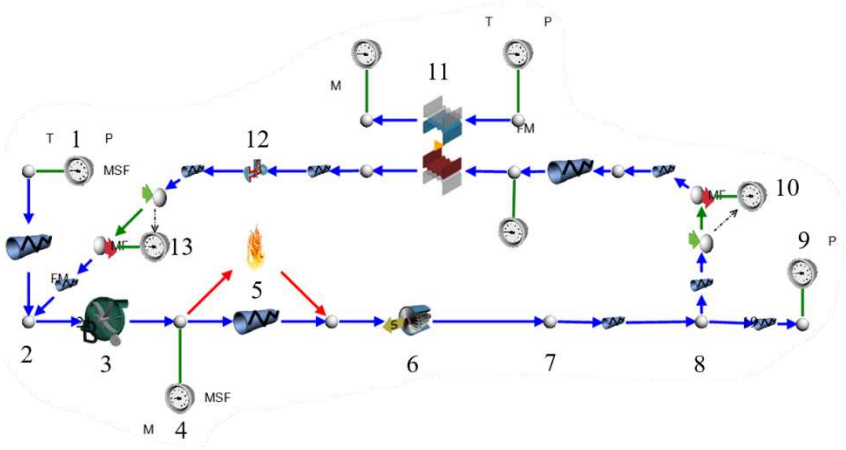

Figure 13: Flownex model of EGR recirculation loop with chemical reaction component. Model replicates gas turbine compressor, combustion chamber, and turbine to provide accurate combustion product compositions for EGR.

Figure 13 shows the Flownex model used to determine combustion composition for input into subsequent simulation studies. This model was validated by utilizing known inlet and outlet conditions of the gas turbine to characterize each component using the “change design” feature in Flownex. Given a constant mass flow, outlet temperature, and pressure ratio found in the Solar Turbines Centaur 40 specification sheet [12], boundary conditions (BC) are set. Using the designer feature to maintain outlet temperature while solving various conditions, such as combustion chamber outlet temperature and fuel injection mass flow, allowed the characterization of the compressor, combustor, and turbine in the system. In an effort to reduce complexity of the system and focus on the combustion characteristics recirculation loop was added with dimensionless components rather than geometric pipes to simplify system, and the recirculation loop was split, only cooling the recirculated gases with the simplest heat exchanger component.

The combustion chamber was modeled with a custom loss component- set to 0.1 flow admittance, and a CEA adiabatic flame chemical reaction component. The CEA adiabatic flame element calculates the exhaust composition and maximum temperature for a chemical reaction given the chemical composition specified [29]. The CEA element reactions are calculated with a secondary program, the NASA-Glenn Chemical Equilibrium program CEA2 [29].

2.5 Actual EGR Modeling

As depicted in Figure 10, the EGR schematic consists of an ambient air entry, mixer, gas turbine, heat exchanger, and exhaust recirculation splitter. The gas turbine will not be modeled in this section, as the focus is at the recirculation system level and the gas turbine sequence adds unnecessary complexity.

The EGR model is a representation of the real-world conditions. Figure 14 depicts the baseline EGR model with indirect cooling, water drop out, and fan simulated redirection. Each component is labeled with a number, which is described in Table 3.

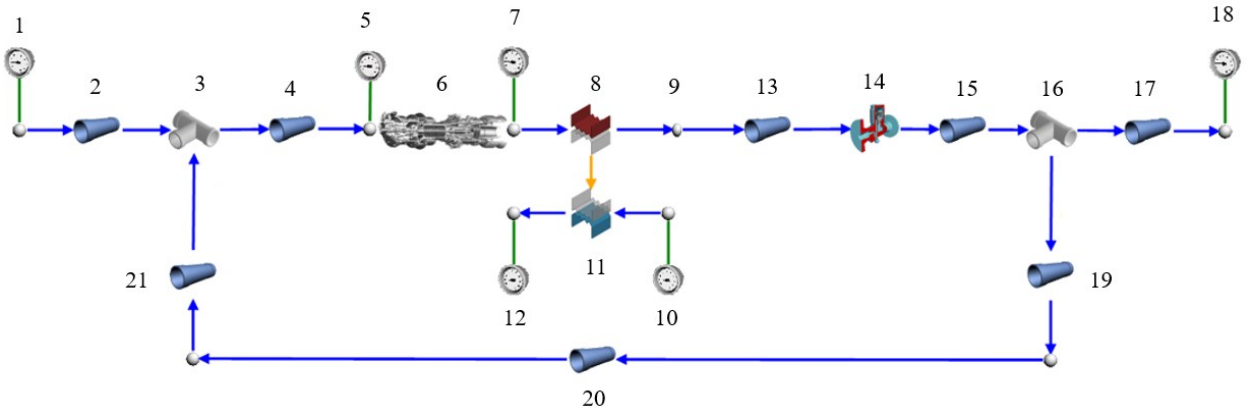

Figure 14: Actual EGR Flownex Model with component descriptions corresponding to Table 3.

Table 3: Actual EGR Flownex Model Indicator Chart Corresponding to Figure 14.

Label	Description
1	Ambient Air Intake
2	Intake Duct
3	Mixer
4	Intake Duct
5	Compressor Inlet Boundary Condition
6	Centaur 40 Gas Turbine
7	Turbine Outlet Boundary Condition
8	Heat Exchanger Primary
9	Heat Exchanger Outlet Node
10	Cooling Water Inlet
11	Heat Exchanger Secondary
12	Heat Exchanger Outlet
13	Exhaust Ducting
14	Water Separator
15	Exhaust Ducting
16	EGR Diverter
17	Exhaust Ducting
18	Ambient Exhaust/ CC Inlet
19	EGR Loop Ducting
20	EGR Loop Ducting
21	EGR Loop Ducting

The application-based EGR system was modeled with a heat exchanger, recirculation diverter and fan, and re-entry mixer. The applied EGR system Flownex model depicted in Figure 14, illustrating the full circulation loop and indicating where the gas turbine is placed along the circuit. The model is a simplified representation of the recirculation system and therefore does not include an active gas turbine component. However, the exhaust composition at point 7 in Figure 14 is set to represent the first cycle exhaust composition before recirculation, as described in Table 2 which imitates the role of the turbine at the first cycle.

2.5.1 Heat Exchangers

The heat exchange component is a major factor in the full EGR system. Two methods of cooling exhaust gas will be considered in this work: (1) indirect cooling and (2) direct contact cooling using a bulk air cooler. Indirect cooling presents opportunity for heat recovery steam generation, which can increase system efficiency by providing additional power generation from the exhaust flow. Direct contact cooling is known to have a high heat transfer rate but is associated with other complications such as fully saturating the exhaust air and requiring a large water makeup flow due to evaporation and drift.

To understand a reasonable footprint requirement for a heat exchanger in this application, a manufacturer was contacted to provide a size and cost estimate for the specified cooling range. The heat exchanger design is theoretically able to cool the exhaust gas from 445 °C to 35 °C with a fin-tube heat exchanger with a footprint of about 10x10 feet for the price of $215,000. This standard will be kept in mind for comparison to heat exchangers designed in this study.

First, we will consider indirect cooling through the generic heat exchanger element in Flownex, pictured in Figure 15.

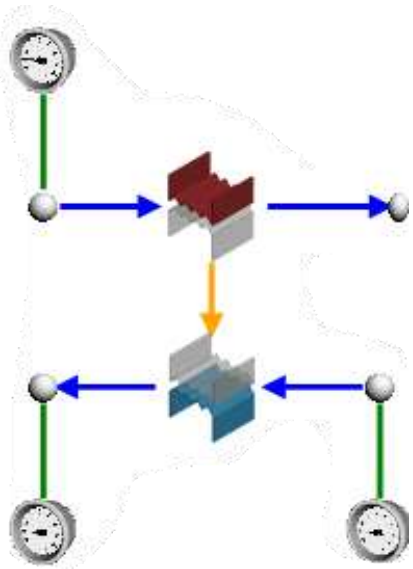

Figure 15: Indirect Contact Cooler Flownex Model showing the generic heat exchanger element.

This heat exchanger model is used when the geometry is unknown and calculates heat transfer using the effectiveness-NTU method [29]. The generic heat exchanger serves as the initial model and is modeled to process dry air through the primary component.

Another form of indirect cooling model is the fin-tube heat exchanger element in Flownex. Fin-tube heat exchangers are commonly used in water-air heat transfer. Air typically passes through the fin side of the heat exchanger, where the fins increase the available surface area to increase heat transfer.

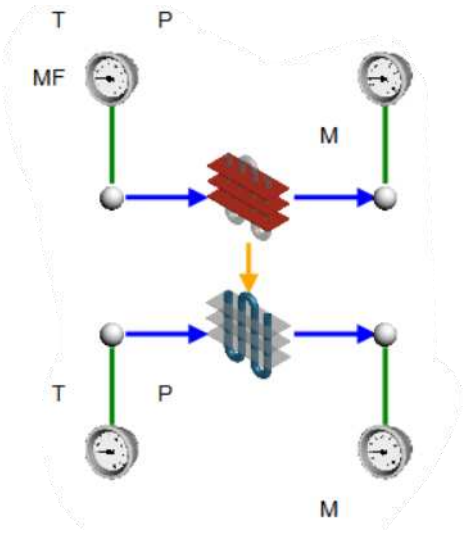

Figure 16: Fin-tube heat exchanger element model in Flownex simulation Environment.

This method of indirect cooling provides an opportunity for steam recovery since the air flow and water coolant do not mix. Therefore, the entirety of the steam produced can be directed to a recovery unit. The finned-tube heat exchanger element is modeled in a discretized fashion rather than a lumped system, or as a series of many heat transfer components [29].

Direct contact cooling is modeled using the bulk air cooler element in Flownex. Direct contact cooling is a common practice in industrial heat transfer. In direct contact coolers, water is injected near the top of a container. The water can be injected as a film or, more commonly because of the difficulty of maintaining film condition, a spray. The spray interacts with splashboards near the top of the cooler, called packing, to increase the surface area contact between water and air. The packing determines the heat exchange capability of the setup. The hot exhaust air enters the cooler near the bottom of the package. Cooling towers can be natural draft towers or forced draft, the later being more common as well as effective. In forced draft towers, fans can be located either at the top or the bottom of the cooling tower.

The bulk air element available in Flownex is modeled using the factor of merit model, rather than the Merkel method which is used in the similar cooling tower method. Common F values in the factor of merit calculation are listed in Table 7.

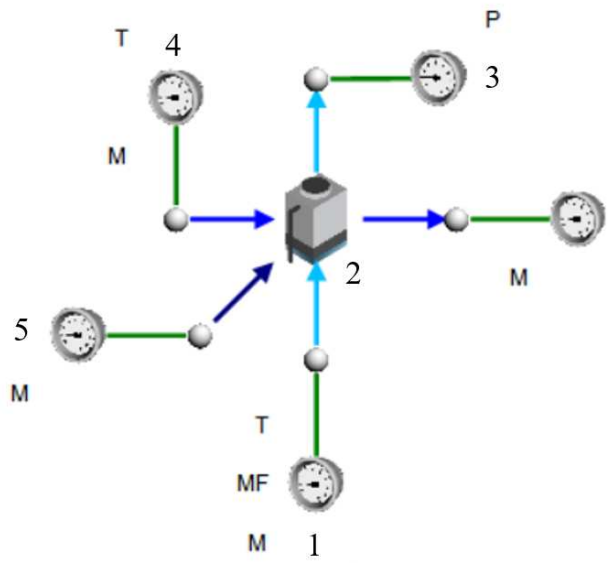

Figure 17: Bulk air cooler complex system modeled in Flownex.

Table 4: Bulk Air Cooler Flownex Model Indicator Chart Corresponding withFigure 17.

Label	Description
1	Hot Exhaust Air
2	Bulk Air Cooler
3	Cooled Exhaust Air
4	Cooling Water Injection
5	Makeup Water Inlet
6	Cooling Water Outlet

The required water makeup for the cooling system is calculated using the designer feature in Flownex. The designer feature allows the user to solve for one independent variable, while proving a range of values for the associate dependent variable.

The direct contact cooler in this study will be simplified and modeled as water injected directly to air flow for use in full recirculation systems. Modeling direct contact cooling in this manner allows for additional fluids to be used, as the bulk air cooler fluids are restricted to two-phase H_2O and a mixed Steam-water-air fluid.

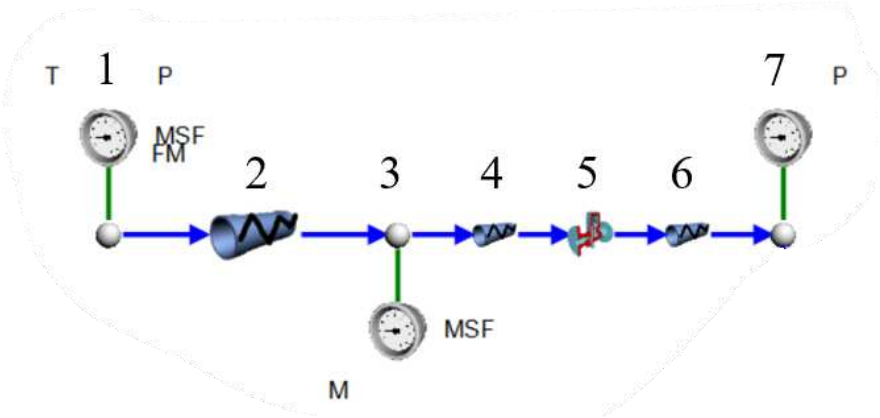

Figure 18: Simplified Direct Contact Cooler Flownex Model.

Table 5: Direct Contact Cooler Flownex Model Indicator Chart Corresponding to Figure 18.

Label	Description
1	Hot Exhaust Flow
2	Exhaust Ducting
3	Direct Contact Water Injection
4	Exhaust Ducting
5	Water Separator
6	Exhaust Ducting
7	Mixer Point EGR & Intake
8	Intake Ducting
9	Ambient Intake Air

Table 6 explains each component in the simplified direct contact cooler model depicted in Figure 18.

.

Table 6: Typical F value in Factor of Merit Model Calculation for Heat Exchange [29].

Type of tower/chamber	Typical F
Vertical Towers	
No packing:	
High water loading	0.5 - 0.6
Low water loading	0.6 - 0.7
With packing:	
High water loading	0.55 - 0.65
Low water loading	0.65 - 0.75
Industrial packed tower	0.7 - 0.8

2.5.2 Cooling water

Cooling exhaust gas comes with auxiliary concerns. The cooling water for a closed cycle system must enter through a secondary cooler after it passes through the exhaust stream. All the previously stated cooling methods will need a chiller for the cooling fluid in the closed loop system. Direct contact cooling will require the additional consideration of make-up water to replace evaporated cooling fluid. The cooling water heat load will be studied in a parametric table, based on the universal heat transfer Equation 2.

Equation 2 $$Q = m * C_p * dT2$$

2.5.3 Redirection methods

Splitting the gas flow between recirculating back to the inlet or exiting to the carbon capture system is an important consideration. Two methods of EGR redirection will be analyzed: (1) blower/fan component and (2) orifice driven pressure differential.

The blower presents an obvious option for flow redirection. They are readily available off-the-shelf components with an extensive selection of flow rates and pressure drop.

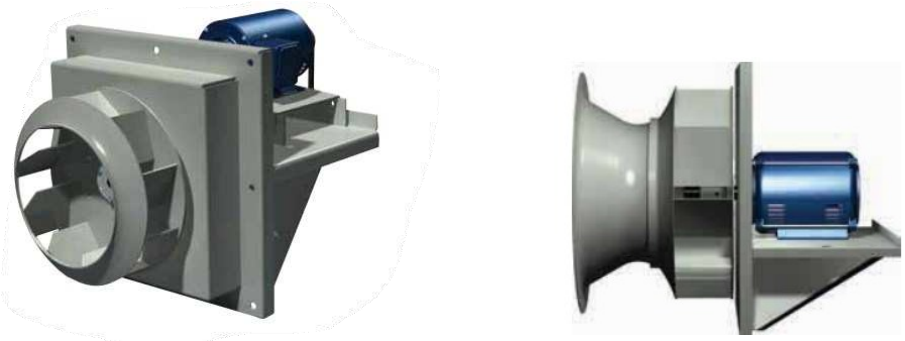

Figure 19: Greenheck centrifugal industrial blower designed to operate in a broad range of applications including clean and hazardous air. PLG model with 900-71,000 cfm capacity and up to 8 in wg allowable [30].

While blowers are common in industrial applications and readily available for system integration, they can present challenges. The presence of water in the exhaust flow may present problems, especially with electric motor configurations. Even with belt driven blowers, water and exhaust particulates can compromise the fan blades. Additionally, blowers in the exhaust flow present a parasitic power load on the overall system, which can diminish the overall efficiency. Lastly, complications with startup or maintenance of the fan can complicate the EGR process.

An alternative to using a blower for flow redirection is to use an orifice along the EGR loop to create flow restriction, ultimately causing the desired flow diversion. This method would require a remotely controlled, variable capability valve for remote control of a variable EGR system. The need for variability is a demand from both lab setting testing and from industrial level plants, to allow for response to changing demands of the plant.

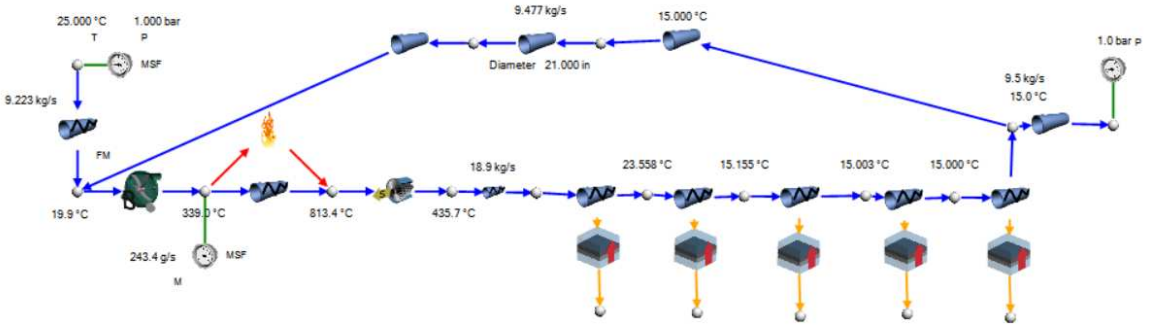

Figure 20: EGR Flownex model using orifice to regulate pressure differential and flow through the system. Orifice located at the center of the EGR loop.

If the desire is for variable EGR flow capability, then an actuated, proportional control or automatic valve would be necessary for the system. Controlling EGR redirection through flow restriction would also influence outlet velocity, which must be considered when choosing the post combustion carbon capture system, as flow velocity is a driving factor in size specification.

Alternatively, if one fixed EGR rate is desired, a simple nozzle or flow restrictor could set the EGR rate given fixed exhaust mass flow.

2.5.4 Opportunity for HRSG with steam production

Heat recovery steam generation (HRSG) is a common application used in many power plant setups. HRSG provides and avenue to improve plant efficiency through heat reclamation and reuse in powering a bottoming cycle turbine. High cooling loads present opportunity for HRSG use and will be evaluated in this study. The quality and volume of cooling water post exhaust cooling will be measured and analyzed to determine HRSG opportunity for the different cooling methods analyzed through a parametric table. By adjusting cooling mass flow as the independent variable, the dependent variable quality will vary as well, allowing determination of the maximum amount of steam as a function of cooling water mass flow.

2.6 Surrogate EGR Modeling

2.6.1 System Components and Given Parameters

The surrogate EGR apparatus was designed with vaporization, mixing, and flow control capabilities to approximate actual exhaust gas composition prior to injection into engine intake. The fluid model is a mixture of air and EGR, which is comprised of CO_2 and N_2. Figure 21 illustrates a simple model of the surrogate system, with component representations called out in

Table 8. This model informs required surrogate delivery gas pressures and pressure drop throughout the system for various pipe sizing cases.

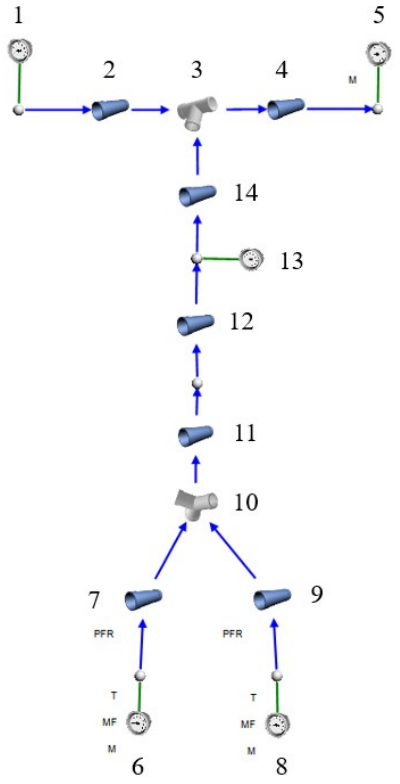

Figure 21: Surrogate EGR Flownex Model.

Table 7: Surrogate Gas System Flownex Model Indicator Chart Corresponding to Figure 21.

Label	Description
1	Ambient Air Intake
2	Intake Ducting
3	Mixer
4	Intake Ducting
5	Compressor Inlet Boundary Condition
6	CO_2 Trailer Exit Boundary Condition
7	Gas Piping
8	N_2 Trailer Exit Boundary Condition
9	Gas Piping
10	Surrogate Gas Mixer
11	Gas Piping
12	Diffuser Pipe
13	Surrogate Gas Inlet Boundary Condition
14	Gas Piping Connector to Mixer

The ambient air intake is fixed in the model at mass flow 14.44 kg/s, and temperature 20°C. The compressor inlet is set to a mass flow rate of 18.7 kg/s, according to manufacturer

specifications [12]. The mixed surrogate gas mass flow rate at point 10 is set to 4.26 kg/s. Although the model is considered a 50% EGR case, in which an even split between EGR and intake air might be assumed to conserve mass flow at the compressor inlet, the surrogate system uses some percentage of ambient air to supplement the bottled gas requirement by supplying the combined oxygen content from the air intake and the EGR streams. Hence, the mass flow rates of ambient intake air and surrogate gases are 14.44 kg/s and 4.26 kg/s, respectively.

At the vaporized gas inlet points 6 and 8, the gas temperature and flowrate are fixed. The flowrate is fixed to represent surrogate requirements depicted in Figure 32 Figure 33 and will be controlled by upstream regulators. The temperature is specified by vaporizer values and the pressure was solved with the restricted range of existing vaporizer technology. The two gases blend at the surrogate gas mixer, which is modeled as a pipe Y-junction at point 10. The flow is mixed at pipe 11 where it travels 100 feet [30.48 meters] into the building. Pipe 12 models a cone shaped diffuser, where the pipe grows from its size at point 11 to the ideal mixing diameter, presented in §3.3 of Jeremiah, Harrod, et al [22]. At the mixer, the surrogate gas blend converges with ambient air and flows into the compressor at the specified mass flow rate 18.7 kg/s.

CHAPTER 3 - RESULTS OF ACTUAL EGR MODEL

Chapter 2 discussed assumptions, conditions, and methods for all of the simulation studies. Chapter 3 will discuss the results of those studies and their implication at the system level.

3.1 Combustion Model

The combustion model in Figure 13 is set to approximate the Solar Turbines Centaur 40 engine compressor, combustor, and turbine. Using the CEA adiabatic flame chemical reaction element to combust a typical chemical composition of natural gas, the results in Table 9 are found for 0% and 50% EGR.

Table 9: Composition Results of EGR Loop with Chemical combustion component for Natural gas fuel.

Component	0% EGR	50% EGR
Carbon dioxide	0.031939	0.056966
Nitrogen	0.759347	0.724823
Nitric Oxide	0.000087475	0.000086614
Nitrogen Dioxide	0.000010021	0
Oxygen	0.18314	0.12113
Water	0.025477	0.096994

The 50% EGR case is similar to the composition found in literature. At 0% EGR the concentration of CO_2 in the exhaust is about 3%, which is similar to findings both in Burnes et al. [7] and findings of the Centaur 40 offsite testing results shown in Figure 2. At 50% EGR, the fraction of CO_2 in the exhaust multiplies by a factor of 1.78, nearly double the non EGR case, which is also similar to the findings in Burnes et al. [7] of nearly doubling the concentration. The

~10% error in the Flownex model versus other literature studies is likely due to inaccuracies in the element characteristic setting process. However, the relative similarity in CO_2 change validates the model as accurate for use in the simulation experiments conducted in this thesis.

3.2 Actual EGR System Model

The purpose of the actual EGR Flownex model is to assess the practicality of the applied system and determine the feasibility of conducting full scale experiments on a Centaur 40 gas turbine. Key parameters informing these assessments are the pressure loss in the turbine exhaust, the cooling load required, the EGR diversion valve design and auxiliary fan power, and fluid composition and vapor quality.

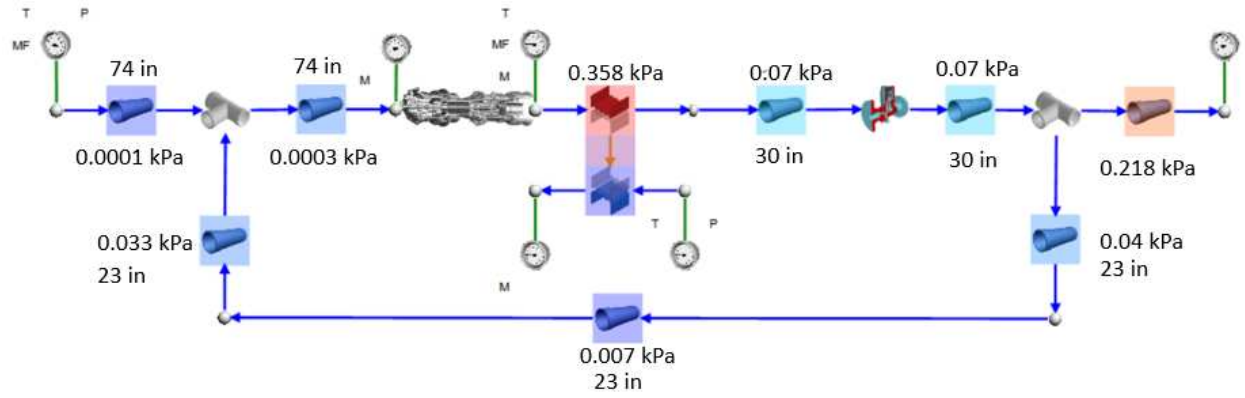

Figure 22: Real EGR System with indirect cooling using a generic heat exchanger pressure drop.

Shown in Figure 22 is a breakdown of the pressure throughout the system. It was necessary to maintain within the maximum pressure drop threshold, as specified by the OEM . This study found that the total pressure drop across the system was 0.658 kPa. This is well within the manufacturer's allowable pressure drop limit; therefore, the designed ducting geometry would be an acceptable feature in an EGR system for this GT.

3.3 Bulk Air Cooler

Validity of the bulk air cooler component is restricted to a maximum air inlet temperature of 373°C, as the critical point of water is at 374°C. Despite the actual turbine outlet temperature being 445°C, the exhaust outlet temperature is modeled at the maximum allowable temperature. This gives a sense of the heat exchanger function within the component specific range of validity. In actual application with exhaust temperatures of 445°C, the difference from the model would be lower cooling capacity at the cooling rates specified in the model.

The typical ratio of mass flow to cooling water for bulk air coolers is between 0.4-2 [29] as specified within the range of validity. Given the exhaust mass flow rate of 18.7 kg/s, the liquid flow rate based on the typical ratio should be 7.48 kg/s-37.4 kg/s, both of which are modeled in Figure 23 and Figure 24, respectively.

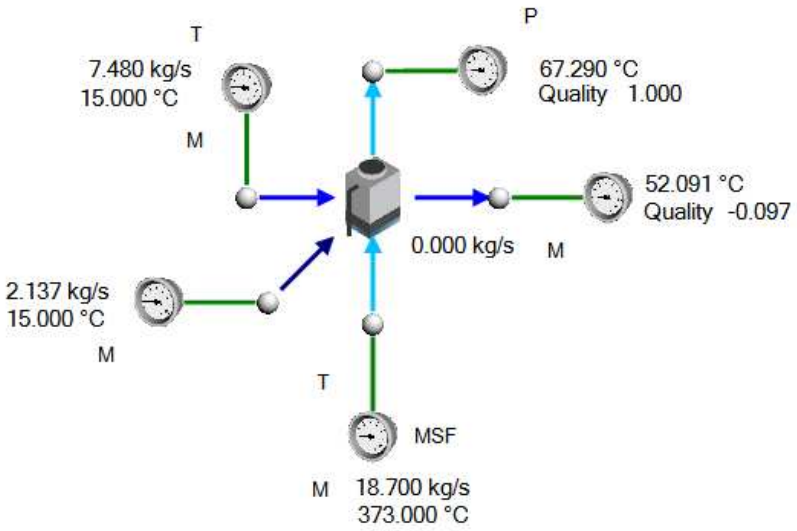

Figure 23: Complex model of direct contact cooler in Flownex minimum typical flow ratio.

As seen in Figure 23, the cooling water inlet flow rate is set to 7.48 kg/s and 15°C. Given the exhaust inlet temperature and the cooling flow rate, the make-up water requirement is specified at 2.137 kg/s. The designer tool in Flownex was utilized to solve this value, holding constant the

pond level mass imbalance shown at the bulk air cooler element. A pond level imbalance of zero indicates the element is functioning without overflowing or emptying the existing pond of water inside the heat exchanger.

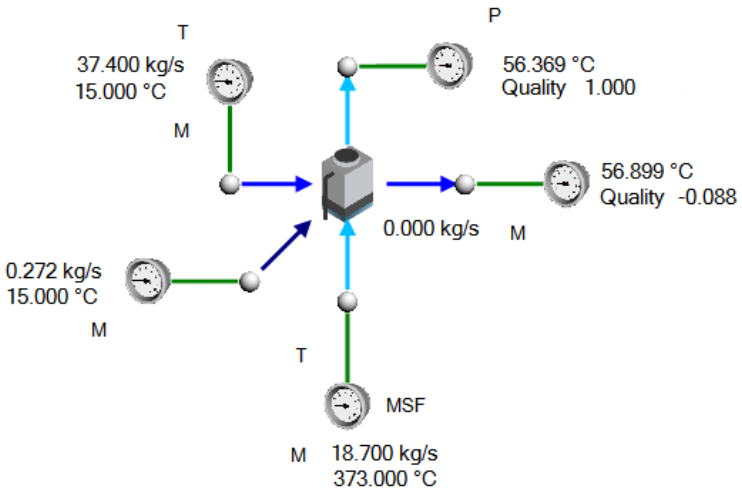

Figure 24: Complex Model of direct contact cooler in Flownex maximum typical flow ratio.

In Figure 24, the upper validity range limit for liquid to gas flow ratios is set at 37.4 kg/s. All the same input parameters as the simulation depicted in Figure 23 are held constant, including cooling water temperature of 15°C, exhaust air temperature of 373°C, and fluid compositions. At this cooling rate, the exhaust reaches a cooled temperature of 56°C.

Comparing the results of simulations resembled in Figure 23 and Figure 24 it is obvious that increasing the cooling fluid flow rate reduces the exhaust temperature. The relationship between cooling water mass flow rate and exhaust temperature can be examined in Figure 25.

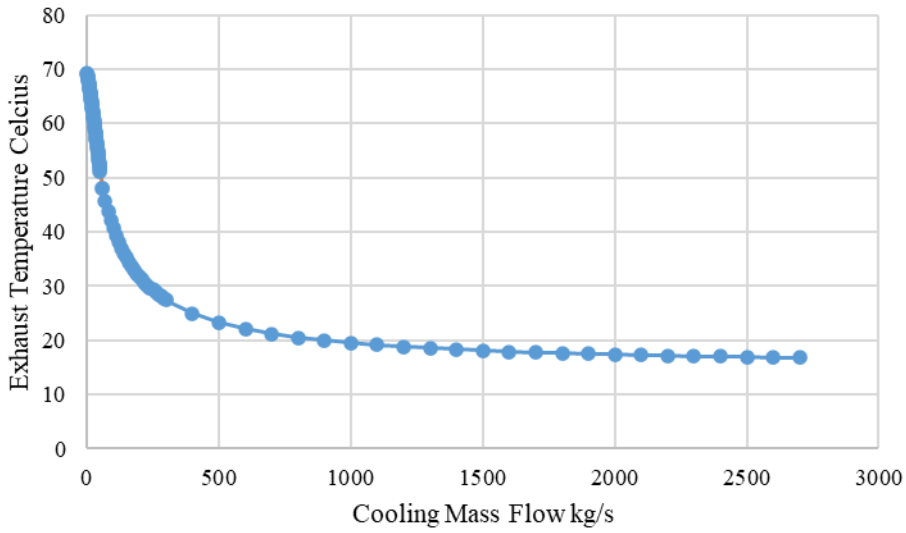

Figure 25: Exhaust air temperature as a function of cooling fluid mass flow rate at 15°C and ambient pressure.

As shown by the complex DCC model, increasing the cooling water mass flow increases the cooling capacity of the element. However, the water begins to condense at 44 kg/s of cooling flow, requiring a drainage of excess pool water. With cooling mass flow rates less than 44 kg/s, the makeup water requirement is directly related to water loss in the system due to evaporation of the cooling fluid.

The makeup water requirement is shown in Figure 26, and pictured on the chart is the threshold for the end of boiling and the beginning of water condensation in the heat exchanger. Once the boil-off mass flow rate reaches zero, make-up water requirement reverses, as the condensed fluid must be drained from the pond to maintain a constant level within the heat exchanger.

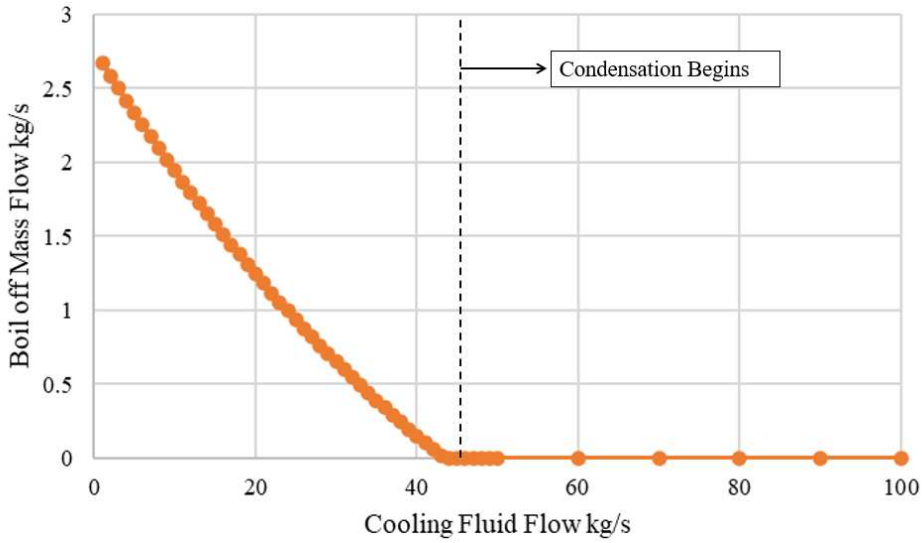

Figure 26: Boil off mas flow rate as a function of cooling water flow rate. Boil off is directly related to and equivalent to makeup water requirement, given the system mass flow is in balance and the water has not begun to condense.

It was found that makeup water flow is primarily effective in maintaining the pond water level within the bulk air cooling, and, within the model, does not have a relevant impact on the outlet cooling and exhaust temperatures.

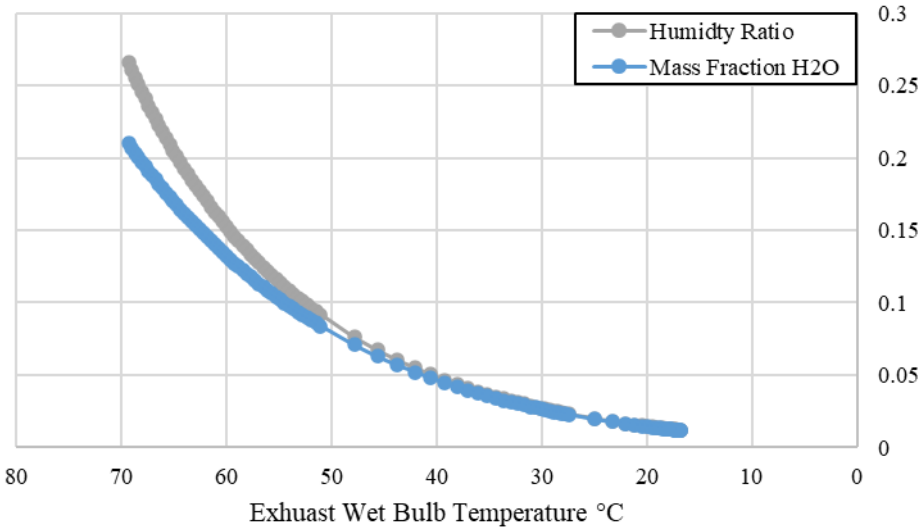

Figure 27: Humidity ratio and Mass fraction of H2O in exhaust gas at constant relative humidity as a function of Exhaust wet bulb temperature in °C.

As shown in Figure 27, the mass fraction of water in the exhaust is reducing with the decreasing wet bulb/temperature, as well as humidity ratio, but the relative humidity is remaining constant. This model assumes fully saturated air leaves the cooler, therefore the relative humidity is constant at fully saturated. We can conclude from the reduced mass fraction and humidity ratio that as a result in reducing temperature, the colder air is able to hold less water than hotter air, therefore leading to an overall reduction in water content in the exhaust. This is desirable due to complications with high water content in the exhaust later down the line, but the greatest reduction in H_2O mass is achieved at excessively large cooling flow rates. As water air separators can achieve similar H_2O mass fraction (MF) reductions, it may be more desirable to choose a separator if an abundance of cooling water is not an available resource. The capital expenses and tradeoffs must be compared with information about the site to make the most advantageous system process decision.

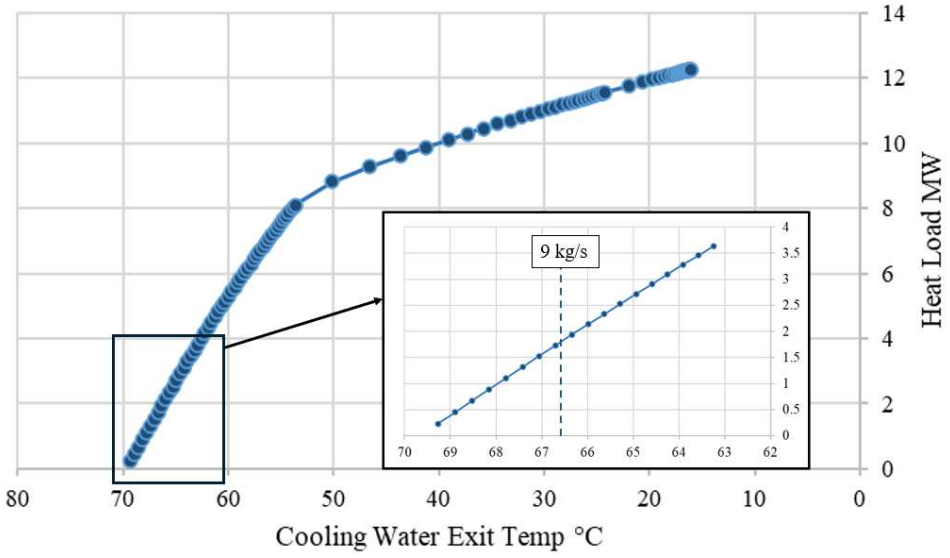

Figure 28: Heat load to rechill water exiting bulk air cooler and recirculating back into inlet in semi-closed loop system.

In Figure 28 the heat load to cool the recirculating cooling fluid is shown as a function of cooling water exit temperature, which is directly related with cooling fluid mass flow, after it has been used to cool the exhaust air flow. While it might be expected that the cooling load to reduce once the cooling water reaches its lowest temperatures, mass flow is a driving component of cooling load and indicates the cooling load is still quite significant, even as the temperature difference drops. However, even at the low mass flow rates the system will likely be operating in a real application condition, the cooling load is still significant and would need to be considered in its impact on overall system efficiency.

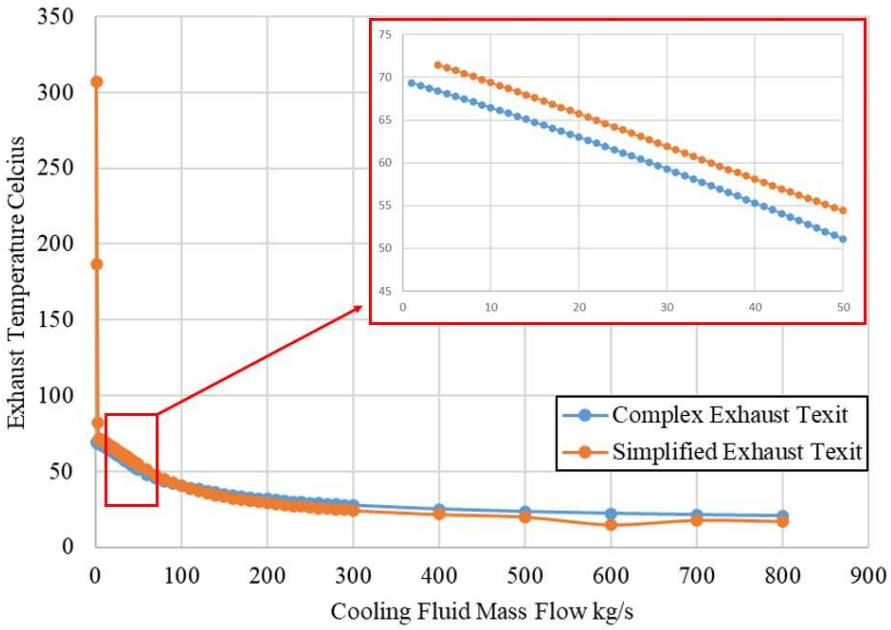

Figure 29: Simplified DCC model results in full EGR loop, showing that the complex model of the direct contact cooler is relatively similar to the simplified direct contact cooling model.

Figure 29 shows the close similarity between the complex model of the direct contact cooler and the simplified model of the direct contact cooler. While this does present an opportunity to use the simplified model in complex fluid networks, the complex direct contact cooler model provides valuable information on both fluids inlet and exit conditions. The simplified model flow results

are showed in Figure 30, and we can see that with a cooling rate of 7.48 kg/s, the exhaust air is cooled to 70.3°C from 445°C.

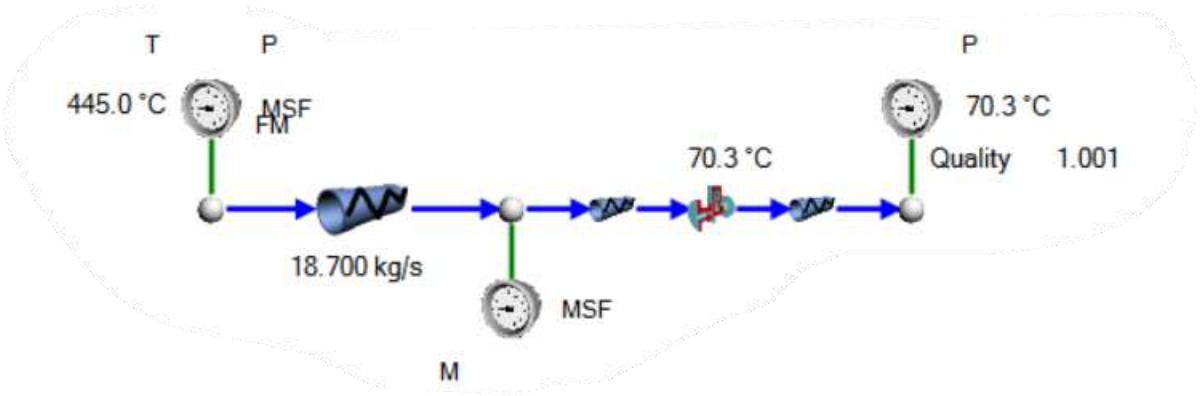

Figure 30: Real EGR simplified direct contact cooling system results of minimum typical gas to liquid cooling ratio 0.4, at 7.48 kg/s.

It was found that the cooling load is directly dependent on the mass fraction of the process fluid. Higher mass fraction of water increases cooling load, and is especially for the indirect cooler. Adding a water separation unit did not significantly reduce mass fraction of water and had a negligible effect on overall system cooling capacity in the simplified direct contact cooling model.

3.4 Recirculation Redirection Blower Method

The fan load redirection duty and power requirement will be explained based on a selected component available for commercial use. In this study, the Greenheck centrifugal industrial fan line was selected from, specifically the PLG model line due to the high CFM capacity of the line in addition to the design considerations for hot air, high mass flow, and hazardous air processing [30]. The specific fan selected for this application was the PLG model capable of handling the 17,000 CFM gas redirection load demanded by the EGR system while consuming about 22kW of power [31]. The fan load required to redirect 50% of the exhaust gas was determined by the volumetric flow rate, solved for by fixing mass flow rate and creating a split exhaust stream in the

Flownex model depicted in Figure 22. The fan selected for this application was the PLG-27 which has a wheel diameter of 27 inches [31]. The specific fan was selected by a quick analysis considering the required process volume, a minimum static pressure, and the installation elevation accounted for in a product specified correction factor.

3.5 Recirculation Redirection Orifice Method

Figure 31 depicts the orifice results of simulating a diffuser in the recirculation loop to control mass flow.

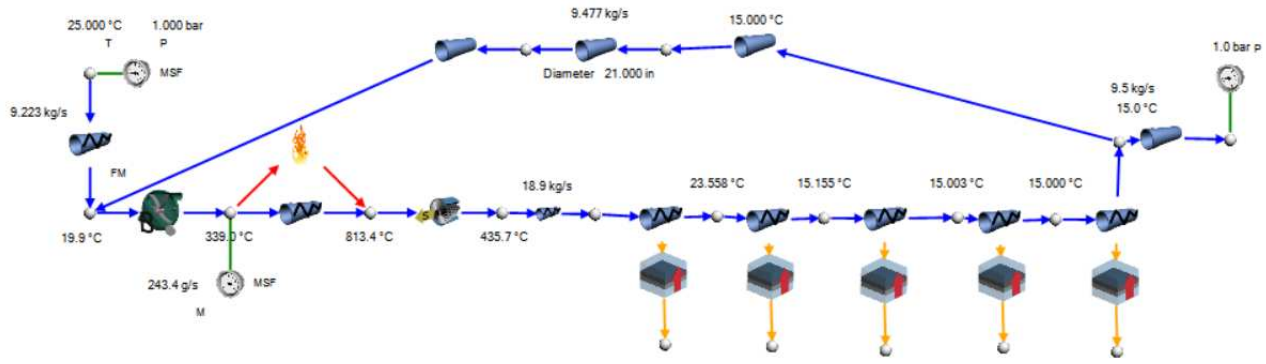

Figure 31: Flownex model of the exhuast gas recirculation system utilizing a restrictive orifice in the EGR loop as a method of gas redirection. Significant mass flow, pressure, temperature, and geometry values and results called out on the drawing page.

The EGR loop is shown in Figure 31 at the same diameter as the exhaust pipe. Changing the diameter of the orifice restricts flow through the EGR loop, resulting in varying mass flow. It is important to note that this model does not consider the flow impact of scrubbers, heat exchangers, or other auxiliary components that would be necessary to conduct actual EGR testing. All components other than the exhaust pipe and EGR loop are non dimensional components, with no impact on pressure changes throughout the system.

A parametric study of the model was conducted, changing the orifice diameter from 10 inches to 50 inches, shown in Figure 32.

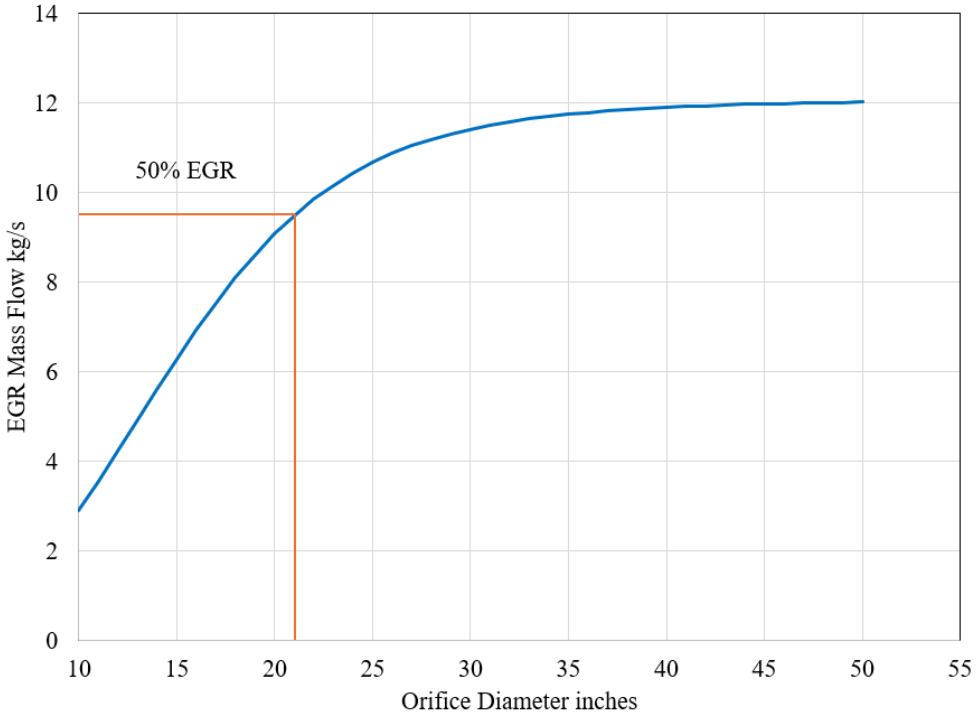

Figure 32: Plot corresponding to Figure 32 changing EGR diameter to simulate an orifice with changing diameter as a method of EGR control. Plot shows that EGR flow changes with orifice diameter, with smaller diameter resulting in less mass flow through the EGR loop.

As shown in Figure 32, changing the orifice diameter results in a varying mass flow, validating an orifice as a feasible method of EGR redirection in actual EGR testing. The orifice diameter variable is used to simulate a change in area, or the opening and closing of a passageway for exhaust flow through the EGR loop. The measured pressure drop throughout the recirculation system ranges from 0.23 kPa at the smallest diameter to 0.17 kPa at the widest orifice diameter, a range well within the acceptable pressure drop of 0.99 kPa.

3.6 Steam Production Calculation for HRSG Opportunity

To determine the cooling load required to reduce the exhaust temperature from 445 °C [12] to a target value of 20 °C, an energy balance was conducted. The required exhaust air cooling load was determined by the energy balance calculation described in this section is 8.3 MW.

The temperature and pressure of the cooling water inlet was set at 15 °C and 101 kPa respectively. The temperature of the hot exhaust air with mass flow 18.7 kg/s was set to 445 °C [12] with ambient pressure and a 2% humidity ratio, and a goal exit temperature of 20 °C and 0% humidity. The enthalpy of both the air and water was solved by using the engineering equation solver (EES) psychrometric library. Given the stated variables, the cooling load to reduce exhaust air from 445 °C to 20 °C was solved using the following equations. Equation 3 finds heat load given efficiency, mass flow, specific heat, and temperature difference.

Equation 3 $$Q = \varepsilon * \dot{m}_{air} * C_{p,air}(T_{air\_in} - T_{water\_in})$$

Equation 3 solves for the sensible heat transfer, considering only the difference in temperature between the hot exhaust air and cooling water. When efficiency (ε) is set to 1, the heat transfer is found to be 8.8 MW. Equation 3 solves for heat transfer in terms of enthalpy at defined humidity ratios of 2% at turbine exhaust and 0% in the cooled state, assuming all water has dropped out.

Equation 4 $$Q = \dot{m}_{air} * (H_{air\_in} - H_{air\_out})$$

Equation 4 solves for the sensible heat transfer given the change in enthalpy of the air before and after cooling and calculates 8.3 MW heat transfer.

Since Equation 3 does not account for enthalpy change during the cooling process, the solution found through calculating Equation 4 will be referenced to solve for total steam generation capacity. Given the stated assumptions and calculation process, the cooling load was estimated to be 8.3MW.

Determining the capacity for steam generation, assuming the cooling fluid is liquid water, was then calculated assuming all the cooling water is vaporized at 100 °C. The turbine exhaust air is cooled by sensible heat transfer as well as latent heat transfer from evaporating water, therefore,

Equation 5 can be used to find the mass flow of cooling water to reach the exhaust cooling heat load, when Equation 6 is true.

Equation 5 $$Q_{air} = \dot{m}_{water} * (h_{vap\ water} + \Delta h)$$

The enthalpy of vaporization of water was calculated from the engineering equation solver thermophysical properties library.

Equation 6 $$\Delta h_{water} = \dot{m}_{water} * C_{p\ water} * \Delta T_{water}$$

Assuming all the water is evaporating to steam, the calculated mass flow value represents the steam production capability of the system that could be used in a HRSG application. The mass flow of water was found to be 3.2 kg/s when the inlet temperature is 15°C and the water fully evaporating to steam. The stated capacity for steam generation can be utilized in the consideration for the efficacy of a HRSG application. In application, an additional burner could be implemented to add additional heat, however, the reduction in O_2 in the exhaust would need to be considered.

CHAPTER 4 - RESULTS OF SURROGATE EGR MODEL

In Chapter 3, the results of the actual EGR system components were analyzed. In Chapter 4, the results of the surrogate gas flow requirements and surrogate system model will be analyzed.

4.1 Surrogate Gas Requirement Calculations

The surrogate gas requirement was first calculated by analyzing the recirculated exhaust gas composition for each EGR% and converting the values from mass fraction to mass flow, using the gas turbine inlet air flow of 18.7 kg/s [12] for the conversion. Once the mass flows of nitrogen, argon, oxygen, and carbon dioxide were determined for each EGR%, the surrogate gas requirement was reconstructed to reduce the actual surrogate gas flowing. As supplementing exactly half the inlet airflow to recreate 50% EGR would be very difficult and require a large amount of gas flow, a portion of the inlet air that would be considered “displaced air” if the system was actually recirculating flow, was considered as EGR. Using this method, the surrogate gas flow requirement was reduced, as a portion of the nitrogen and carbon dioxide already present in ambient air was considered as a fraction of the EGR flow. The adjusted values and actual gas delivery requirements are shown in Figure 33.

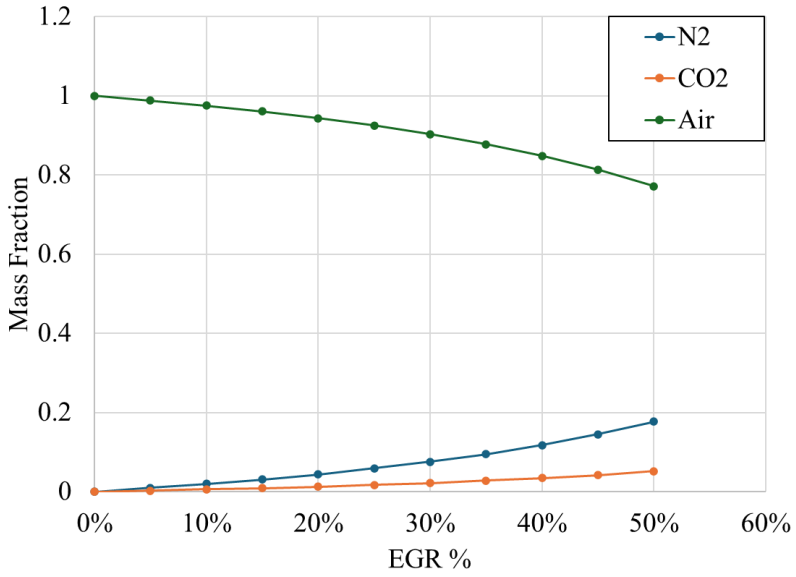

Figure 33: Surrogate Gas Requirements in Mass Fraction as a function of EGR%.

As seen by the Figure 33 plot, the air never converges with the surrogate gases, this is because of the ambient air replacement method for reducing surrogate gas flow. Despite the effort to reduce experimental gas flow, the capacity of gas required in this application is on an industrial scale. Local bulk gas suppliers were surveyed for available gas capacity and delivery capabilities.

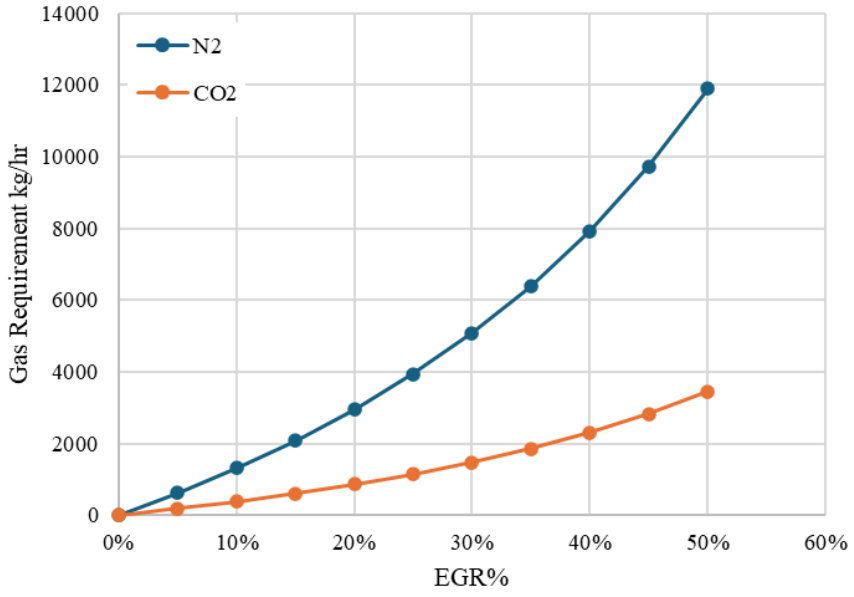

Figure 34: Surrogate gas requirements by EGR% at full engine load.

Figure 34 plots the surrogate gas requirement for CO_2 and N_2 as a function of EGR %. The high flow rates required are due to the high volume of air typically processed by the engine and would increase and decrease with higher and lower engine classes, as air flow rates increase and decrease. Nitrogen holds a higher percentage of the surrogate gas composition, at 11901 kg/hr mass flow required for 50% EGR, or 361,970 SCFH. The largest bulk delivery option for gaseous Nitrogen is 130,000 SCFT, which can only deliver about 20 minutes of the required amount in the 50% case. Therefore, nitrogen must be delivered in liquid form and vaporized with an ambient air vaporizer.

The liquid mass flow required before vaporization for the 50% N_2 case was found to be 1992 CFH. The available liquid nitrogen capacity supplied by Airgas suppliers is 43482 kg, or about 50 tons. Given the required mass flow rate of nitrogen and the available tanker capacity, N_2 surrogate supply at the 50% EGR case limits runtime to about 3.6 hours.

The CO_2 tanker capacity was determined based on a 20ton CO2 estimate (within a 50 ton trailer). Assuming typical liquid CO_2 transport conditions of 362 psi (25 bar) and -15°C, the standard gaseous capacity of the tank is 45,351 SCF. The required CO_2 surrogate volume flow is 66,509 SCFH, allowing about 13 hours of runtime at the 50% EGR full load case, as shown in Figure 35.

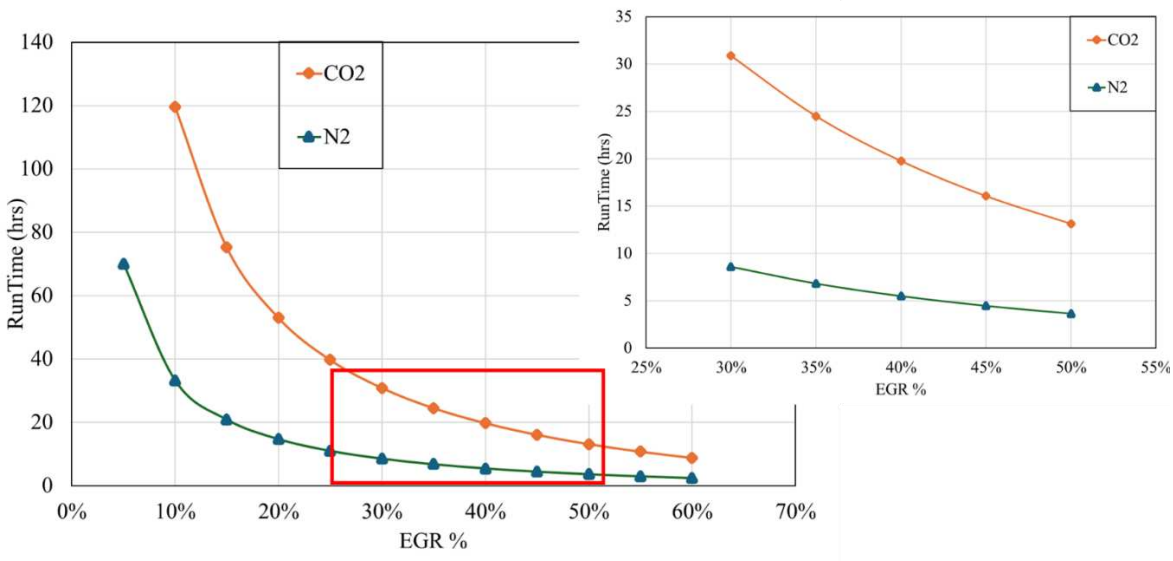

Figure 35: Plot of surrogate gas testing runtime given tanker capacity at various EGR%.

4.2 Gas Vaporization

Gas vaporizers are necessary to transition the compressed liquid CO_2 and N_2 into gaseous phase. Ambient air vaporizers are used for nitrogen, which do not require any heat input to vaporize the gas, only natural convection [27]. Carbon dioxide must be vaporized with heat input, and has an associated footprint, along with the N2 vaporizer, that must be accounted for in packaging design [32].

Figure 36: CO_2 electric vaporizer. [32]

Figure 37: Nitrogen ambient air vaporizer. [33]

Gas vaporizers are shown in Figure 36, the carbon dioxide vaporizer, and Figure 37, the nitrogen vaporizer. The component sizing and footprint analysis of the gas vaporizers will be conducted based on the two selected options available for commercial use. The ambient air nitrogen vaporizer's largest model has a max flow rate of 186,600 SCFH. Given the Nitrogen flowrate is 361,970 SCFH, two vaporizers are required to accommodate the required flow rate. The dimensions of each are WxDxH : 101x114x534 inches, and total weight is 9,070lbs. The CO_2 vaporizer largest size available has a maximum flowrate of 6434 lb/hr of CO_2. The surrogate gas requirement of CO_2 is 7613 lb/hr. Therefore, two electric CO_2 vaporizers are required to accommodate the total required flowrate for the 50% EGR case. The dimensions of each vaporizer are LxWxH:56.75x65.75x31.0625 inches.

4.3 Surrogate Gas Flownex Model

The Flownex model of the surrogate gas delivery system was paramount in deciding the required gaseous delivery pressures and allowable pipe diameters. The model also informed

Reynolds number in the piping system, suggesting that a designated mixing skid was not required, as the flow is turbulent and therefore creates a homogeneous mixture in the transport piping.

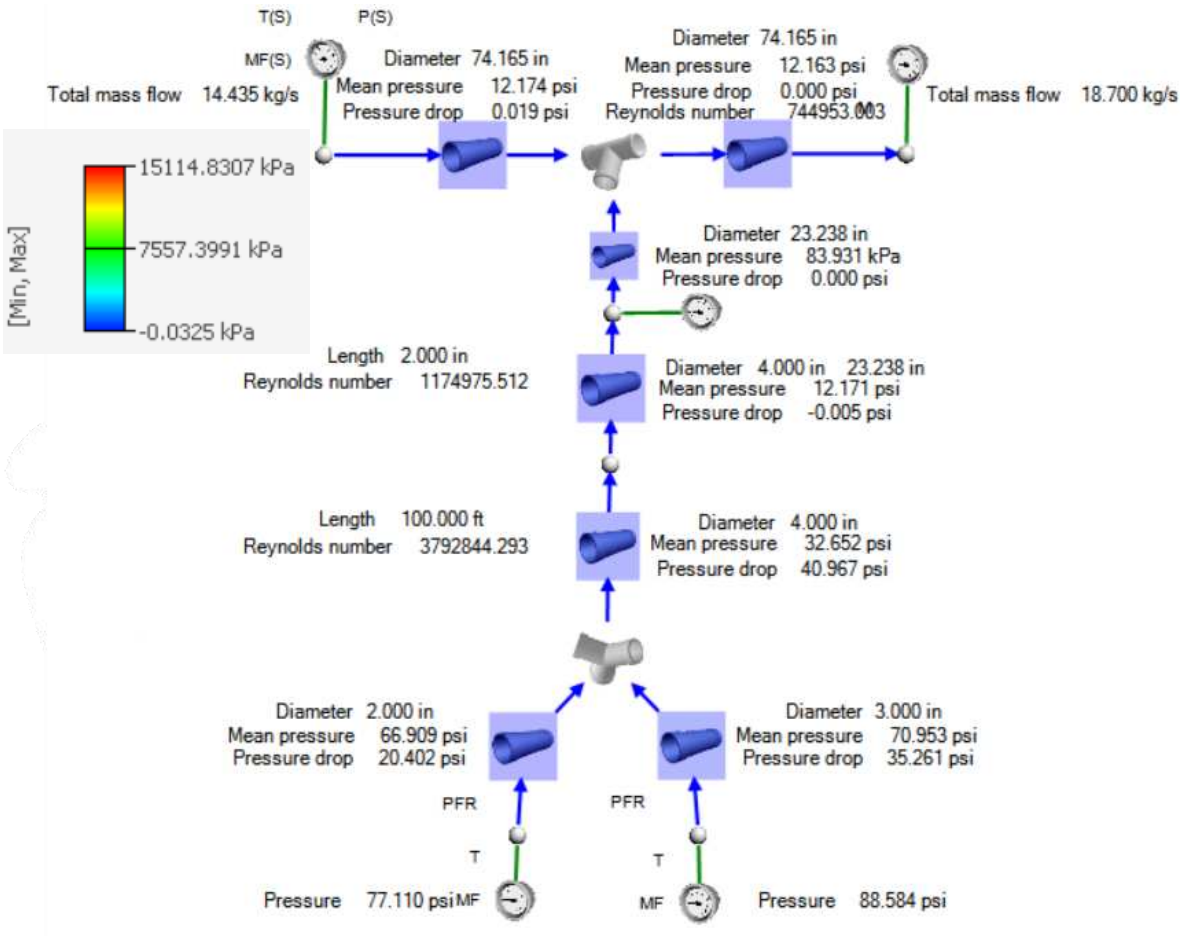

Figure 38: Surrogate gas system with minimum pipe diameters showing gas delivery pressure requirements, pressure drop, and Reynolds number.

The surrogate system in Figure 38 shows the set diameter for each pipe element, as well as the solved for average pressure and pressure drop in each element. Furthermore, it shows the Reynolds number and length of the longest pipe sections, suggesting that no mixing skid is needed for the gas. From this figure, the gas delivery pressure for CO_2 is at least 77.1 psi to overcome pressure drop throughout the piping system. For N_2, the delivery pressure must be at least 88.5 psi to

overcome pressure drop throughout the system. As both of these values are well within deliverable range specified by Airgas suppliers, the piping system design is acceptable.

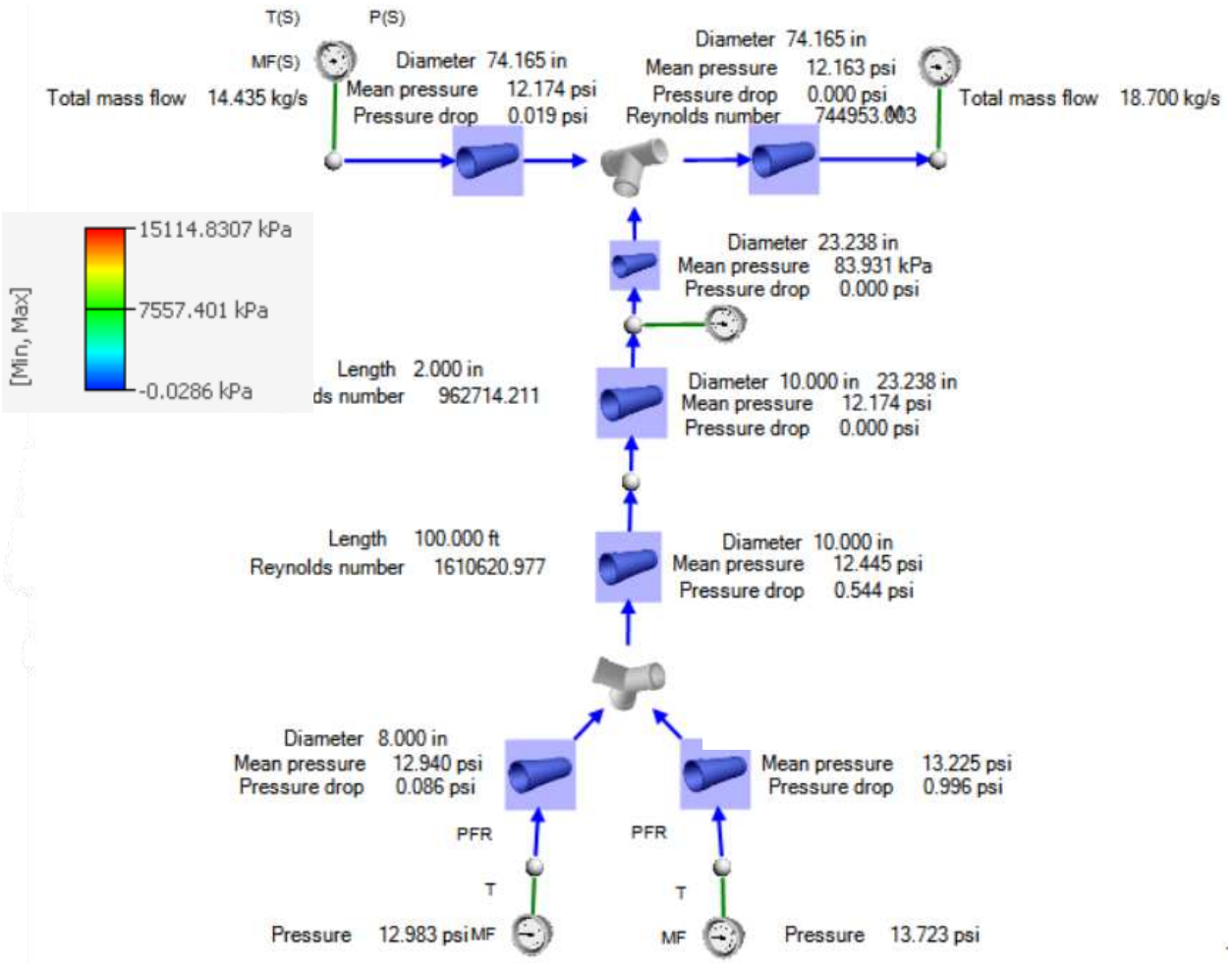

Figure 39: Surrogate Gas system at large pipe diameters.

The surrogate gas delivery system model shown in Figure 39 shows the pipe diameter of each element as well as the average pressure and pressure drop. As seen from this model, the delivery pressure requirements are much lower than compared to the minimum pipe sized system, at 12.9 psi for CO_2 and 13.7 psi for N_2. As the delivery pressures are also well below the maximum pressure before additional pumping systems need to be incorporated, this piping setup is another acceptable design. Similarly with the minimum pipe study, the Reynolds number after gas mixing

points is shown on the plot, and is well above the turbulent region, indicating good mixing and flow. This negates the need for a gas mixing skid, as the fluids have ample time to mix as they transport from the gas delivery tanks to the mixing point before the compressor inlet.

CHAPTER 5 - COMMISSIONING RESULTS

The previous chapters dictated modeling efforts and results of the actual and surrogate EGR systems. Chapter 5 will describe commissioning of the exhaust system on the Solar Turbines Centaur 40 in CSU's research facility at the Powerhouse Energy Campus, including design challenges and restrictions specific to the location. Since the Powerhouse is categorized as a historic building in the city of Fort Collins, there are restrictions that prohibit the permanent change of the street-facing building image. This presented a challenge in designing a functioning exhaust stack for the gas turbine. Furthermore, the internal structure of the building presented design challenges is routing and installing the exhaust, as major structural components could not be altered without major reconstruction, and had to be incorporated into the design or worked around. The specific commissioning restrictions, objectives, and results will be addressed in this section.

5.1 Construction Objectives

To facilitate investigation of EGR on the Solar Turbines Centaur 40, an integral effort of this research was to complete commissioning of the exhaust system. Several challenges were presented in the process of installing the exhaust system, most notably in the geometry and features of the existing research facility building. The commissioning tasks consisted of the following:

- Exhaust pipe extension installation to bridge distance from package installation point to silencer installation point.
- Design and manufacture of exhaust pipe extension stand to support weight during thermal expansion.
- Installation of Silencer, including mounting to acceptable height and alignment with turbine.

- Installation of exhaust chimney extension and associated roof protection thimble.
- Design and manufacture of adjustable chimney cart.
- Designing specifications for internal insulation of exhaust system, and installation.

Several obstructions to the originally intended installation sequence for the gas turbine exhaust system arose due to the existing building conditions. The need for a pipe extension was determined by a few factors, 1) the installation sequence 2) the existing building geometry and features and 3) building safety standards.

To understand the full system layout, a SolidWorks model of the full assembly, including the exhaust system, gas turbine package and components, and building features, is shown in Figure 40.

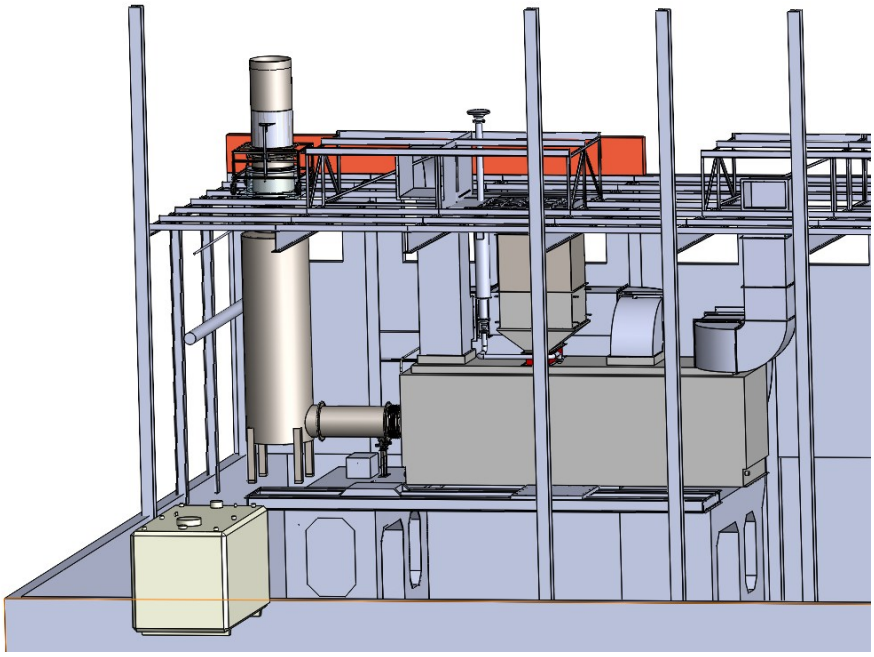

Figure 40: SolidWorks model of full assembly, including gas turbine package and ducting and components as well as full exhaust system.

Each component in the commissioning process will now be explained in sequence.

5.2 Silencer Positioning and Mounting

Given the limited space availability of the research facility, the turbine package was installed where it best fit the floor space of the facility. This was at the southwest corner of the CSU powerhouse campus, situated under roof monitors, open window recesses, and near legacy engine skid footprint on the ground, with varying floor material and geometries. This arrangement required integration consideration of both the roof and ground conditions.

Due to the legacy engine footprint, there was a considerable amount of ground discontinuity, shown in Figure 41 as the red section of ground. This, coupled with the existing structural beams running east-west and north-south, and the requirement of concentricity between the turbine exhaust and silencer intake, the location of the silencer was mostly pre-determined. Additional considerations were the proximity of the silencer to the south wall and the requirement for accessibility to pass through the building, as well as the fire extinguisher line at the ceiling partially obstructing the mobility of the silencer.

Figure 41: Internal building exhaust system comprised of expansion bellows, exhaust pipe extension, and silencer.

Foremost, the distance of the silencer from the package face was determined to be 90.5 inches to avoid collision with the uneven floor and supporting roof beams, and to allow adequate space between the silencer and closest wall according to the standard 36 inches, as shown in Figure 42.

Figure 42: Silencer final position from south wall of research facility, maintaining standard 36 inches required for passageways.

The final location of the silencer required the fire control line to be routed around the silencer by Front Range Fire, which was done in advance of the installation process dictated in section 5.6.

5.3 Chimney Exhaust Extension

To channel the exhaust fumes through the silencer and roof to the ambient air outside, an exhaust pipe chimney extension was needed. The chimney extension was designed to extend the top of the silencer through the roof, and to terminate below the street-view visibility plane to adhere with county historical building codes, described further in section 5.9. The required length was found to be 60 inches, and was modeled as a continuation of the silencer, maintaining the inner

diameter and wall thickness of the existing geometry. Once the part was modeled, it was sent to inExhaust for manufacturing, the drawing pictured in Figure 43.

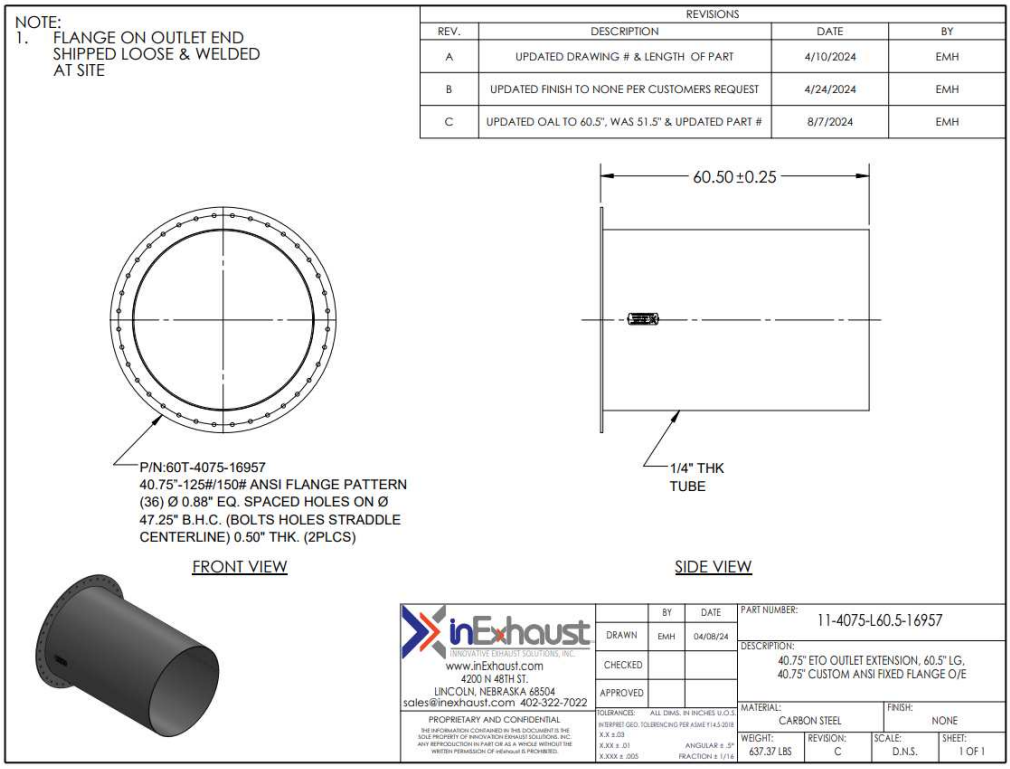

Figure 43: Exhaust Pipe Chimney extension drawing sheet from inExhaust.

5.4 Thimble Component and Installation

As the exhaust had to terminate through the roof, it was required by standard building code that the exhaust be insulated from combustible roof material through use of a thimble. Therefore, a custom thimble had to be manufactured based on the given specifications. The custom part drawing sheet is pictured in Figure 44.

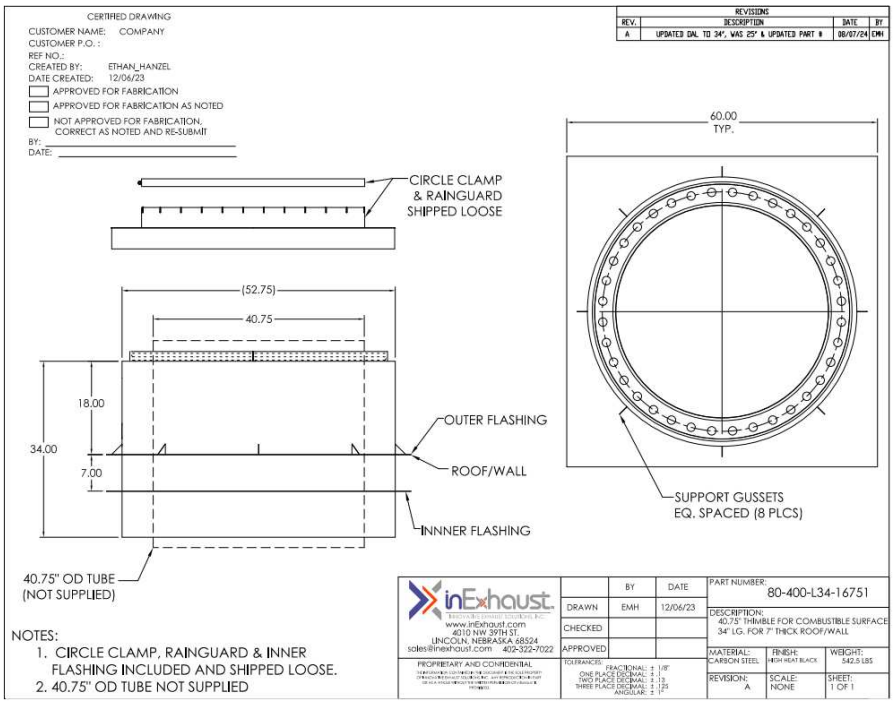

Figure 44: Thimble drawing sheet from inExhaust.

As shown in Figure 44, the thimble insulates the exhaust pipe extension from the top of the thimble through the roof. The thickness of the roof was determined by plunging and measuring through the roof membrane to measure insulation and overall pitch and combining that with the thickness of the concrete decking blocks. The thickness was found to be between 3.75-4 inches, and the concrete decking panels to be 3" tall, summing to a roof thickness of 6.75-7 inches. This is represented in the 7-inch dimension between the outer and inner flashing shown in Figure 44.

5.5 Roof Reconstruction

To accommodate the added weight and allow for the proper installation of the thimble, it was deemed necessary to replace the concrete decking with steel sheet decking. Additionally, one section of cross member support was removed and reinforced to accommodate the exhaust extending through the roof, as the original cross member would have completely obstructed the

passage. In this endeavor, Corbel Engineering was contracted to redesign the roof support, the final drawings shown in Figure 45.

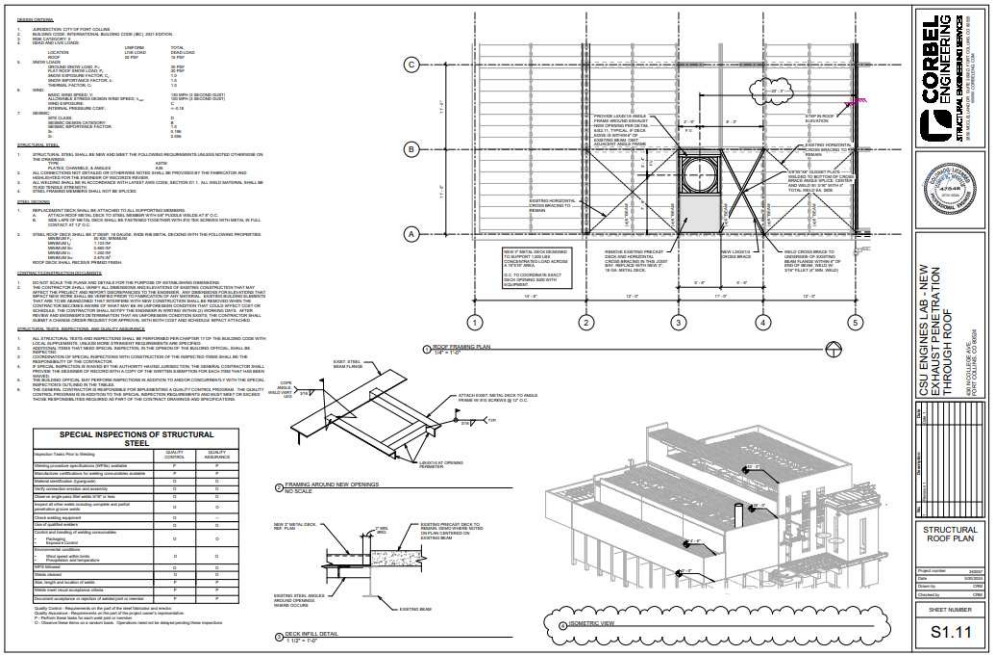

Figure 45: Corbell engineering roof redesign for additional load bearing of thimble installation.

The design depicted in Figure 44 was executed in a joint effort between the CSU powerhouse team and hired contractor, Hillside Construction.

5.6 Silencer and Thimble Installation

The assembly sequence of the silencer, chimney pipe extension, decking, and thimble was paramount in the successful completion of this installation phase. First, the silencer was moved out of the way to allow the installation of the new roof support system, pictured in Figure 45. Once roof supports were installed, the silencer was moved back into place. The roof membrane was opened and concrete decking tiles removed to make way for the new decking. The silencer, weighing approximately 8,542 pounds, was lifted through the opening in the roof into place by a

crane. Then, the chimney pipe extension was lifted onto the roof and lowered into place, where it was installed with gasket and hardware, pictured in Figure 46.

Figure 46: Decking and thimble installation process.

Once the chimney pipe extension and silencer were in place, the thimble was lifted and lowered onto the support beams, shown in Figure 46. Figure 47 shows the thimble in place with the upper and lower flashings installed.

Figure 47: Thimble and pipe extension 2 installation process.

Figure 48: Completed installation of pipe extension and insulation thimble at roof.

After the thimble was fully installed, the remaining decking was installed and the roof membrane was sealed with high heat materials, shown in Figure 48.

5.7 Silencer Shims for Vertical Alignment with GT Package

The GT package installation guide required the entire package be mounted on a 2-inch-high platform of grout. To maintain the axial alignment of the turbine exit with the silencer entrance, the silencer was mounted on shims, shown in Figure 49. The shims were designed with an outer geometry and center hole to match the silencer feet for easy mounting.

Figure 49: Two-inch shims under silencer feet, required to lift the silencer to match concentricity of the turbine exhaust, as the GT package was installed on 2 inch slabs, raising it above concentricity.

During the initial alignment process of the silencer, markings were made to indicate the final location of the feet, pictured in Figure 48, to allow for realignment during the final installation process.

Once the silencer final location was known, center holes were drilled into the ground to place concrete anchor bolts. The shims were placed in the marked location, with the anchor bolt through their center hole. Then the silencer was lifted above the concrete bolt and lowered back down onto the shims, where it was then torqued into place.

5.8 Exhaust Pipe Extension Design and Installation

The dimensions of the horizontal pipe extension (EP1) were designed to be a continuation of the existing components, maintaining the inner diameter and wall thickness of the silencer. This also ensured additional protection from possible hazardous ejections. The designed pipe extension is pictured in Figure 50.

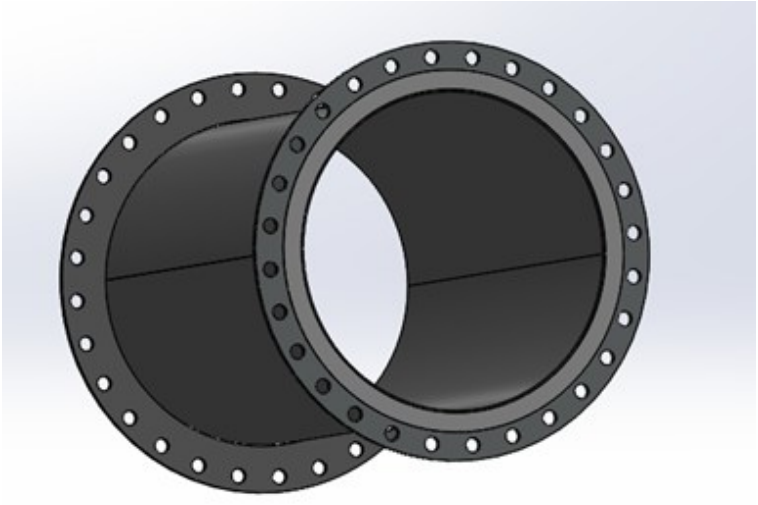

Figure 50: SolidWorks model of horizontal exhaust pipe extension design sent to manufacturer for production.

To ensure lead time and manufacturing did not delay the final installation of the exhaust system, the horizontal pipe extension was ordered to the manufacturer before the final silencer position was known. To account for the possibility of lateral adjustments during the installation process, the pipe extension was specified longer than required, at 70.5 inches long, pictured in the manufacturer drawing in Figure 51.

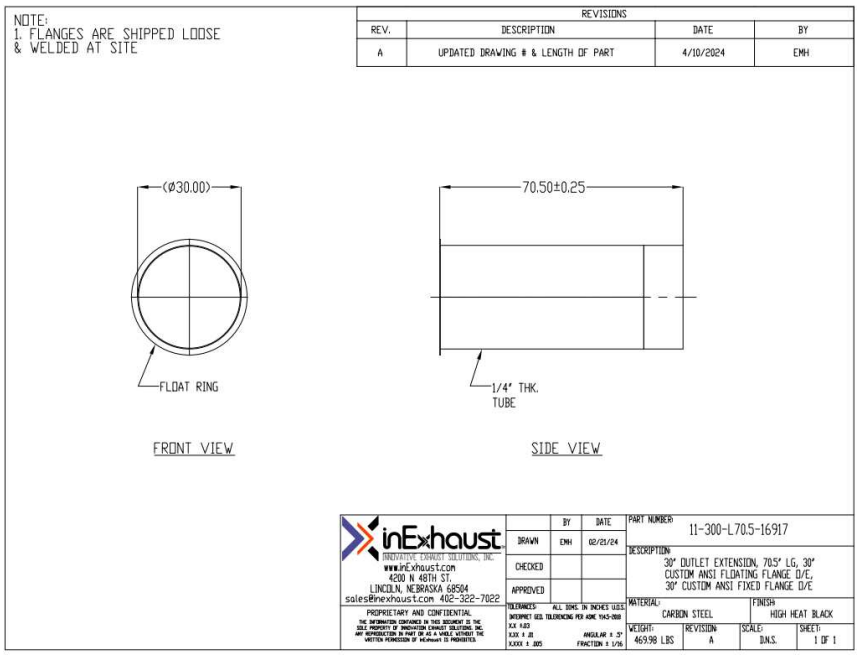

Figure 51: Horizontal exhaust pipe extension manufacturer drawing sheet.

As mentioned in section 5.2, the distance between the silencer and turbine package faces was determined to be 90.5 inches. After accounting for the expansion bellows lateral installation distance of 24 inches, it was found that the exhaust pipe extension needed to be 66.5 inches from face to face. The pipe was cut to the determined length.

In anticipation of a variable length, the manufacturer included the flange face separately to be welded on site and included a floating flange to allow for easy alignment during installation.

When planning the installation of EP1, it was necessary to consider the entire system and the impact adding a custom retrofit part might have on the original equipment manufacturer (OEM) design. One notable complication was in support of the additional pipe extension. It was specified in the OEM installation documents that additional ducting above a particular weight must be independently supported. Further, the expansion bellows, which exists between the turbine package and pipe extension, has a maximum allowable displacement, noted in Table 10.

Table 9: Expansion Bellows joint allowable displacement.

MODEL LINE	Axial Compression From Installation	Axial Extension From Installation	Lateral Movement Allowable (+/-)	Radial Movement Allowable (degrees)
Centaur 40/50–Taurus 60/65/70	2.0 in (5.1 cm)	0.625 in (1.588 cm)	0.50 in (1.27 cm)	0.0

It was known that the vertical expansion of the silencer could be as much as 0.5 inches, with varying local expansion, and axial expansion to be as much as 0.2 inches. Given the allowable displacement stated in Table 10, this would be acceptable, but it does not consider the addition of EP1.

As EP1 exceeded the allowable dependent weight support threshold, it was necessary to conduct thermal and static calculations on the system to determine the total displacement of the system. Through modeling, the impact of adding a component to OEM design was clear.

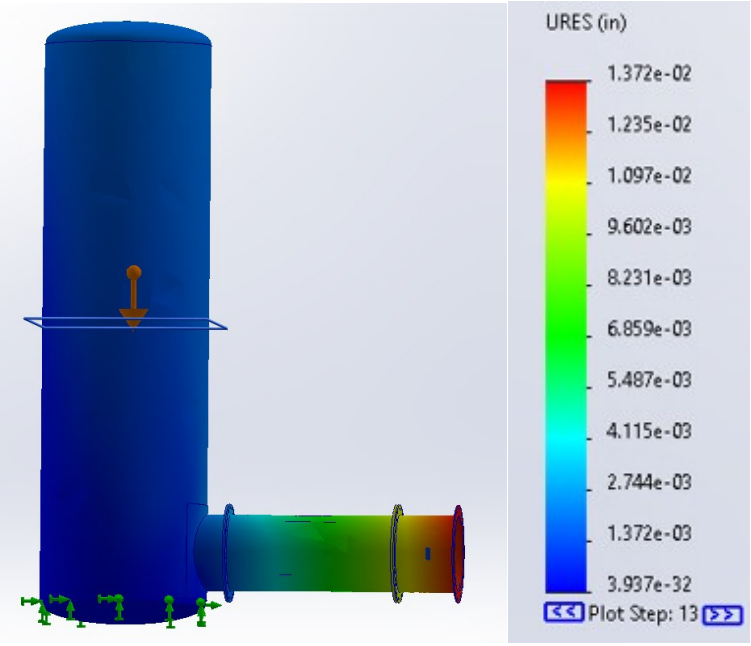

Figure 52: Static simulation of exhaust assembly without thermal load.

As shown in Figure 52, the silencer can withstand the additional weight of the pipe extension without buckling or bending beyond the acceptable displacement. However, when the exhaust system reaches operating temperature, as modeled in Figure 53, the displacement is beyond the acceptable limit and compromises the expansion bellows.

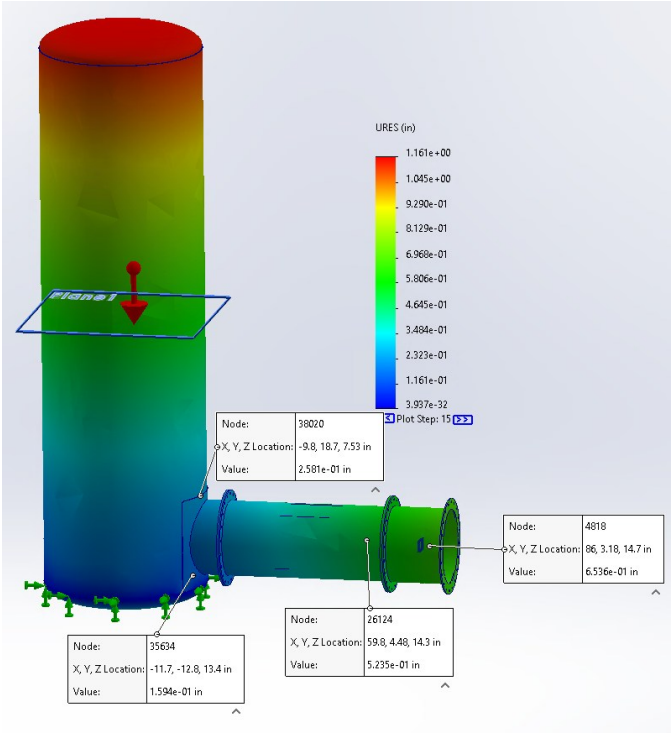

Figure 53: Study of EP1 Displacement on Silencer with thermal and static considerations.

Furthermore, a stress studies were conducted on the silencer supporting the weight of the cantilevered pipe extension and bellows, one without thermal load (Figure 54) and one with thermal load (Figure 55).

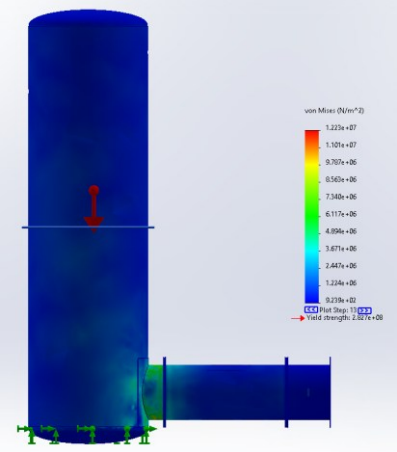

Figure 54: Stress study of silencer with cantilever weight of exhaust pipe extension and bellows without thermal load performed in SolidWorks.

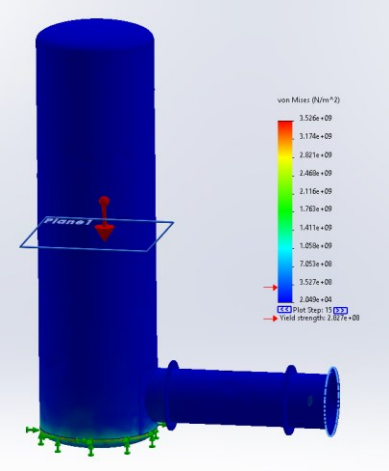

Figure 55: Stress study of silencer with thermal load performed in SolidWorks.

It can be determined from these studies that the silencer cannot support the weight of the exhaust assembly (pipe extension and bellows) when under thermal load, as is indicated by the yield strength marker in Figure 55.

In response to this deformation problem, a stand was designed and manufactured to allow both vertical and horizontal movement while maintaining support. When reaching operational temperatures, the silencer can expand as much as 0.5 inches vertically and 0.2 inches horizontally. This is compounded when considering the thermal expansion of the carbon steel pipe extension, which can be up to 0.24 inches horizontally and 0.17 inches vertically, as determined by a thermal simulation shown in Figure 56 .

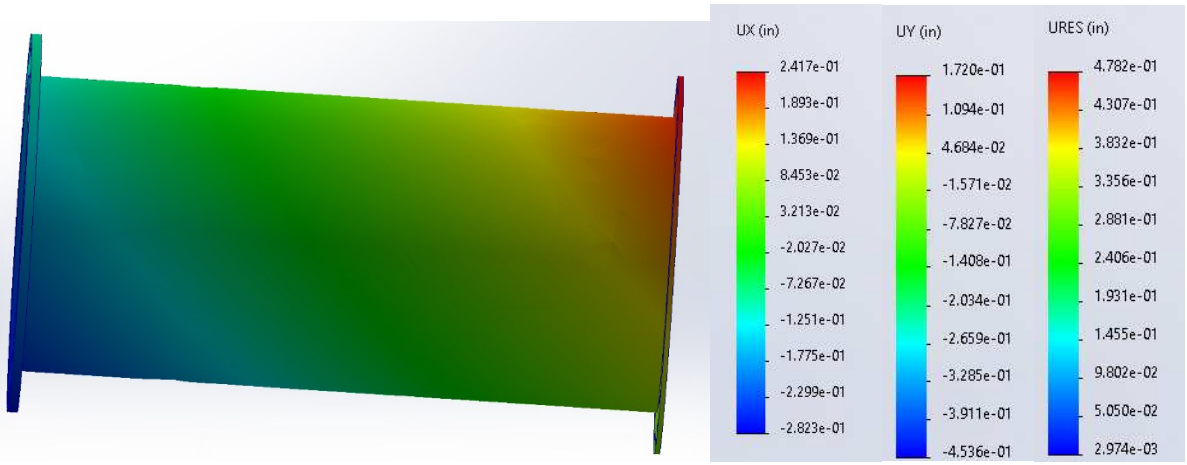

Figure 56: Thermal expansion study performed on horizontal pipe extension in SolidWorks; with thermal load across all surfaces set to temperature 445 °C.

To allow horizontal movement, a saddle and roller assembly was selected to fit the diameter of the pipe extension. For vertical movement, two heavy duty springs are mounted beneath the roller. The springs are installed partially compressed, allowing for maintained support through vertical movement.

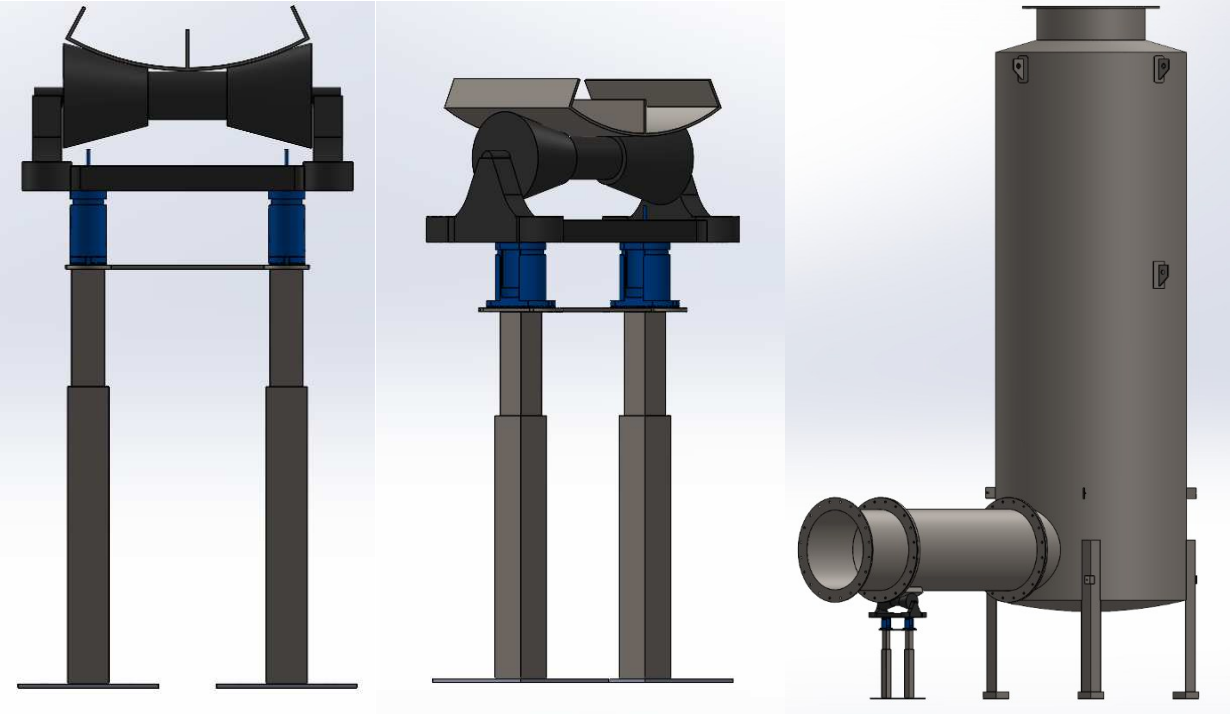

Figure 57: Exhaust Pipe Extension stand SolidWorks CAD model.

Figure 57 depicts the design for support the horizontal exhaust pipe (EP1) in the exhaust system. The exhaust system material will expand as the temperature of the exhaust system rises and stabilizes with combustion. The bellows is in place to accommodate lateral movement from expansion. EP1 was added to overcome the existing building limitations of the research facility, which requires analysis of the silencer in its ability to support the additional weight. Solidworks FEA studies were conducted to observe the material behavior of the silencer at a range of temperatures, from ambient to operating. At ambient temperature, the silencer is fully capable of supporting the pipe extension, but the problem of displacement presents itself when at operating temperature.

Figure 58: Images of installed Exhaust pipe extension support.

5.9 Mobile Cart for Chimney Extension Design and Installation

The chimney will be exhausting gas at operating temperature 445°C. This presents complication both in terms of heat transfer and exhaust fumes when considering the surrounding building and roof material. To prevent exhaust gas from melting surrounding roof membrane, which is rubber based, or exhaust flue entering into nearby building windows, the chimney height was set to 128 inches above the roof membrane. The actual chimney is 84 inches in height, as shown in Figure 59, but it rests on top of the chimney pipe extension, which terminates about 34 inches above the membrane.

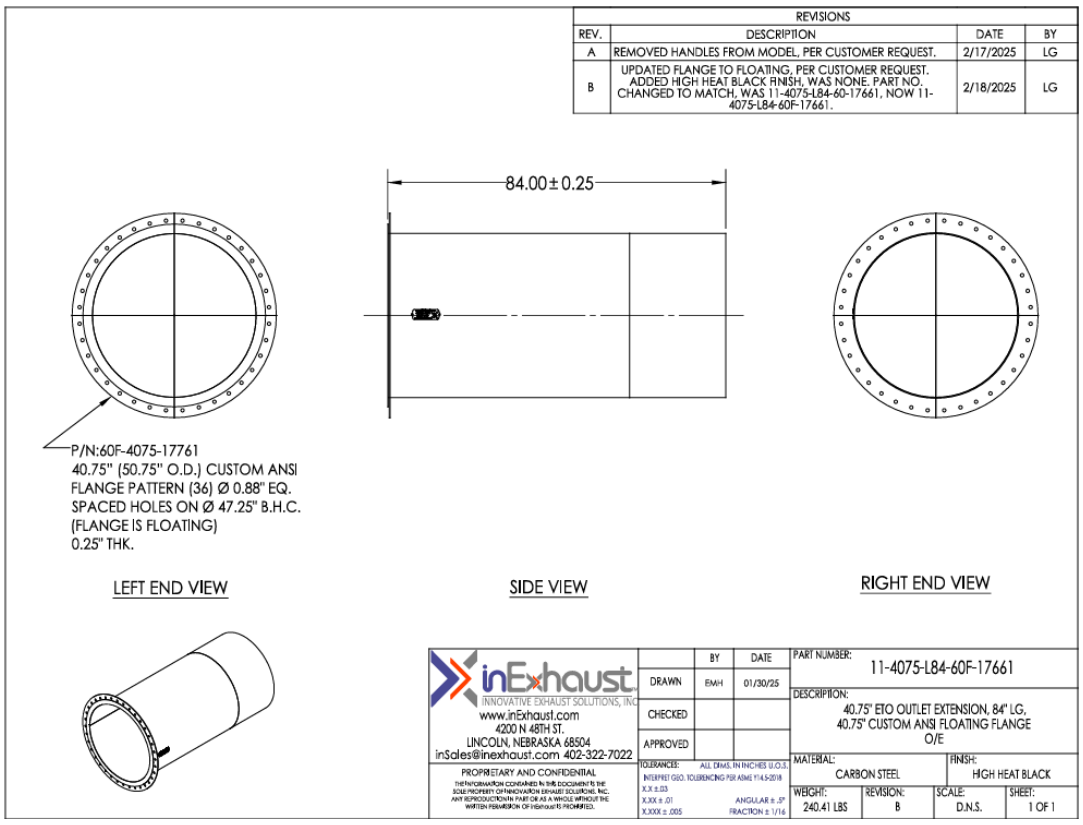

Figure 59: Drawing sheet of chimney extension supplied by custom manufacturer inExhuast.

In addition to heat and exhaust concerns, street visibility of the exhaust chimney stack was a consideration in the system design. A design challenge of maintaining exhaust chimney function while adhering to historic building defacement restrictions presented itself in this phase of the commissioning process. Historic buildings, of which CSU's Powerhouse Energy Institute is, must maintain a historically accurate street view. This regulation demanded that the chimney be out of sight for all or some of the time, but safe exhaust ducting practices and building codes demanded an extended chimney during testing operations, as the Solar Turbines Centaur 40 exhaust was required to terminate at an appropriate height to not destroy the roof membrane and to adhere with building codes, which placed it above the visibility limit. To both terminate the exhaust at a safe height for building structure and adhere to the city's historical society requirements, a temporary chimney with a mobile uplifted and demounted positions was deemed necessary. The chimney

design iterated through a series of functional designs, which included a telescoping system, a hinging system, and finally, a mobile chimney cart with vertical height adjustment. The mobile cart design is pictured in Figure 60.

Figure 60: SolidWorks model of mobile, vertically adjusting chimney cart assembly in upright (left) position and lowered (right) position.

To facilitate repeated vertical movement on the roof, support wings were added to the chimney stack as mounting points for the lifting jacks mounted to the stand on opposite sides, as seen in Figure 60. To ensure the wings were adequate in material and geometry to support the entire 240 pound stack, force analyses were conducted in SolidWorks, as seen in Figure 61 and Figure 62.

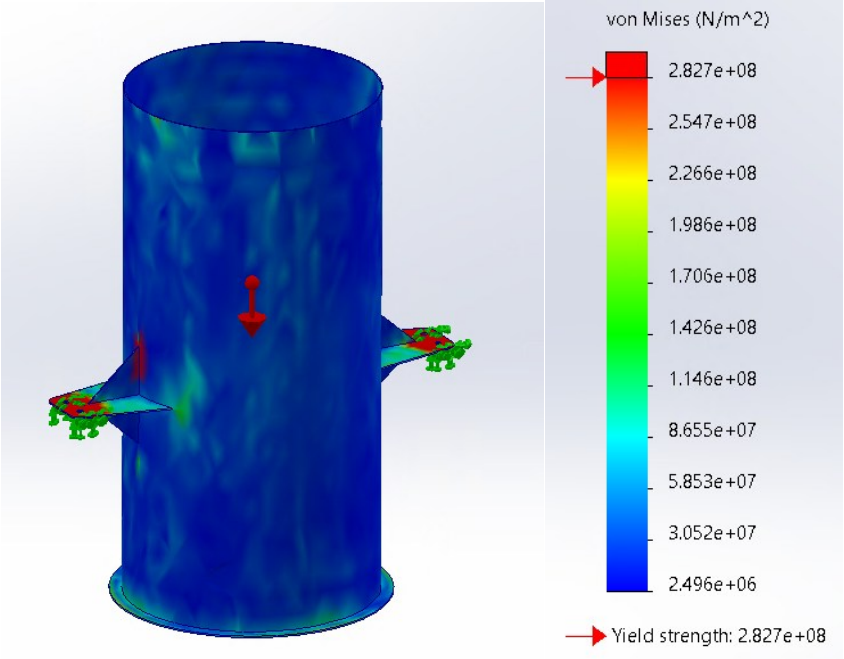

Figure 61: Stress study of winged chimney with thermal temperature load and gravity acting. Scale max set to yield strength of material.

Figure 61 shows the results of a stress study conducted on the winged chimney. The scale is set to put yield strength of the material as the maximum, so any red areas on the figure are exceeding the yield strength. The study shows that the mounting points of the lifting jacks undergo a high amount of stress at temperature and exceed the yield strength. However, the deformation is maintained within the ultimate strength of the material. Furthermore, deformation results shown in Figure 62 show minimal deformation at the mounting point and the surrounding area.

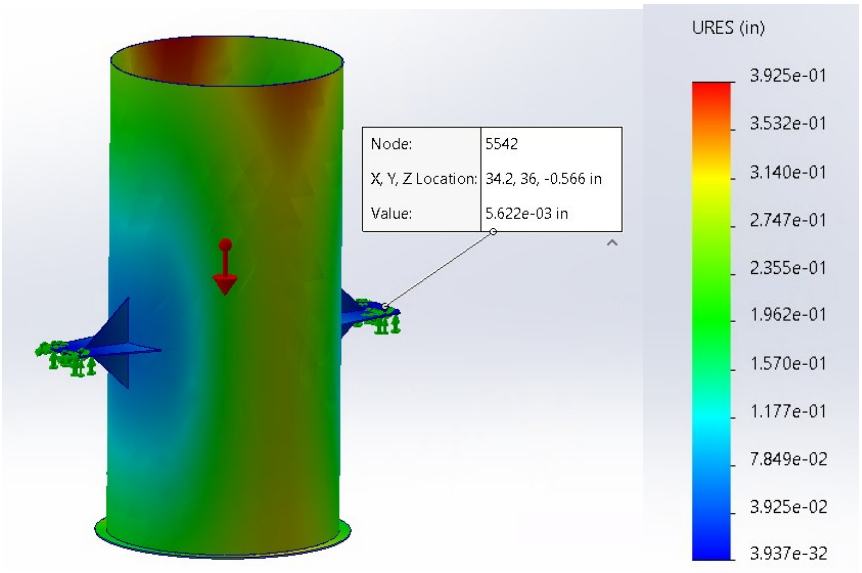

Figure 62: Deformation study of winged chimney with thermal load and gravity acting.

The maximum displacement of the study in Figure 61 is 0.39 inches. Given the size of the chimney and the slight predicted deformation and stress maintenance being below the ultimate strength point, the studies indicate that the chimney can support itself while withstanding the max operating temperature of 445°C.

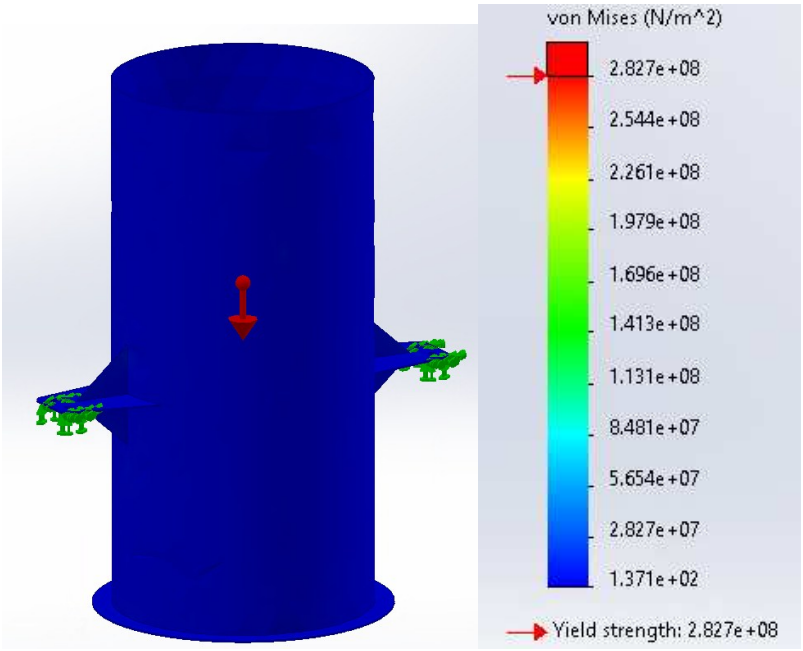

Figure 63: Solidworks FEA stress plot with gravity load, no heat load.

As shown in Figure 63, the chimney FEA stress plot is shown under conditions of weight load but without heat load. The stress points are well below the yield point of the material, showing no stress when heat is not applied. Figure 61 indicates that the chimney wings would be reaching the material yield point, causing deformation at the mounting plates if supported in that manner during full engine firing, reaching operating temperatures. However, when not at operating temperatures, the chimney weight can be fully supported by the wings and cart assembly, as shown in Figure 63 and pictured in Figure 64.

The cart design depicted in Figure 60 as a solution to the visibility restriction was manufactured and installed on the roof, as shown in Figure 64 and Figure 65.

Figure 64: Mobile cart for raising and lowering exhaust stack.

Figure 65: Mobile cart of raising and lowering exhaust stack view.

As is shown from the manufactured model in Figure 64 and Figure 65, deformation of the chimney around the support wings proved to be negligible. The chimney cart allows the chimney to be

upright and in place during testing and lowered and out of the way when not testing. It can easily be installed and removed by two people in less than 15 minutes. The installation of this component completes the exhaust ducting components of the commissioning process.

5.11 Insulation Motivation and Installation

The exhaust gas temperature of the Solar Turbines Centaur 40 can reach up to 445°C, therefore the exhaust system must be insulated to reduce safety hazards such as contact burns and proximity heat exposure. To ensure proper fitting of insulation blankets, the exhaust system was canvased and modeled in SolidWorks showing each protrusion, including custom lifting lugs added during the silencer installation process. The drawing was then sent to the insulation manufacturer, Insultech, for custom fiberglass blankets.

Figure 66: Image of exhaust system insulated with insultech blankets.

As pictured in Figure 66, the insulation blankets are fully installed. The blankets covering the silencer and horizontal pipe are 2-inch-thick silicone coated fiberglass cloth blankets with internal

wire mesh, and springs and rings closures. They will reduce the contact temperature from 445°C to below 73°C (164°F), with a 96.95% insulation efficiency.

5.12 Commissioning Summary

The exhaust system is fully commissioned. The exhaust is ducted continually from the turbine package exhaust through the silencer and terminates outside the building. The chimney and mobile cart assembly is stationed on the roof and has been tested to ensure proper function. The exhaust system is fully insulated to prevent injury and comply with building specific safety recommendations.

CHAPTER 6 - CONCLUSION AND DISCUSSION

Exhaust gas recirculation is a promising technology and step toward retrofitting existing gas turbine infrastructure to bridge the gap between the available decarbonization strategies of today and the zero-carbon systems of the future. As technology improves and the renewable fuel network matures, a zero-carbon energy industry becomes nearer, but there is still a long way to go. This study contributed to the progression of decarbonization strategies through system modeling and physical commissioning that laid the foundation for future experimental testing of EGR for decarbonization. The results of this study find that simulated EGR through surrogate gases is more feasible than actual EGR at the CSU Powerhouse campus, given the available resources and restrictions, as described below.

EGR for carbon capture is a feasible option for large scale power plants and has been theoretically proved to increase net efficiency of large systems. However, some complications of this system prove it impossible in some applications, such as for the laboratory setting at CSU's Powerhouse energy institute. The high mass flow requirement for cooling fluid coupled with the required cooling load is beyond what is feasible at our facility. The cooling load to reduce the exhaust gas from 445°C to 20°C is about 8.5 MW of cooling load, which is a massive load to take on as an auxiliary system component. Furthermore, it was found that the mass flow rate for a typical bulk air cooler is between 7.48 kg/s and 37.4 kg/s, depending on the selected exhaust temperature reduction, with the higher flow rate only achieving a temperature reduction to 56°C, despite the cooling mass flow being double the GT air flow (potentially due to heat transfer capacity restrictions of the modeled system). The makeup water requirements for the stated typical bulk air coolers were found to be 2.137 kg/s and 0.272 kg/s of water to account for boil off mass flow. When the effects of drift are considered, these values are likely to increase even further.

Furthermore, if the cooling water is recirculated in a direct contact semi closed system, which would be optimal for reducing required resource cost in water usage, cooling loads and water purification systems would have to be considered. Cooling loads to recirculate the cooling fluid were found to be about 1.75 MW to maintain a cooling fluid flow of just 9 kg/s, less than half the mass flow of the exhaust air. Given the high resource requirements necessary to implement and cool a true EGR system, it is not feasible with the limitations of the specified research facility without major reconstruction of infrastructure.

However, surrogate exhaust gas recirculation presents a feasible alternative to actual EGR while still allowing for experimental testing of the theory. It was found that the gas delivery rate for CO_2 and N_2 is 3453 kg/s and 11901 kg/s respectively to replicate 50% EGR. This value is calculated from an adjusted EGR requirement that considers the composition of ambient air in the intake as a partial contributor to the EGR makeup. The experimental surrogate flow run time limitations of available bulk air trailers was found to be 3.6 and 5.5 hours, with nitrogen being the limiting factor due to its high mass flow requirement. The Reynolds numbers in both surrogate pipe size cases examined were well above the turbulent flow range for turbulent flow in pipes,10,000, at 3792844 and 1610620 for each case directly after mixing the gases, suggesting the two gases become fully mixed as they travel together through the pipe. This removed the need for a surrogate gas mixing skid, as the gases can be assumed to be fully homogeneously mixed by the time they reach the ambient air mixer point. The required gas delivery pressures for CO_2 and N_2 were solved to be 77 and 88 psi at the most, which is well within the allowable delivery pressure specified by Airgas.

This simulation-based study assessed the practicality and the performance implications of implementing an EGR system for a gas turbine to enhance exhaust CO_2 concentration and thus

permit the use of smaller, less-energy demanding carbon capture systems. Two system layouts were evaluated, 1; an applied “real-world” EGR system requiring exhaust gas cooling to extract condensate prior to recirculation, and 2; a laboratory appropriate configuration using high flow rate CO_2 and N_2 as surrogate gases to simulate EGR without the power and space demand associated with actual recirculation. The systems were modeled in Flownex to determine appropriate component sizing and analyze the impact on exhaust pressure loss, required redirection flow and power, heat transfer load and water requirements to cool the exhaust gas, and the impact of various boundary condition inputs on the overall system. Given the high resource cooling and scrubbing requirements of the actual EGR system, my recommendation is a surrogate gas system that will simulate EGR for the purpose of testing its impact on the Centaur 40 at CSU. In the case of implementing EGR for carbon capture for a land-based power generation facility, actual EGR with heat recovery and a bottoming steam generation cycle would be most energy efficient. For the case of naval application of EGR for carbon capture, further consideration must be made weighing the usefulness of an indirect heat recovery and generation unit given the available onboard space, as direct contact cooling may be a more feasible way to cool the exhaust for recirculation without implementing a secondary power generation cycle.

To facilitate testing of the engine with an EGR loop, extensive commissioning procedures were required to fully install the engine to operating status. The commissioning work completed in pursuit of this project involved design, manufacturing, and installation of the exhaust system and auxiliary components. The exhaust system included the alignment and installation of the provided expansion bellows and silencer, as well as the design, manufacture and installation of the horizontal exhaust pipe extension, the silencer extension pipe, the exhaust thimble and roof reconstruction, and the chimney stack and mobile cart. The exhaust system was fully completed to

the specifications for normal engine operation. The completion of exhaust commissioning enables the recommended EGR testing method of surrogate gas injection.

CHAPTER 7 - FUTURE WORK

The future work in this study is two-fold, first in the actual EGR system and second in the surrogate EGR system.

To understand the full load and requirements of the actual EGR system, it is necessary to consider a fully closed loop system for the indirect cooling method. Additional work would include calculating fouling in the pipe system as well as loss of effectiveness due to corrosion from exhaust particles. Furthermore, the implications of CO_2 scrubbers on pressure drop and power consumption are necessary to consider in the case of implementing real EGR. Additionally, sizing and selecting a component to replicate the orifice would be necessary in validating the method of using flow restriction to change pressure and redirect flow. The most likely application would be a variable butterfly or solenoid valve. Finally, a secondary heat exchanger system to cool the recirculating gas should be sized and considered, as well as a water purification unit to ensure recirculating gas is not accumulating any undesirable solids or chemical adjustments. A valuable continuation of the real EGR system would be in studying repeat firing and the efficiency implications of a complete HRSG system in conjunction with EGR.

The surrogate system requires specifications for every aspect of the gas delivery system, including surrogate gas tank footprint, cost of operating, and bill of materials for system assembly. The design of the surrogate gas delivery system for application in impending on-site testing is currently in progress.

Once both designs are fully considered in terms of resource availability and cost, it will be necessary to compare them to make an informed financial decision and recommendation to small

lab or small power generation facilities, as to pave the way for EGR system research and wide scale implementation for carbon capture.

Flownex provides an opportunity to model the selected EGR system to its fullest extent, including the capability of modeling a digital twin of the EGR GT system. Digital twins are virtual models representative of a real-world system. Creating a digital twin of the EGR and GT system would provide insight into how different components would react in the real world given various input changes. It would be possible to model a digital twin of the Centaur 40 with EGR but would require extensive modeling and knowledge of the transient solving condition in Flownex. Furthermore, each individual component would need near-exact replication, as any small individual component inaccuracies can compound into major inaccuracies as a full system. Furthermore, there is the complication of individual components and fluid restrictions, as some components cannot process two-phase or mixed fluids. One example is the direct contact cooler component that only allows water-steam-air in the solver, creating complications given the process exhaust is comprised of various combustion products in addition to pure air. These complications can be circumvented with the data-transfer link utilized between components, if some inaccuracy is allowable. In all, it would be possible to create a digital twin to replicate the GT EGR system, given careful consideration of all modeling sensitivities and inaccuracies.

The final step in future work is to implement surrogate EGR for testing on the Solar Turbines Centaur 40. This includes procurement of N_2 and CO_2 gas tankers and vaporizers that can deliver a surrogate mixture at the scale necessary to imitate actual EGR. Furthermore, piping infrastructure design and installation is necessary to integrate a surrogate gas injection with the engine. The surrogate gas manifold will need to account for variable EGR rates and allow for

injection gas volume and composition regulation. Finally, exhaust flue composition testing must be created for accurate EGR data acquisition.

BIBLIOGRAPHY

[1] T. Stein, "Greenhouse gas pollution trapped 49% more heat in 2201 than in 1990, NOAA finds - NOAA Research," NOAA Research, 24 May 2022. [Online]. Available: https://research.noaa.gov/greenhouse-gas-pollution-trapped-49-more-heat-in-2021-than-in-1990-noaa-finds/. [Accessed 23 June 2025].

[2] "U.S. Energy-Related Carbon Dioxide Emissions, 2024," U.S. Energy Information Administration, Washington, DC, 2025.

[3] "Turbine Installation Fleet Interactive Map," National Energy Technology Laboratory, 2023. [Online]. Available: https://netl.doe.gov/carbon-management/turbines/turbinesmap. [Accessed 11 June 2025].

[4] "U.S. Energy Facts Explained," Energy Information Administration, 15 July 2024. [Online]. Available: https://www.eia.gov/energyexplained/us-energy-facts/. [Accessed 11 June 2025].

[5] "Electric Power Sector Emissions," United States Environmental Protection Agency, 31 March 2025. [Online]. Available: https://www.epa.gov/ghgemissions/electric-power-sector-emissions. [Accessed 28 June 2025].

[6] W. Muras, K. FLetcher, C. Bradley and R. Khan, "Navy Decarbonization Research Consortium | Operational Navy Decarbonization Roadmap," Office of Naval Research | Naval Postgraduate School, Monterey, Ca, 2023.

[7] D. Burnes, P. Saxena and P. Dunn, *Study of Using Exhaust Gas Recirculation on a Gas Turbine for Carbon Capture,* Controls, Diagnostics, and Instrumentation; Cycle Innovations; Energy Storage ed., vol. 5, Virtual, Online, 2020.

[8] R. G. Narula and H. Wen, "The Battle of CO2 Capture Technologies," in *ASME Turbo Expo*, Glasgow, 2010.

[9] "Supply, Underground Injection, and Geologic Sequestration of Carbon Dioxide | US EPA," United States Environmental Protection Agency, 14 January 2025. [Online]. Available: https://www.epa.gov/ghgreporting/supply-underground-injection-and-geologic-sequestration-carbon-dioxide. [Accessed 23 June 2025].

[10] M. Fajardy and C. Greenfield, "CO2 Capture and Utilization - Energy Ssytem - IEA," International Energy Agency, 25 April 2025. [Online]. Available: https://www.iea.org/energy-

system/carbon-capture-utilisation-and-storage/co2-capture-and-utilisation. [Accessed 24 June 2025].

[11] "Clean Fuels & Products Shot Media Kit," U.S. Department of Energy, 2023. [Online]. Available: https://www.energy.gov/eere/bioenergy/clean-fuels-products-shot-media-kit. [Accessed 24 June 2025].

[12] "Solar Turbines Centaur 40," [Online]. Available: https://s7d2.scene7.com/is/content/Caterpillar/CM20150703-52095-62290. [Accessed 16 December 2024].

[13] M. Sammak, P. Kulkarni, T. Camp, T. Denman and G.-L. Agostinelli, "Gas Turbine Combined Cycle System Integration with Exhaust Gas Recirulation for Boosted Power and Improved Carbon Capture Operations," in *ASME*, Memphis, 2025.

[14] H. Jääskeläinen and M. K. Khair, "EGR Systems and Components," DieselNet Technology Guide, August 2023. [Online]. Available: https://dieselnet.com/tech/engine_egr_sys.php. [Accessed 28 June 2025].

[15] A. M. ElKady, A. Evulet, A. Brand, T. P. Ursin and A. Lynghjem, "Application of Exchaust Gas Recirculation in a DLN F-Class Combustion System for Postcombustion Carbon Capture," *Engineering for Gas Turbines and Power,* vol. 131, no. 3, p. 034505, May 2009.

[16] S. C. Gülen and C. Hall, "Gas Turbine Combined Cycle Optimization for Post-Combustion Carbon Capture," in *ASME Turbomachinery Exposition*, Charlotte, 2017.

[17] A. T. Evulet, A. M. ElKady and M. J. Bowman, "Systems and Methods for Power Generation with Exhaust Gas Recirculation". United States of America Patent 8850789, 7 October 2014.

[18] J. Sholes, "Retrofittable Advanced Combined Cycle Integration for Flexible Decarbonized Generation," GE Gas Power, 2024.

[19] V. Thielens, F. Demeyer, K. P. Geigle, P. Kutne and W. D. Paepe, "Experimental Investigation of the Emissions and Performance of a Micro gas Turbine Setup with Enhanced EGR," *Elsevier,* vol. Applied Thermal Engineering, no. 267, p. 125673, 2025.

[20] L. Badum, F. Schirrecker and B. Cukurel, "Multidisciplinary Design MEthodology for Micro-Gas-Turbines - Part I: Reducing Order Component Design and Modeling," *ASME, J. Eng. Gas Turbines and Power,* vol. 146, no. 10, 2024.

[21] K. Chen, D. Seo and P. Canteenwalla, "The Effect of High-Temperature Water Vapor on Degradation and Faulure of Hot Section Components of Gas Turbine Engines," *Coatings,* vol. 11, no. 9, p. 1061, September 2021.

[22] B. Jeremiah, A. Harrod, T. Fosudo, A. Zdanowicz and B. Windom, "Exploration of Exhuast Gas Recirculation for Improved Carbon Cpature System Performance on a 3.5 MWe Liquid-Fueled Gas Turbine," in *ASME Turbo Expo*, Memphis (TN), 2025.

[23] *CS-061: Gas Turbine Combustor Design.*

[24] *CS-031: Combined Cycle Power Plant.*

[25] K. Zolińska, P. Mirek and M. Panowski, "Modeling of a transient low-temperature waste heat recovery in the plate heat exchanger in Flownex Simulation Environment," *Journal of Physics: Conference Series,* vol. 2412, no. 012004, 2022.

[26] A. S. Muksin and B. Syaiful, "Simple Simulation using Coupling between Flownex and LabVIEW Simultaneously in Case of Indonesian Experimental Power Reactor," *J. Physics,* vol. 1198, no. 022072, 2019.

[27] NAESB, "Natural Gas Specs Sheet," 2004. [Online]. Available: https://www.naesb.org/pdf2/wgq_bps100605w2.pdf. [Accessed 3 July 2025].

[28] S. R. Turns, "Chapter 2 | Combustion and Thermochemistry | Ideal-Gas Mixtures," in *An Introduction to Combustion: Concepts and Applications - 2nd ed.*, Singapore, McGraw-Hill, 2000, pp. 13-15.

[29] *Flownex Library Manual,* Flownex Simuation Environment, 2024.

[30] "Greenheck Blowers," Greenheck Fan Corporation, 2025. [Online]. Available: https://www.greenheck.com/products/air-movement/fans/blowers. [Accessed 2025].

[31] "Plug Fans Model PLG Catalogue," March 2013. [Online]. Available: https://content.greenheck.com/public/DAMProd/Original/10002/PlugFans_catalog.pdf. [Accessed 2025].

[32] "Doucette Industries Refrigeration Application Specialist CO2 Evaporators," [Online]. Available: https://www.doucetteindustries.com/Portals/0/Products/CO2%20Vaporizers/CO2_Vaporizer_Brochure.pdf. [Accessed 21 11 2024].

[33] "Thermafin Supergap Premium Natrual Convection Fin Ambient Vaporizer," 2018. [Online]. Available: https://files.chartindustries.com/PDS3.5.pdf. [Accessed 21 11 2024].

[34] "Toxicological Profile for JP-5, JP-8, and Jet A Fuels," Agency fo Toxic Substances and Disease Registry (US), Atlanta , 2017.

APPENDIX A – FLOWNEX COMBUSTION MODEL

Appendix A describes the method for modeling a gas turbine engine in Flownex using known conditions about temperature output and pressure ratio. Utilizing these variables along with "change design" conditions for certain components in Flownex sets the basic turbine and compressor components to replicate real-world function. This model can be used to measure fuel injection requirements, combustion composition, and component response to various conditions such as inlet temperature. The process will be described in a series of steps that one can follow along with the Flownex simulation software.

Step 1: Initialize Components

This process is useful when inlet and outlet conditions are known, but the compressor and GT charts are unknown. Pressure ratio, mass flow, inlet temperature, and exit temperature must be known. Isentropic efficiencies are assumed. The component circuit is displayed in Figure 67, with components labeled by number as follows; 1: Boundary Condition, 2: Simple Compressor, 3: Basic Pipe, 5: Simple Turbine.

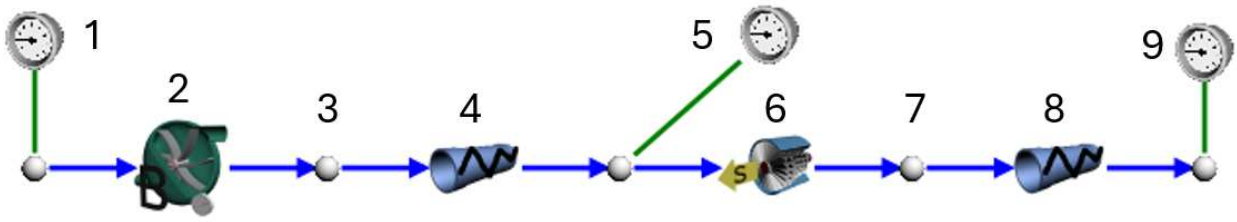

Figure 67: Component system circuit required to initiallize simple compressor and simple turbine component characteristic charts in Flownex.

The initial boundary condition, labeled 1 in Figure 67, represents the inlet air, and must be known as the ambient condition specified for the outlet temperature measured or listed in the engine's technical specification sheet. For our purpose, component 1 will have a set temperature of 20°C and pressure of 100 kPa. Figure 68 shows the property window setup for BC 1.

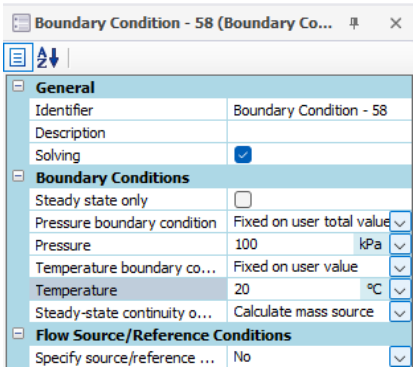

Figure 68: Property window settings for initial boundary condition corresponding to BC 1 in Figure 66.

The fluid for BC 1 and the system circuit is specified by selecting the node associated with BC 1, and setting the fluid option in the property window to Air, found following the fluid drop-down menu in the sequence, Pure Fluids, Gases, Air.

The basic centrifugal pump, labeled component 2 in Figure 67, will be adjusted before and after the initialization run. Before initialization, the efficiency at BEP, fixed mass flow, and design for mass flow options in the property window must be set.

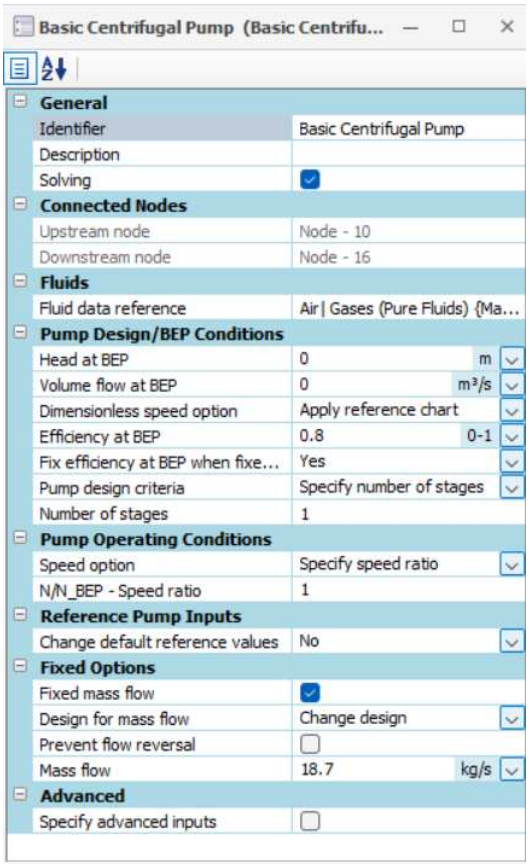

Figure 69: Property window settings for basic centrifugal pump corresponding to component 2 in Figure 67.

To initialize the compressor component, proceed with the following sequence:

1. Set dimensionless speed option to “apply reference chart”
2. Set efficiency at BEP to guess value 0.8 or measured value
3. Select fixed mass flow
4. Set design for mass flow option to “change design”
5. Set mass flow to 18.7 kg/s as specified in technical specification sheet [12]

The efficiency at BEP can be assumed 0.8 for the primary initialization or adjusted to a measured efficiency if available. The mass flow should be set to 18.7 kg/s, as specified in the technical

specification sheet [12]. Once fixed mass flow is selected, the design for mass flow option will appear, and should be set to change design. The change design feature will allow the component to "solve" itself to create a characteristic "chart" given external references and boundary conditions.

Component 3 in Figure 67 is a node, and is used in junction with a major component, such as a compressor, to specify the conditions at that point. The node conditions are specified in Figure 70.

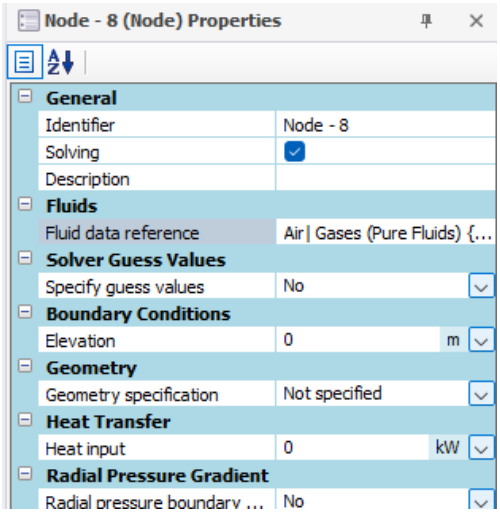

Figure 70: Property window settings for node corresponding to point 3 in Figure 66, showing no heat transfer at that point.

As shown in Figure 70, the heat input is set to zero, specifying the process is assumed adiabatic. The custom loss pipe, labeled component 4 in Figure 67, is representative of the combustion chamber in the gas turbine engine, and must have set resistance and exit temperature values, as shown in Figure 71.

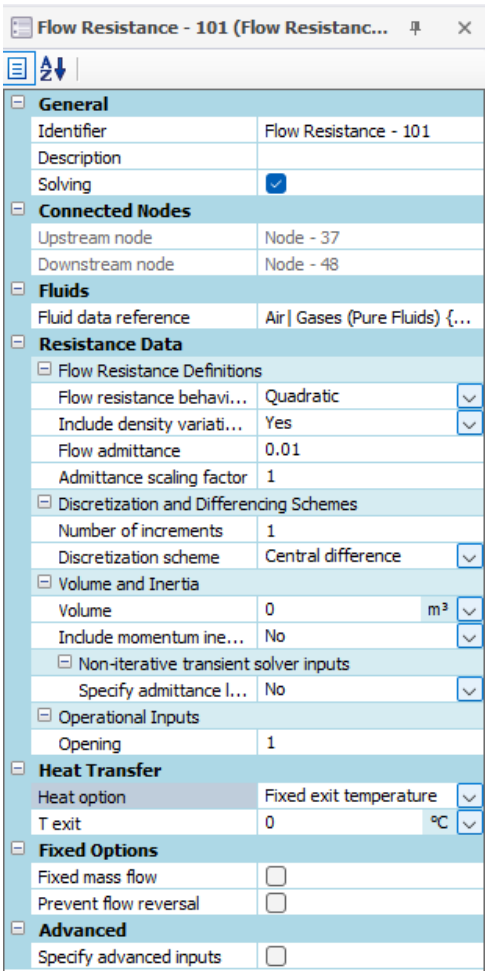

Figure 71: Property window of pipe component corresponding to label 4 in Figure 66, showing no heat transfer specification.

The custom loss component replicates resistance in the combustor. The resistance is set under the flow resistance definition at an assumed 0.01 value. Next, the heat option under the heat transfer section is set to ‘fixed exit temperature’. This allows the user to set the exit temperature of the combustor. For the initialization run, the exit temperature should be set to zero.

The boundary condition, labeled as component 5 in Figure 67, is paired with the simple turbine component 6. It is necessary for the simple turbine component initialization that the boundary condition steady-state continuity setting in the property window be specified as ‘apply element fixed mass flow’, as shown in Figure 72.

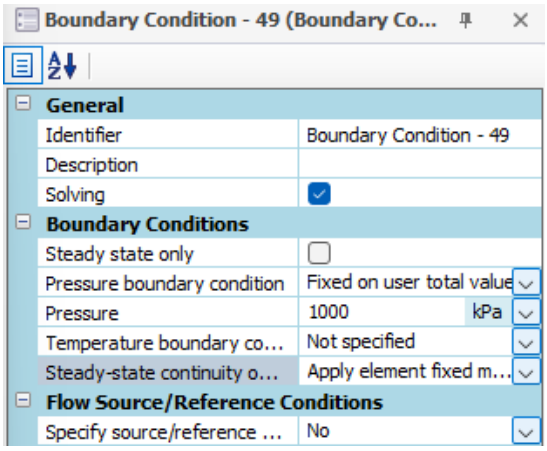

Figure 72: Property window of boundary condition paired with simple turbine, corresponding to components 5 and 6 respectively in Figure 66.

Utilizing the 'apply element fixed mass flow' setting associated the boundary condition with the next component, in this case the simple turbine. The boundary condition specified in Figure 72 specifies the pressure for the simple turbine, allowing it to solve under the 'change design' setting. As shown in Figure 72, the pressure is set to 1000 kPa, which is found by the compressor pressure ratio 10:1 specified in the engine technical spec sheet [12], and calculated from the inlet pressure set at BC 1 in Figure 68.

The simple turbine, labeled 6 in Figure 67, is specified as shown in Figure 73.

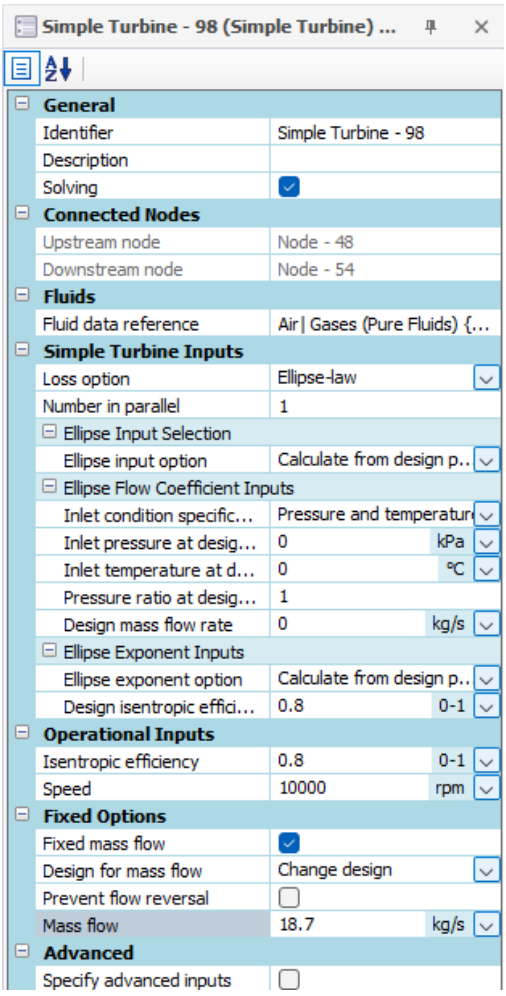

Figure 73: Simple turbine property window, corresponding to component 6 in Figure 67.

The pre-defined property window settings in Figure 73 are as follows; design inlet pressure is set by the boundary condition at 1000 kPa, design mass flow rate is set by the centrifugal pump, and the ellipse flow coefficient inputs are set by the system after the initialization run. The user must set design isentropic efficiency and operational isentropic efficiency to 0.8, which is a starting assumption and can be reconfigured to represent actual efficiency performance given more detailed engine information. The user should also set the speed to 10000 rpm, or the assumed operating speed, and select fixed mass flow and set to 18.7 kg/s, as specified by the specification sheet [12]. Set the design for mass flow option to ‘change design’ for the initialization run.

The exhaust pipe in the system is modeled by the custom loss flow pipe, labeled component 7 in Figure 67. The property window settings for this component are shown in Figure 74.

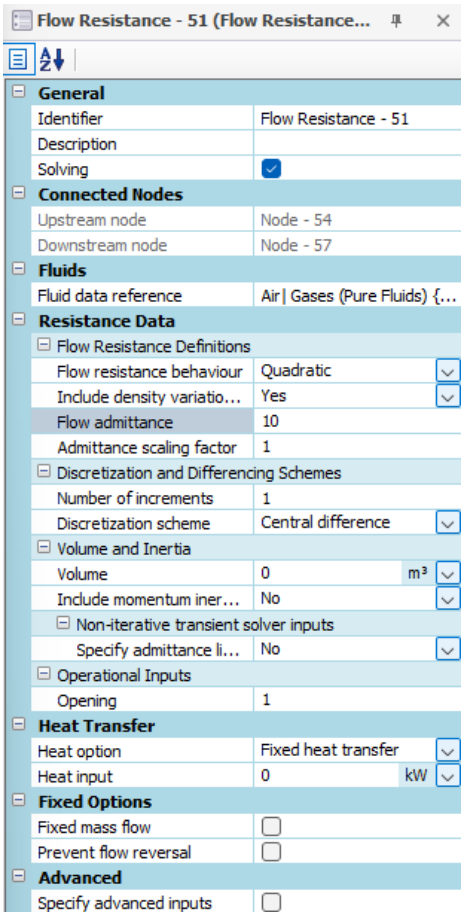

Figure 74: Property window settings for the exhuast of the combustor model, associated with component label 7 in Figure 66.

The flow admittance should be set to 10, simulating no resistance in flow from the exhaust pipe.

The exit boundary condition, labeled component 8 in Figure 67, represents the end of the combustion system. The parameter window settings are shown in Figure 75.

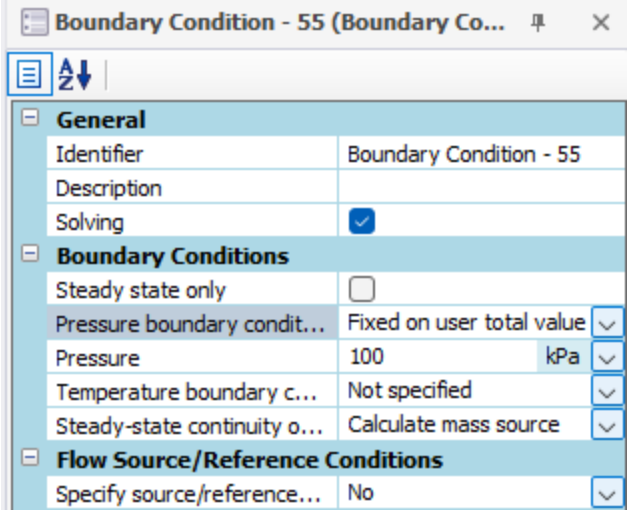

Figure 75: Parameter window settings for exit boundary condition, corresponding to component 8 in Figure 66.

The exit BC specified in Figure 75 should have pressure specified at 100 kPa, matching the inlet BC, noted in Figure 68.

Now that the components are set, the system can be initialized. Solve steady State once.

The results depicted in Figure 76 should appear if fixed exit temperature of "combustor" pipe is set to zero.

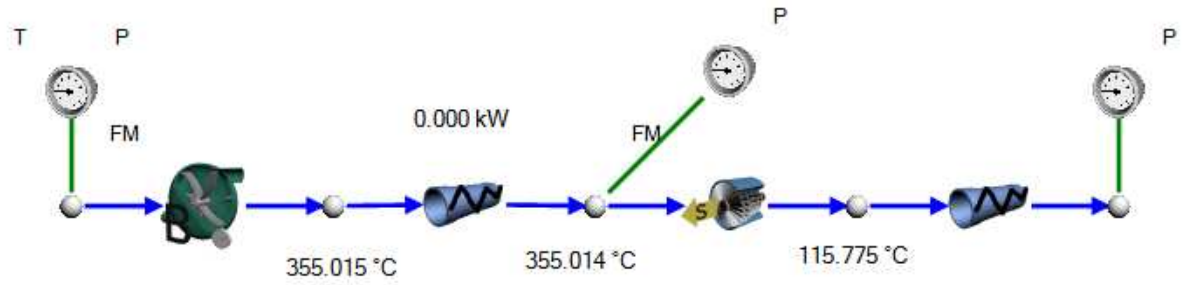

Figure 76: The gas turbine model initialized in Flownex, showing temperatures and power results associated with individual components.

Step 2: Set Compressor and Turbine Characteristic Charts

The second phase of the engine system modeling process is to set characteristic charts for the compressor and turbine.

If the combustor exit temperature is known, set that value under exit temperature in the property window of component 4 in Figure 67. If the actual exit temperature is not known, a guess value can be estimated, with the solver variables depending on the system inlet and outlet temperatures and the pressure ratio. First, find barrier guess values for exit temperature of combustor, referenced in Figure 77.

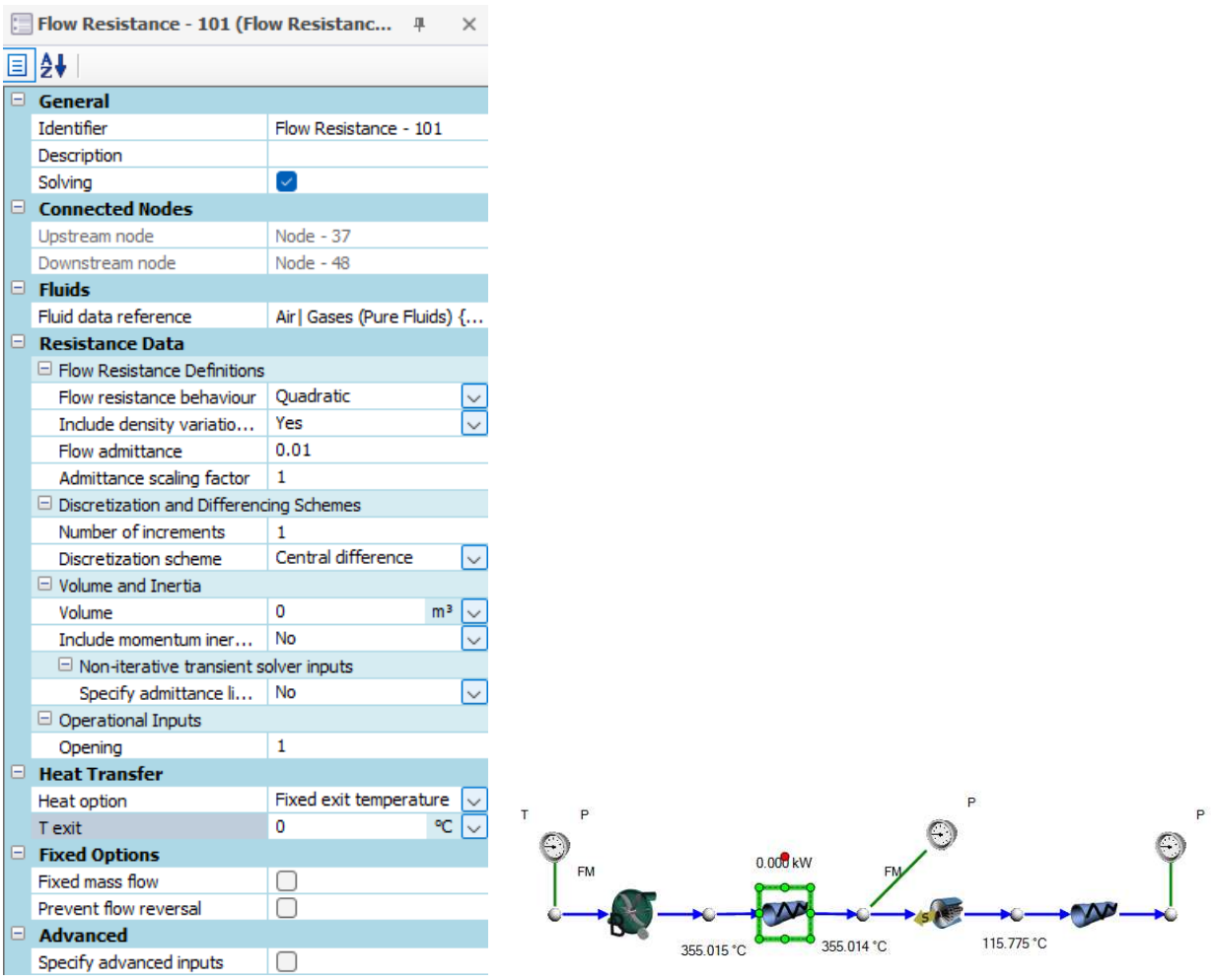

Figure 77: Combustion chamber component model property window and component in Flownex system prior to combustion th exit temperature determination.

To determine the appropriate combustor exit temperature that achieves the known exhaust temperature of 445 °C [12], the Flownex designer can be used. The designer functions using a user-set numerical range and a target value. The temperature range is determined by manually entering guess values into the exit temperature until a target range is determined. The range 800 °C– 900 °C for the combustor exit temperature achieves the known outlet node temperature of 445 °C [12] at point 7 in Figure 67, and is used for this process.

Given the designer tool configuration shown in Figure 78, the designer tool solves for the unknown variable using the Newton-Raphson method, solving within the specified range.

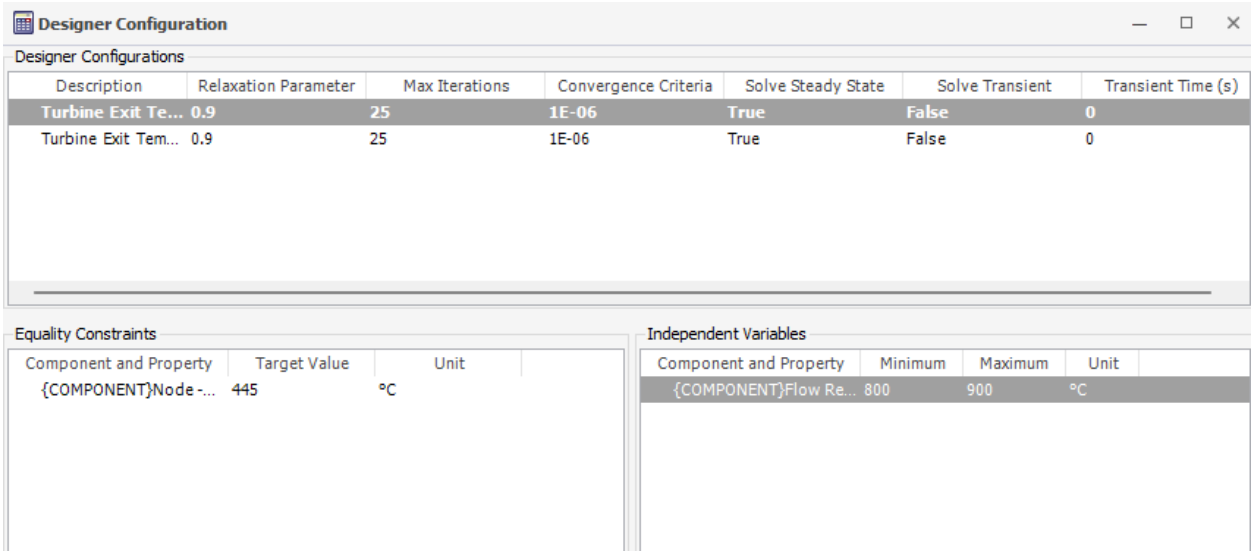

Figure 78: Designer configuration window solving for combustion chamber exit temperature between 800 °C to 900 °C to achieve target value 445 °C as specified by Solar Turbines Centaur 40 specification sheet [12].

The designer tool solved for a combustor exit temperature of 845 °C using the method described, but study of the Solar Turbines Centaur 40 operating system by Kinglsey Atomboh found a more accurate exit temperature to be 962 °C (1236 K). In future modeling, the exit temperature should be adjusted to accurately reflect the temperature at the combustor exit, set at 962.85 °C.

Running the designer tool should converge to show the component temperature and heat transfer results depicted in Figure 79.

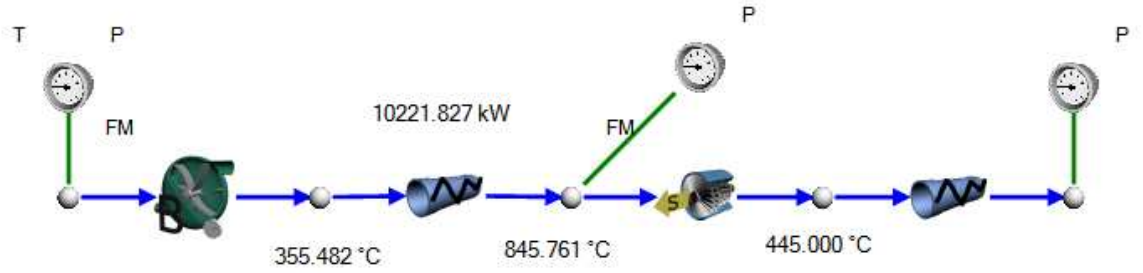

Figure 79: Results of running preliminary system circuit in Flownex with fixed combustion chamber exit temperature, showing turbine and compressor component characteristics set to produce the desired outlet temperature.

The compressor and turbine charts are now set to produce the appropriate combustion chamber outlet temperature given known system inlet and outlet temperatures. Now, the system model can be reconfigured to allow for dynamic conditions after the following steps are completed:

1. Deselect fixed mass flow and remove boundary condition from simple turbine component.
2. Deselect fixed mass flow from compressor component.

The property table after deselecting the simple turbine fixed mass flow component is shown in Figure 80, and should be similarly represented in the compressor component. Additionally, the boundary condition corresponding to component 5 in Figure 67 should be deleted.

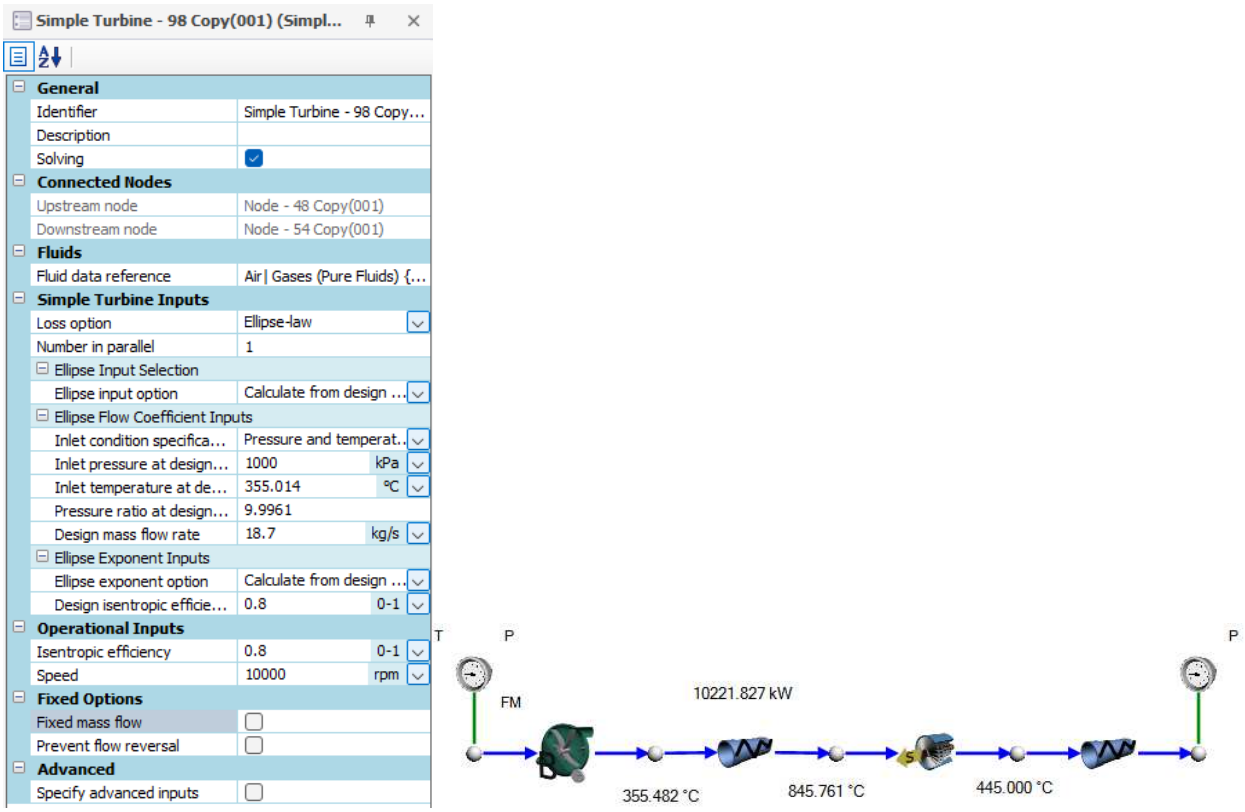

Figure 80: Simple turbine component property window and system model solver results with compressor and turbine initialized and set, allowing for variable mass flow, inlet temperatures, and inlet pressures.

After the compressor and turbine have been initialized and set, the user can change intake temperature and mass flow variables to produce various system results while maintaining gas turbine operating characteristics representative of the Solar Turbines Centaur 40.

Step 3: Add combustion

Adding combustion to the gas turbine system model is the last step in creating a digital replica of the engine. Figure 81 shows the model with a the CEA adiabatic flame component added to replicate the combustion chamber chemical reaction.

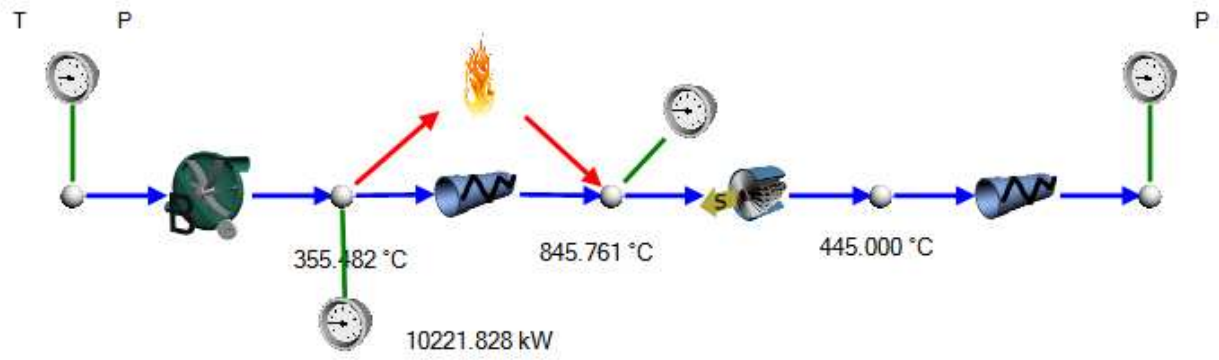

Figure 81: Component system circuit for gas turbine model with chemical reaction in the combustion chamber, represented by the CEA adiabatic flame component and custom loss pipe component.

The model combustion chamber properties must be set to replicate a GT chemical reaction. The boundary conditions labeled as component 4 and 7 in Figure 82 represent the fuel injection and combustor exhaust, respectively.

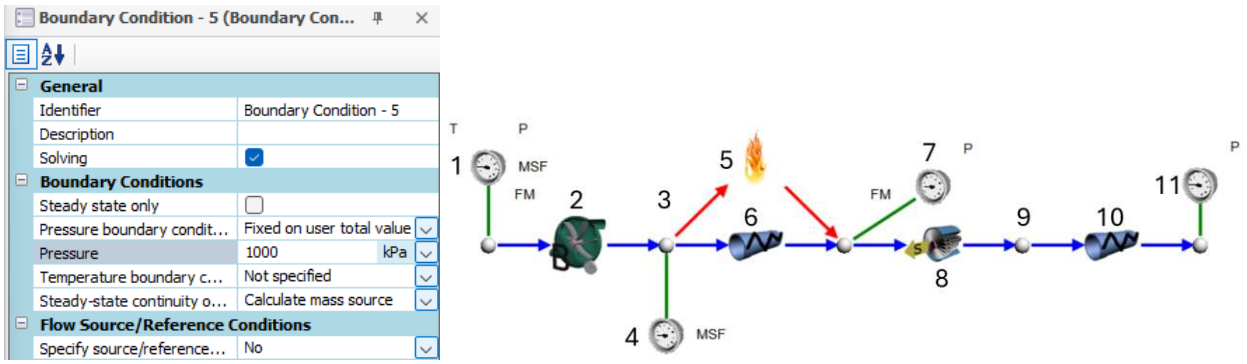

Figure 82: Gas turbine system modeled in flownex with boundary condition at point 7 represented in the property window, with combustor exit presure set to 1000 kPa.

The combustor outlet BC at point 7 in Figure 82 is set to the specified pressure ratio 1000 kPa [12]. Point 4 in Figure 82 represents fuel injection to the combustion chamber. In order to add natural gas to the system model, natural gas/air mixture must be created as a new fluid in Flownex. Figure 83 shows the mixed fluid dialog window, where the air/natural gas fluid can be created.

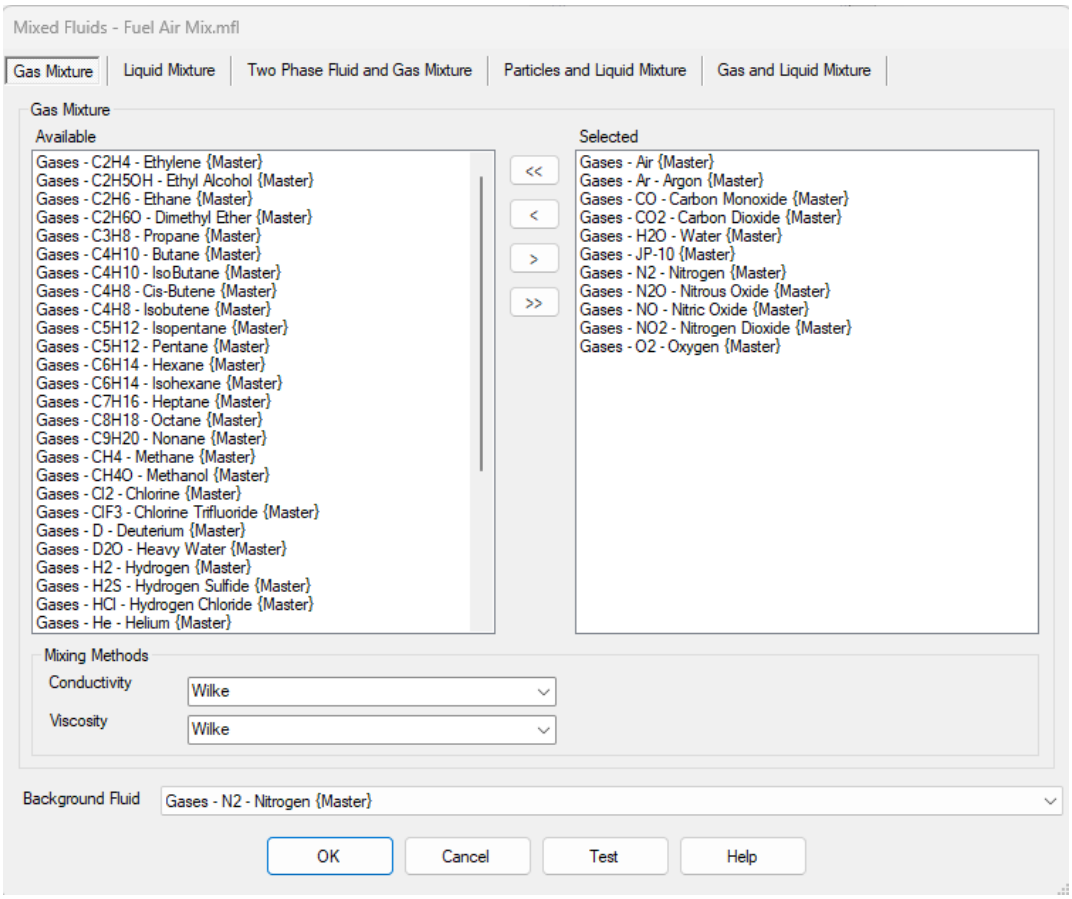

Figure 83: New mixed fluid dialog window displaying the elements used to create the fuel air mixture for the combustor chemical reaction.

For a proper chemical reaction to take place, the new mixed fluid must include all possible combustion inputs and products, with JP-10 as the fuel to represent natural gas. The background fluid is set as N2 to avoid confusion when viewing the combustion products. The N_2 fraction is large, so additional N_2 combustion products would make a negligible difference in product results when compared to Air, for example.

Set the new fluid and define the mass fraction for the ambient air intake and fuel injection points as shown in Figure 84.

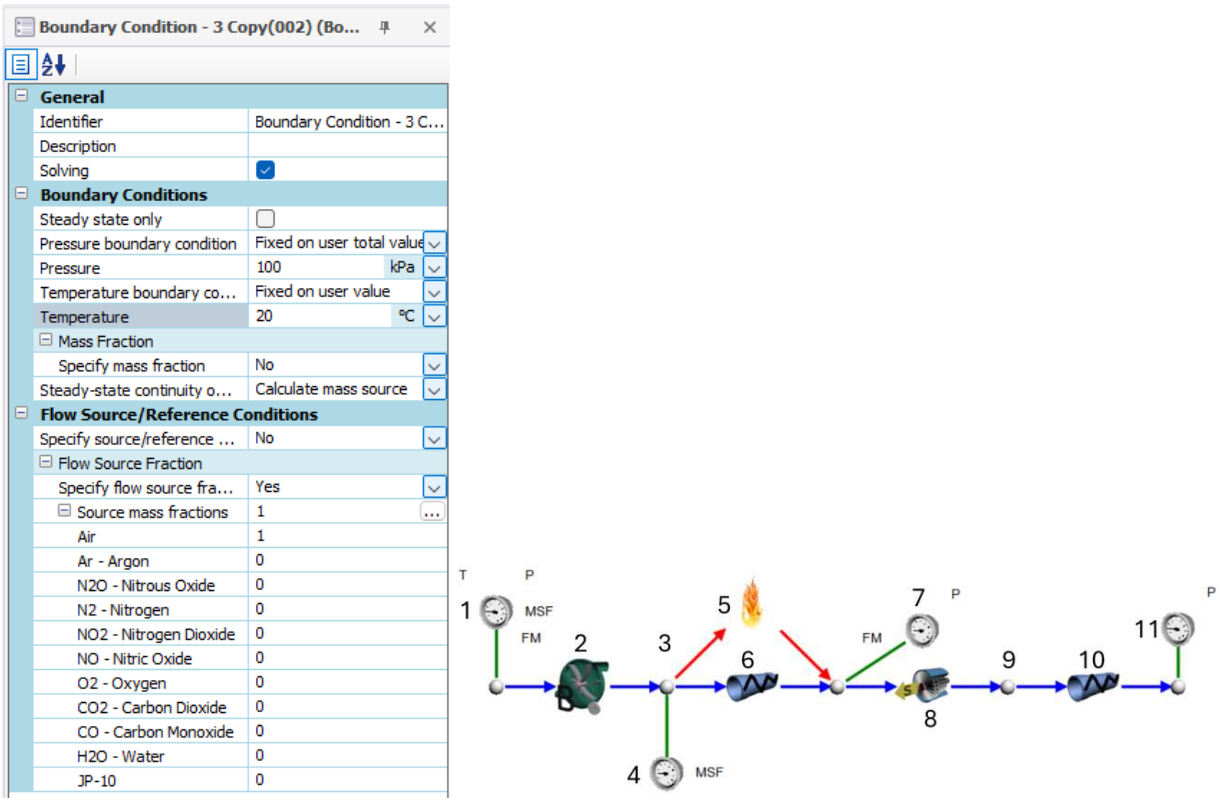

Figure 84: Property window of the combustor fuel injection boundary condition showing fluid flow mass fraction breakdown at point 1.

The fuel injection boundary condition at point 1 in Figure 84 should be set to represent 100% Air, and the boundary condition at point 4 should be set similarly to 100% fuel JP-10 to represent a pure fuel injection. When specifying the fuel mass fraction, it is important to set the flow source/reference conditions rather than the generic boundary condition mass source.

To replicate the combustor in the Flownex model, the following procedure should be followed:

1. Set the flow source fraction to 100% JP-10.
2. Change compressor and simple turbine to “fixed mass flow-change design” but do not reset the mass flow. It will solve itself given the new fuel input

3. Add boundary condition to simple turbine, and set pressure to 1000 kPa, or the pressure ratio specified relative to ambient. Set the mass fraction steady state continuity to “apply element fixed mass flow” as shown in Figure 85.

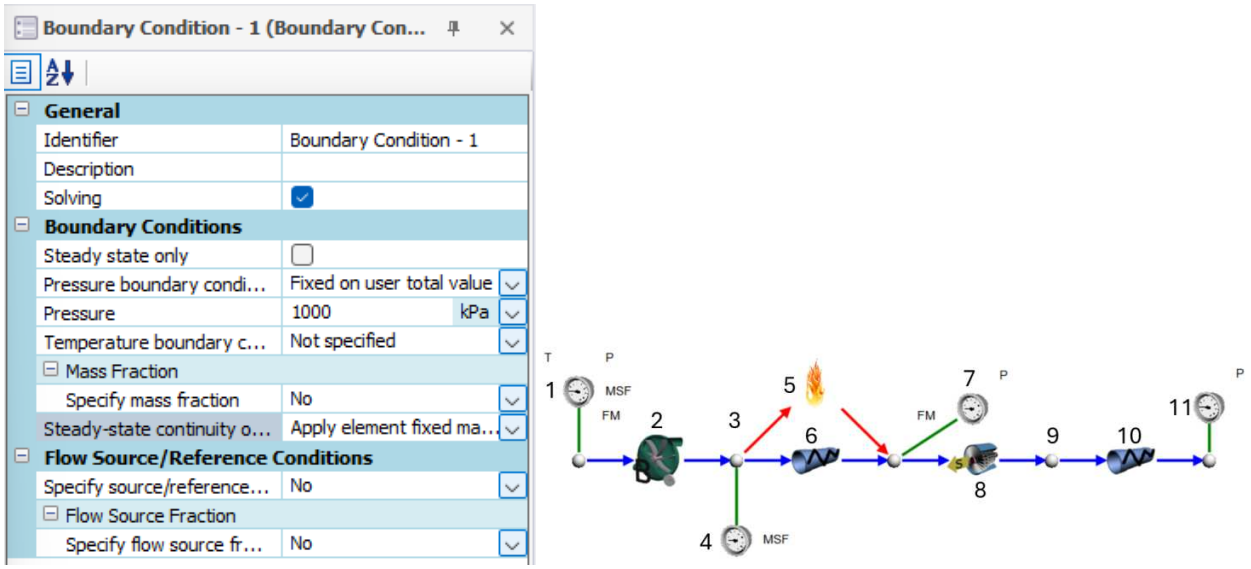

Figure 85: Property window of boundary condition at point 7, showing the pressure set to 1000 kPa, representing the defined pressure ratio in the Solar Turbines Centaur 40 specification sheet [12].

To determine the required fuel injection mass flow to maintain the turbine outlet temperature of 445 °C, the designer can be used. The designer tool setup is shown in Figure 86, solving for a target exhaust temperature of 445 °C given fuel injection boundary conditions 100 g/s – 500 g/s.

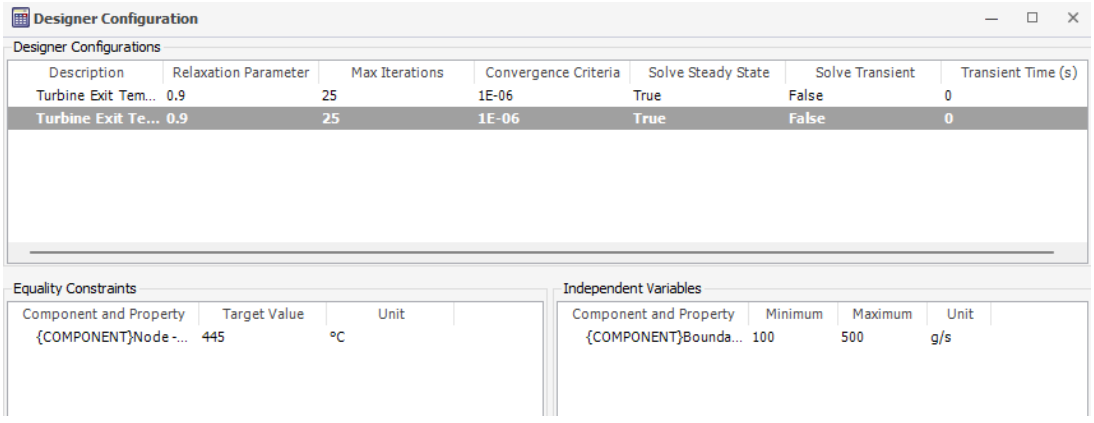

Figure 86: Designer dialog window solving for combustor fuel injection to maintain exhaust temperature of 445 °C.

The designer should converge, adjusting the simple turbine mass flow to account for the additional mass from fuel injection. Once the designer has converged, deselect fixed mass flow from turbine and compressor to fix the new configuration, and remove the boundary condition associated with the simple turbine.

This concludes the process for creating a Flownex model to replicate the compressor, combustion chamber, and turbine of a gas turbine engine given mass flow, pressure ratio, combustion chamber outlet temperature, and turbine outlet temperature. The completed model is shown in Figure 87.

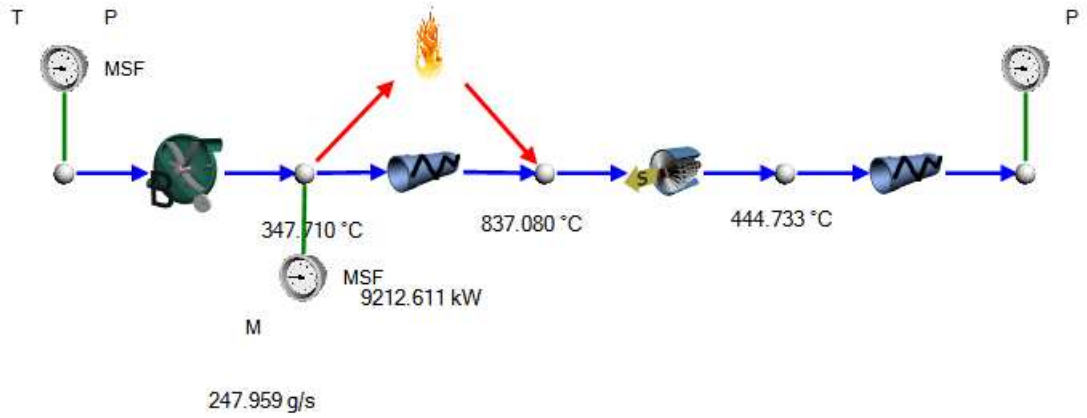

Figure 87: Completed component system replicating a Solar Turbines Centaur 40 GT with compressor, combustion chamber, and turbine.

The model can be adjusted to account for different known engine variables. It should be noted that this model is a rough replication of the system, and various real-world differences exist, such as the actual ambient air intake value inaccuracy. In addition to entering the combustor, intake air is channeled to auxiliary uses in the GT, such as air cooling, sealing, and other accessory functions. The model assumes all intake air is entering into the combustor, which will result in more fuel-lean combustion than in actual engine performance. Additionally, this model doesn't account for fuel injection adjustments by the engine to maintain an adiabatic flame temperature or adjustments made to the pilot flame to reduce blowout, which also has a notable impact on combustion product

composition. Therefore, the stated model sensitivities should be considered when analyzing model results.

This model can be used as the basis for creating a complete EGR loop in Flownex, in which a recirculation channel with cooling, scrubbing, and water separation can be added.

A preliminary model of the EGR loop added onto the GT system is shown in Figure 88.

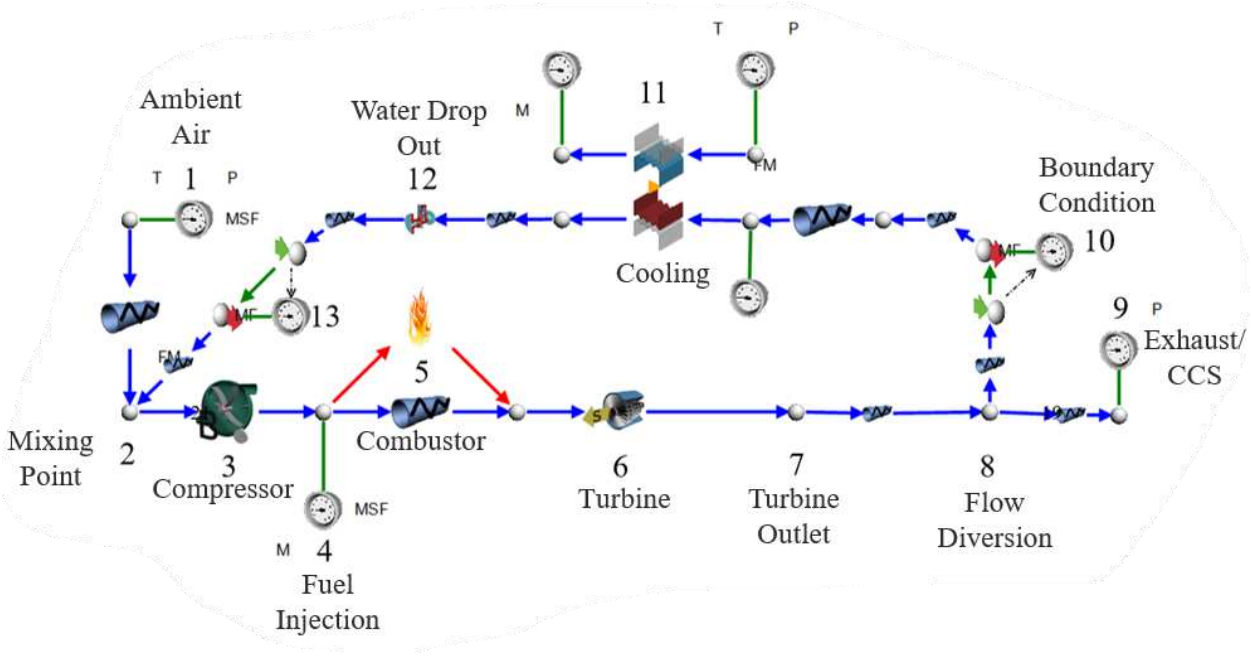

Figure 88: Preliminary model of GT with EGR loop, including exhaust diversion, cooling, and water drop out.

The system layout depicted in Figure 88 can be used as a starting point for creating an actual EGR system in Flownex. The model utilizes various components that create compounding inaccuracies and should be reconfigured in a second iteration of the recirculation loop. The depicted model cools only the recirculated portion of the exhaust, which does account for the CCS low temperature requirement, resulting in a false system cooling load result at point 11 of Figure 90. It is important to consider the boundary conditions at point 10 and 13 in Figure 90, which utilize data transfer links to allow two types of fluid in the circuit. The data transfer links are needed to allow both

gaseous and liquid H_2O in a single circuit, which accounts for fluid requirements of the GT circuit, namely the compressor and turbine which do not allow for liquid fluid, as well as the heat transfer component used, which requires liquid fluid to replicate a realistic cooling circumstance. The model also neglects to include a scrubbing component necessary to remove corrosive compounds from the exhaust flue before entering the GT.

APPENDIX B – INDIRECT HEAT EXCHANGER MODELING

The indirect heat exchanger can be simply modeled as the composite heat exchanger component in Flownex. It has been found that the generic heat exchanger component is not suited for phase change and therefore cannot be accurately used to model heat exchange and the effect on cooling water. Preliminary modeling has been done on this front, but further study is needed to accurately replicate a realistic heat exchanger. However, it is known that the heat exchanger should be comprised of the composite heat exchanger transferring heat between the upper process section (exhaust air) and the lower cooling section (cooling fluid), both fluids flowing through pipes with defined geometry, or alternatively, non-dimensional flow restriction component pipes. The boundary conditions are defined individually, noting that T=Temperature, P=Pressure, M=Mass Flow. An example layout for configuring this model is shown in Figure 89.

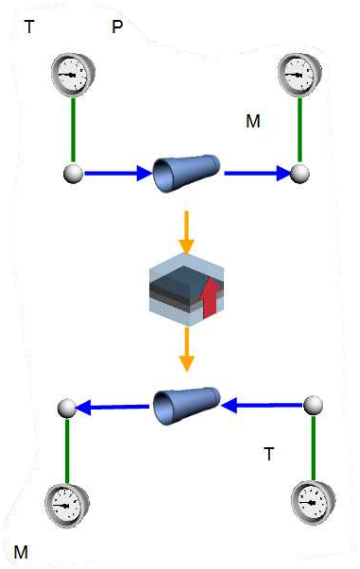

Figure 89: Indirect contact heat exchanger Flownex model using the composite heat transfer component with upstream exhaust air and downstream cooling fluid flowing through pipes with specified boundary conditions.

The heat transfer component should be configured to represent a realistic heat exchanger. It is suggested to use the constant h value method for each stream rather than the NTU-effectiveness method, and to set the “temperature differencing scheme” setting to “average temperature difference” for convection on the upstream and downstream sides of the CHT component. Additionally, flow components connected to the CHT should be incremented.

APPENDIX C – MOBILE EXHAUST STACK CART

Operating the chimney stack mobile cart assembly is best done with two people. There are two positions the chimney stack should be in, standby and firing. The standby position is assumed when the engine is not being run and the stack is positioned as far east as possible next to the brick wall to eliminate visibility from the street. The firing position is assumed when the engine is undergoing testing and the chimney stack has to be mounted to and supported by the chimney pipe extension flange. The chimney stack mobile cart assembly is depicted with red labels in Figure 90.

Figure 90: Exhaust stack and mobile cart assembly installed in the firing assembly.

The chimney stack can be raised and lowered by cranking jack stands A and B in synchrony until the desired height is achieved. The jack stands will self lock, and will not “self crank” or unwind

along the travel path. When in the standby position, the stack should be lowered to the lowest possible height. Similarly, while rolling into position, the stack should remain as low as possible until lifting is required to clear the mounting flange height. The jack stand should never be removed from the jack mount.

The cross members shown disassembled in Figure 90 should be attached at the open side of the cart with the associated hardware. These members should be in place when the cart is stationary in standby and when moving. The cross members should be removed to allow for cart and chimney stack disassembly when the stack is mounted in the firing position. When the chimney stack is installed on the exhaust pipe extension flange in the firing position, the mobile cart assembly should be detached from the stack and rolled to its non-firing standby position. This is done by removing the mounting bolts at the wing mount to release the cart from the stack.

The wheel lock on each castor wheel should be in the open position when moving and locked when stationary or when lifting and lowering the stack.